The steady-state visual evoked potential in vision research: A review

Anthony M. Norcia — Department of Psychology, Stanford University, Stanford, CA, USA

L. Gregory Appelbaum — Department of Psychiatry and Behavioral Sciences, Duke University, Durham, NC, USA

Justin M. Ales — Department of Psychology & Neuroscience, University of St. Andrews, St. Andrews, UK

Benoit R. Cottereau — Université de Toulouse, Centre de Recherche Cerveau et Cognition, Université Paul Sabatier, Toulouse, France; CNRS UMR 5549, CerCo, Toulouse, France

Bruno Rossion — Psychological Sciences Research Institute and Institute of Neuroscience, University of Louvain, Louvain-la-Neuve, Belgium

Periodic visual stimulation and analysis of the resulting steady-state visual evoked potentials were first introduced over 80 years ago as a means to study visual sensation and perception. From the first single-channel recording of responses to modulated light to the present use of sophisticated digital displays composed of complex visual stimuli and high-density recording arrays, steady-state methods have been applied in a broad range of scientific and applied settings. The purpose of this article is to describe the fundamental stimulation paradigms for steady-state visual evoked potentials and to illustrate these principles through research findings across a range of applications in vision science.

Introduction

Evoked potentials, consisting of stereotypic changes of electrical activity evoked by sensory stimuli and measured at the scalp, were first recorded in the middle of the last century (Adrian, 1944; Adrian & Matthews, 1934b; Dawson, 1954; Walter, Dovey, & Shipton, 1946). Since then, they have become an important tool for understanding the relationships between physical stimuli, brain activity, and human cognition (Handy, 2005; Luck & Kappenman, 2012; Regan, 1989). The goal of this article is to describe, at both the conceptual and technical levels, the core principles underlying a particular type of visual evoked potential—the steady-state visual evoked potential (SSVEP)—and its application to human sensory and cognitive processing.

Evoked potentials can be generated not only as a result of physical stimulation by a sensory stimulus (exogenously generated evoked potentials) but also by internal cognitive or motor processes (endogenously generated evoked potentials). These two types of responses comprise event-related potentials (ERPs), which are "the general class of potentials that display stable time relationships to a definable reference event" (Vaughan, 1969, p. 46). In their most common form, ERPs are recorded in response to an isolated, discrete stimulus event. In order to achieve this isolation, stimuli in an ERP experiment are typically separated from each other by a long and/or variable interstimulus interval, allowing for the estimation of a stimulus-independent baseline reference. In contrast to these transient ERPs, exogenous ERPs can also be generated in response to a train of stimuli presented at a fixed rate. Because the responses to such periodic stimuli can be very stable in amplitude and phase over time, those

Citation: Norcia, A. M., Appelbaum, L. G., Ales, J. M., Cottereau, B. R., & Rossion, B. (2015). The steady-state visual evoked potential in vision research: A review. *Journal of Vision, 15*(6):4, 1–46, http://www.journalofvision.org/content/15/6/4, doi:10.1167/15.6.4.

doi: 10.1167/15.6.4 Received September 24, 2014; published May 5, 2015 ISSN 1534-7362

responses have been referred to as the steady-state visually evoked potential (Regan, 1966).

Steady-state evoked potentials in response to visual stimuli were first reported by Adrian and Matthews (1934a) in a remarkable article that also demonstrated suppression of the alpha rhythm by attention. As was typical of the time, some details are left to the imagination, but the following quote from the article leaves little doubt: "At a signal the eyes are opened and the shutter lifted to turn on the flickering light. The result is a series of potential waves having the same frequency as that of the flicker" (p. 378). Interest crescendoed in the 1960s among researchers who studied the processing of luminance information (Kamp, Sem Jacobsen, Storm Van Leeuwen, & van der Tweel, 1960; Regan, 1964, 1966; Spekreijse, 1967; van der Tweel & Lunel, 1965; van der Tweel & Spekreijse, 1969). The signal processing methods used at the time were rudimentary (Regan, 1989) and have been steadily improved over time (Nelson, Seiple, Kupersmith, & Carr, 1984; Norcia, Clarke, & Tyler, 1985; Tang & Norcia, 1995; Tyler, Apkarian, Levi, & Nakayama, 1979). More importantly for the purpose of this article, the technique has been extended to stimuli of increasing complexity, from luminance flicker to pictures of faces, and therefore this method has become more broadly applicable in visual science research.

In this article, we describe the key features of the SSVEP and its generalization from single stimuli to multiple simultaneous stimuli. In the process, we cover many different applications of the SSVEP for understanding visual perception and attention. At each stage, we point to prominent results that have been obtained with the method. We end with a discussion of work that has used the method in conjunction with computational modeling to understand nonlinear processing in the visual cortex.

Responses to single periodic visual inputs

When a single stimulus attribute is modulated periodically as a function of time, the evoked response generated by that stimulus has a periodic time course. While SSVEPs can be recorded at a wide range of frequencies, in most studies the stimulus frequency (i.e., presentation rate) tends to be above 8–10 Hz. At these high frequencies, the interval between stimuli is substantially shorter than the duration of the response that follows an individual stimulus presented in isolation, so that responses to individual stimuli overlap. If the rate is above 10 Hz, the SSVEP is nearly sinusoidal (i.e., an externally driven oscillation), and some researchers consider this to be the prototypical case of an SSVEP response. Below this stimulation rate, responses to individual stimuli overlap but some features of the responses to each event remain preserved, such as responses at frequencies that are multiples of the stimulus frequency (Heinrich, 2010). Here we consider that what is critical for the definition of a response as an SSVEP is not the temporal frequency of the stimulus but rather the fact that the stimulus and the response are each *periodic*. SSVEPs have been recorded at very low frequencies (Eizenman et al., 1999; Norcia, Candy, Pettet, Vildavski, & Tyler, 2002); we will review several examples in what follows.

Because the SSVEP response is periodic, it is confined to a specific set of frequencies, and it is thus natural to analyze it in the frequency domain instead of the time domain. The stimulus frequency determines the response frequency content: The response spectrum has narrowband peaks at frequencies that are directly related to the stimulus frequency. To distinguish stimulus frequencies from response frequencies, we will use the following notation: A capital letter F will be used to refer to a stimulus frequency, and a lowercase italic letter f will be used to refer to a response frequency. This distinction in notation will become important when we discuss stimuli that contain more than one frequency (e.g., $F1$ and $F2$) and responses occurring at multiple harmonics of a given stimulus frequency (e.g., $1f$, $2f$, and $3f$).

The relationship between periodic signals in the frequency domain and their corresponding representation in the time domain is shown in Figure 1, with the first column showing the signal waveform in the time domain and the second column showing the spectrum, which is the corresponding representation of the signal in the frequency domain. The example in Figure 1a consists of the simplest case—a periodic signal consisting of a single sine wave. The sine wave shown has a frequency F of 2 Hz. In the time domain, there are two peaks and troughs over a period of 1 s. In the frequency domain (Figure 1b), the response consists of a single line (i.e., spectral component) at 2 Hz ($1f$).

An important concept in spectrum analysis is the notion of spectral resolution. Spectral resolution is the fineness of the bins on the frequency axis of the spectrum. The frequency resolution is inversely proportional to the duration of the electroencephalograph (EEG) segment that is transformed to the frequency domain. For example, the frequency domain representation of a 20-s duration periodic response has a frequency resolution of 1/20 s, i.e., 0.05 Hz, and this resolution is independent of the periodic stimulation frequency (see Bach & Meigen, 1999, for details on SSVEP spectral analysis techniques). The spectrum analysis requires that at least one full period of the response of interest be present. Spectrum resolution is important in determining the signal-to-noise ratio

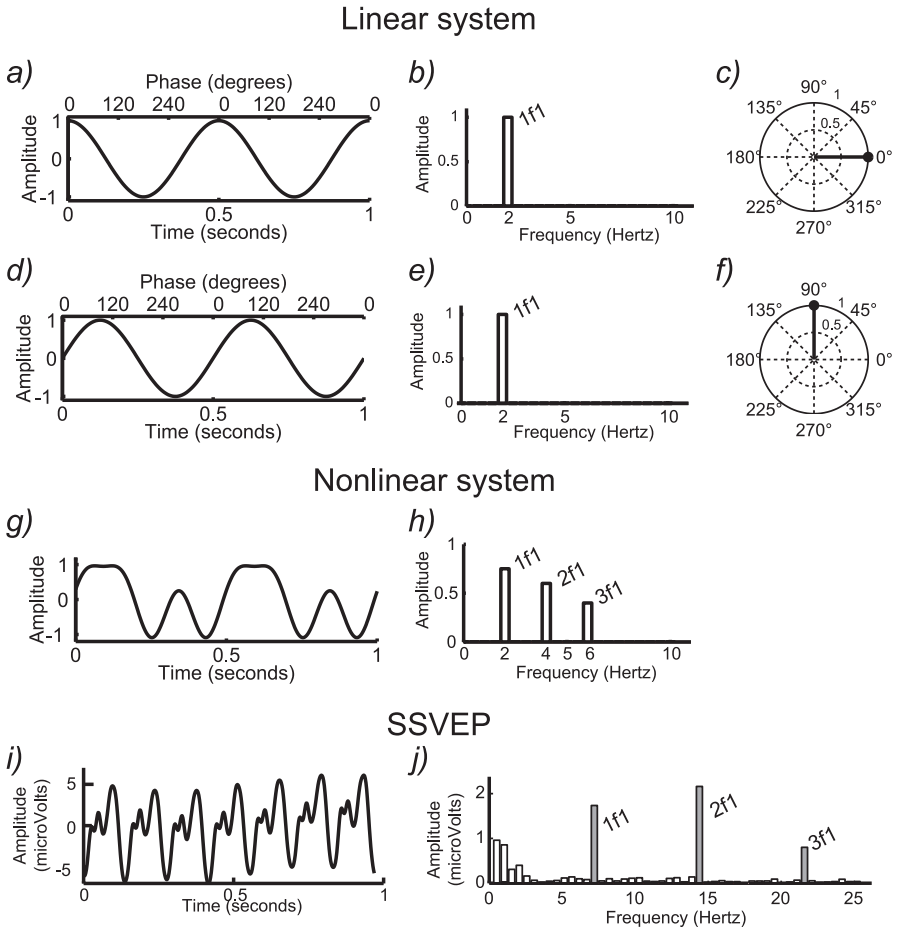

Figure 1. Conceptual illustration of steady-state responses in time and frequency domains. (a) Simulated purely sinusoidal response from a linear system in the time domain. (b) The corresponding response spectrum for the single-sine-wave response in (a). (c) Vector representation of amplitude and phase of the signal in (a). (d) Single sinusoidal response with a quarter-cycle delay relative to the response in (a). (e) The corresponding amplitude spectrum is the same as in (b) because the signal amplitude in (d) is the same as in (a). (f) The vector plot shows a response with the same amplitude as in (a), but with a phase shift of 90°. (g) Simulated multicomponent response of a nonlinear system in the time domain. (h) The more highly structured nonlinear response in the frequency domain contains multiple harmonics (1*f*, 2*f*, 3*f*). (i) Time-domain SSVEP with a stimulus frequency of 7.2 Hz. (j) The SSVEP response spectrum contains multiple harmonics (1*f*, 2*f*, 3*f*).

(SNR) of the measurement and in being able to separately analyze responses that have multiple frequency components in them (see Multiple periodic visual inputs).

In addition to response amplitude, SSVEPs have a second parameter: response phase. The phase value is related to processing delays in the visual system and is a composite of temporal integration times in the retina and cortex and temporal propagation delays between retina and cortex and between areas in cortex. Phase is a circular variable running over 360° or 2π radians. The response amplitude and phase can be represented as a vector in a polar coordinate system (see Figure 1c and f). The length of the vector codes the response amplitude, and the polar angle codes the response phase. In Figure 1, the origin for the phase parameter is at 3 o'clock, where the phase is 0. The waveform in Figure 1a has a phase of 0, consistent with it being a cosine wave with its peak at time 0. The next row (Figure 1d through f) shows another simulated response with the same amplitude but a different temporal delay. Here the delay corresponds to one quarter of a cycle (compare Figure 1a and c). The amplitude and frequency of the response are the same and thus the amplitude spectrum is identical (Figure 1b and e). In the vector representation, the phase has now shifted by 90° (Figure 1f), which directly corresponds to one quarter of the period of the sine wave in the time-domain plot. The relationship between phase and temporal delay is discussed in detail in Appendix 1.

SSVEP responses can contain activity not only at the stimulus frequency F but also at its harmonics. This occurs because either because the stimulus contains multiple temporal frequencies (as when a square-wave

temporal modulation profile is used) or the system is nonlinear, or both. A harmonically related response component is one that occurs at an exact integer multiple of the stimulus frequency—2*f*, 3*f*, and so on—where the use of a lowercase *f* indicates that what is being referred to is a response frequency rather than a stimulus frequency *F*.

The case of multiple response frequencies is illustrated with synthetic data in Figure 1g, where we again show a periodic signal that repeats exactly two times per second, as did the sine-wave signal in Figure 1a. This signal, however, contains additional frequency components that are readily apparent in the spectrum shown in Figure 1h. Here we see additional response components at 2 (2*f*) and 3 times (3*f*) the input frequency *F*. These higher harmonic components distort the shape of the time-domain waveform away from that of a single sine-wave profile.

If the visual stimulus is a perfect sine wave, it does not contain higher harmonics; if the visual response is linear, the response to this stimulus will be confined to the frequency bin corresponding to the stimulus frequency. Only the amplitude and/or phase of the response varies if the system is linear. In contrast, if the system is nonlinear, this will manifest in the presence of higher harmonic responses (for more details on nonlinearity in the SSVEP, see Multi-input interactions as an objective measurement of system nonlinearities and neural convergence). The nonlinear nature of the visual response is illustrated in Figure 1i, which shows data from an actual SSVEP recording where the stimulus comprised a sinusoidal modulation of contrast at a frequency *F* of 7.2 Hz. Here again, the time waveform is periodic but not sinusoidal, and the response spectrum thus contains narrow lines at exact integer multiples of the input frequency (Figure 1j). The presence of frequencies in the response (the output) that were not present in the stimulus (the input) indicates that the response of the visual system is due to the activity of nonlinear neural mechanisms.

In a real SSVEP recording, the signal of interest is inevitably contaminated by measurement noise. This measurement noise consists predominantly of additive EEG noise (Victor & Mast, 1991). The experimental noise is present over all frequencies in the spectrum (white bars in Figure 1j), with more noise in low frequencies and in specific broadband frequency ranges such as the alpha band (8–12 Hz; see, e.g., Klimesch, 2012). By contrast, the SSVEP signal that one seeks to isolate experimentally is confined to a set of narrow frequency bins that are directly related to the stimulus frequency. If the frequency resolution of the analysis is high, it has been shown that the SSVEP itself is very narrowband (Regan & Regan, 1989). This means that the SNR of the SSVEP can thus be very high, because only a small fraction of the noise—the noise that is present in the same bins as the response—is relevant (Regan, 1989). Appendix 2 provides technical details on statistical analysis procedures appropriate for determining when an SSVEP is present and distinguishable from the background noise. The appendices also discuss procedures for calculating error statistics on the SSVEP parameters.

One of the key questions in SSVEP recording is the choice of the stimulus frequency. In a seminal study, Regan (1966) reported a maximal response at about 10 Hz for luminance flicker. Subsequent studies have reported a similar (Fawcett, Barnes, Hillebrand, & Singh, 2004; Regan, 1989; Srinivasan, Bibi, & Nunez, 2006) or slightly higher (Hermann, 2001) frequency range. Typically, studies such as these have used low-level visual stimuli and recordings from medial occipital sites. However, the stimulation frequency that gives rise to the largest SSVEP response may depend on the kind of stimulus used and the recording site (Srinivasan et al., 2006). Under the hypothesis that the stimulation rate generating the largest SSVEP is inversely related to the time needed to fully process the stimulus, lower stimulation rates may be necessary to record SSVEPs generated by higher level visual processes, for instance the discrimination of complex stimuli such as faces (i.e., about 6 Hz; Alonso-Prieto, Belle, Liu-Shuang, Norcia, & Rossion, 2013). Relatively low frequencies can also be advantageous because, as we will see later, the phase of the response becomes interpretable (Appelbaum & Norcia, 2009; Cottereau, McKee, Ales, & Norcia, 2011).

In common practice, stimulus frequencies tend to be in the range of 3–20 Hz, but this is not a requirement for recording an SSVEP: Several studies have recorded extremely narrowband SSVEPs at very low frequencies (Alonso-Prieto et al., 2013; Norcia et al., 2002; see also Regan & Regan, 1988), while SSVEP components at fundamental frequencies up to 100 Hz have been reported (Herrmann, 2001). As noted already—and this is an important point—what is critical for the definition of a response as an SSVEP is not the temporal frequency of the stimulus but rather the fact that the stimulus and the response are each periodic.

The sweep VEP

One of the leading applications of the SSVEP has been the sweep VEP. In this paradigm, the SSVEP is measured in response to a stimulus that is parametrically varied (swept) over a range of values, rather than being presented at a fixed, unchanging value (Regan, 1973). The sweep VEP was first used for objective refraction: SSVEP amplitude was measured as the power of a lens was continuously varied (Regan, 1973). The best correcting lens power was taken as the one

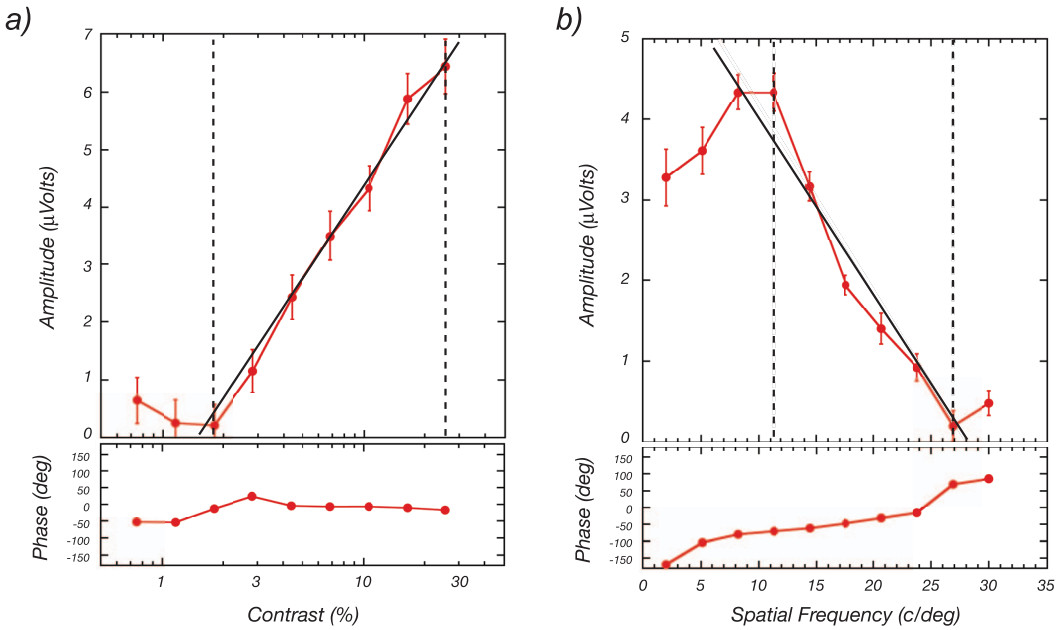

Figure 2. Contrast and spatial-frequency responses measured with the swept-parameter technique. (a) VEP amplitude and phase as a function of log contrast measured as the average of ten 10-s sweeps. (b) VEP amplitude and phase as a function of linear spatial frequency measured as the average of ten 10-s sweeps. See text for details.

that led to the largest SSVEP. The sweep VEP has since been mainly used to measure spatial acuity (Nelson, Kupersmith, Seiple, Weiss, & Carr, 1984; Norcia & Tyler, 1985; Regan, 1977; Tyler et al., 1979) and contrast sensitivity (Allen, Norcia, & Tyler, 1986; Nelson, Kupersmith, et al., 1984; Norcia, Tyler, & Hamer, 1990; Regan, 1975). Spatial acuity is measured by sweeping the spatial frequency (e.g., pattern size) of a high-contrast pattern over a wide range. Similarly, contrast sensitivity can be measured by varying the contrast of a fixed-spatial-frequency pattern over a wide range of contrast values.

Measurement of contrast response and spatial frequency tuning functions is illustrated in Figure 2. On the left is a contrast response function (solid red curve) that was measured by increasing the contrast of a binary noise pattern between 0.8% and 26% contrast while the pattern was exchanged with a blank field at F = 5.1 Hz. The sweeps each lasted 10 s, and the data are from the average of 10 of these 10-s trials. The response at 5.1 Hz increases systematically as contrast increases. As Campbell and colleagues (Campbell & Kulikowski, 1972; Campbell & Maffei, 1970) first noted, the SSVEP is a linear function of log stimulus contrast for a substantial range of suprathreshold contrasts, starting near psychophysical threshold. This behavior can be seen in the data of Figure 2a. Given this, a *sensory threshold* can be estimated from a linear extrapolation of the contrast response function to zero amplitude. The assumption here is that the evoked response will continue to decrease in the same fashion until it disappears entirely. The point at which this occurs is obscured by the background EEG. By regressing through the ambient noise level, one can estimate this point as a constant criterion (zero response). If one has access to several well-measured points on the response function, this estimation technique shows little bias (Norcia, Tyler, Hamer, & Wesemann, 1989).

The right panel of Figure 2 shows a spatial frequency tuning function measured over 2 to 30 c/°. Here the steps are linear, based on the fact that contrast sensitivity falls off linearly when plotted as log sensitivity versus linear spatial frequency (Tyler et al., 1979). Again, a threshold, which in this case reflects the participant's grating acuity, can be estimated by extrapolating the response function to zero amplitude. Sweep VEPs have proven to be useful for measuring acuity and contrast thresholds in a wide range of research and clinical contexts (Almoqbel, Leat, & Irving, 2008).

Stimulus symmetry leads to symmetrical SSVEP responses

In two of the actual SSVEP recordings discussed already (Figures 1i and 2a), the stimulus modulated in a *pattern onset/offset* mode, in which a spatially structured field (a random checkerboard) was alternated with a spatially uniform field (a gray field of the same mean luminance). It is intuitively simple that the visual system should have a large response after the transition from the uniform field to the patterned field but a

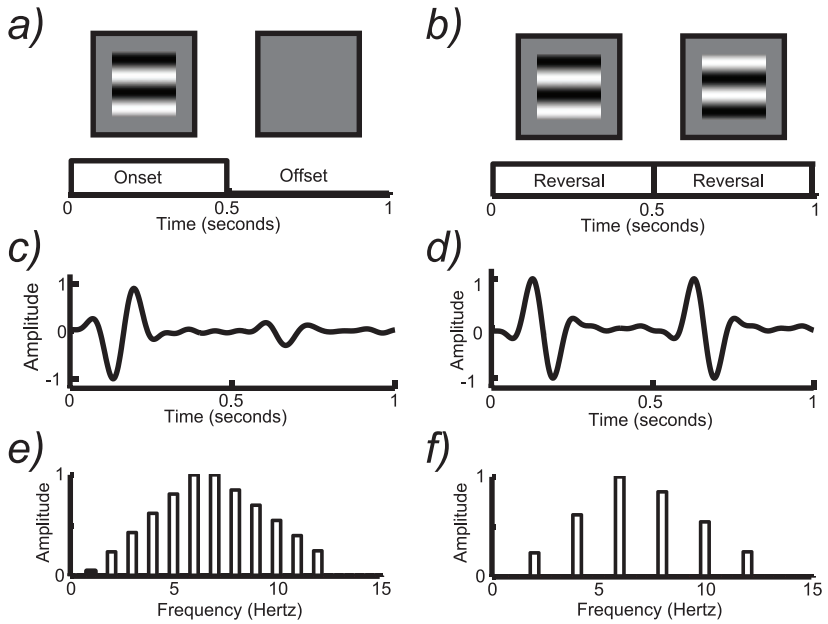

Figure 3. (a) Schematic illustration of the pattern onset/offset stimulation mode. Here a patterned field is alternated with a uniform field of the same mean luminance. (b) Schematic illustration of the pattern-reversal stimulation mode. Here the same pattern is presented in both phases, but with a 180° shift of spatial phase that causes bright bars to be exchanged for dark ones and vice versa. (c) Schematic illustration of one cycle of the response to pattern onset/offset consisting of a large response at pattern onset and a smaller response at offset. (d) Schematic illustration of one cycle of the response to pattern reversal. Here the response to each reversal event in the display is accompanied by an equal response. Note that the period of the response is now one half of the full stimulus cycle in (b). (e) The response spectrum of the pattern onset/offset response contains both odd (1*f*, 3*f*, etc.) and even (2*f*, 4*f*, etc.) harmonics of the stimulus frequency. (f) The response spectrum of the pattern-reversal response contains only even harmonics (2*f*, 4*f*, etc.) of the stimulus frequency.

small(er) one at its offset. This is illustrated schematically in Figure 3a. The pattern of large/small responses repeats at the stimulus repetition rate (indicated by the brackets), and therefore a response is present at the fundamental frequency ($f = 1/T$) and possibly higher harmonics (2*f*, 3*f*, etc.; see Figure 3e). The direct connection between stimulus frequency and response frequency, plus a simple asymmetry consideration (onset is not equivalent to offset), can be generalized to any periodic stimulus containing the onset and offset of patterns going from simple ones such as checkerboards (Spekreijse, van der Tweel, & Zuidema, 1973) to more complex ones such as faces (Ales, Farzin, Rossion, & Norcia, 2012; Rossion & Boremanse, 2011).

Another common presentation mode for SSVEPs is *pattern reversal* (see Figure 3b). In this presentation mode, a pattern (e.g., a checkerboard or grating) alternates between states in which the luminance of bright elements shifts to an equivalent dark value and vice versa. In this way the mean luminance of the pattern is constant and only the contrast of the pattern changes at the stimulation rate. Pattern reversal thus has translational symmetry—one spatial phase of the pattern reversal is simply a (spatial) translation of the other. Pattern reversal stimulation is often referred to as counterphase modulation to reflect this property. The two spatial alternations comprising the pattern reversal stimulus evoke equivalent neural population responses, i.e., there are just as many of the same kinds of neurons that respond to one phase of the stimulus as the other. Because the two phases of the stimulus activate the same number and type of neurons, the response to each reversal is the same, and this leads to an EEG spectrum that contains only even harmonics (2*f*, 4*f*, 6*f*, etc.; Cobb, Morton, & Ettlinger, 1967; Millodot & Riggs, 1970). Pattern reversal stimuli are sometimes referred to by the number of reversals per second they contain (e.g., eight reversals/s for 4-Hz stimulation). There are two pattern reversals per cycle of the stimulus, and the response is largest at the pattern reversal frequency when high reversal rates (~6 Hz and above) are used. For consistency, it is useful to refer to the frequency of a pattern reversal stimulus as the frequency at which the stimulus returns to its original state (e.g., 1 Hz in the example of Figure 3b) and refer to the response harmonics (e.g., $2f = 2$ Hz) as being multiples of this rate rather than the pattern alternation rate (see spectrum in Figure 3f).

The concept of translational symmetry in the stimulus leading to translational symmetry in the response can be generalized to more complex patterns, as will be described later in Generalizations of the

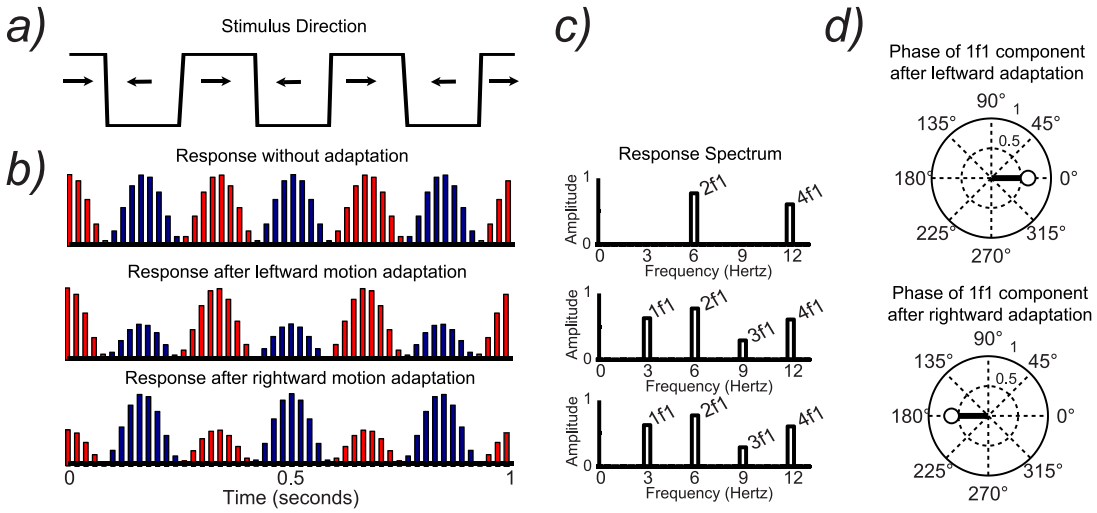

Figure 4. (a) Schematic illustration of a stimulus that changes direction at 3 Hz. (b) Schematic illustration of hypothetical neural responses tuned to rightward motion (red) and leftward motion (blue). Shown before and after adaptation to different directions of motion. (c) Response spectrum generated from the neural responses in (b). (d) Phase of the 1*f*1 component after adaptation to different directions of motion.

pattern onset–offset VEP. The conceptual relationship between symmetry/asymmetry in stimuli and responses and odd and even harmonics exists due to symmetry properties of the Fourier transform—asymmetry is encoded in the odd harmonics and symmetry in the even harmonics.

Breaking symmetry by adaptation: Uncovering tuned populations

The normal relationship between symmetric stimuli and symmetric population responses can be perturbed experimentally; this is useful for uncovering information about the tuning of the neurons in the underlying population. A concrete example comes from studies of the motion-processing system. At early stages of the visual pathway, starting especially in V1, single cells become selective for direction of motion (Hubel & Wiesel, 1965, 1968), and each direction of motion is represented by roughly equivalent numbers of direction-tuned cells. Thus when a stimulus changes direction, the population response after each direction change is approximately the same. This is illustrated schematically in Figure 4. Figure 4a depicts a stimulus that moves leftward for 167 ms followed by rightward motion for 167 ms (for a total stimulus-defined repetition period of 333 ms, or $F = 3$ Hz). This stimulus evokes identical responses for the leftward and the rightward motion (Figure 4b, first row). Because of these identical responses, the repetition rate of the measured response is not 3 but 6 Hz, or a 167-ms period (Figure 4c). This frequency doubling is generated because even though independent sets of neurons tuned for each direction motion are present in the cortex, their summed population response measured at the scalp is not different for left and right directions of motion. Information about the underlying neural tuning (i.e., that there are separate populations of neurons for leftward and rightward motion) has thus been lost.

It is possible to uncover the presence of underlying tuned populations by using selective adaptation (Ales & Norcia, 2009; Hoffmann, Unsold, & Bach, 2001; Tyler & Kaitz, 1977). In the unadapted state, as just noted, both populations respond equally well to each direction and the summed population response at the scalp results in a frequency doubling of the response. However, prolonged exposure to one direction of motion reduces the responsiveness of direction-selective cells tuned to the exposed direction of motion (Priebe, Lampl, & Ferster, 2010), a process known as direction-specific adaptation.

After adaptation to a leftward motion, the responses of individually tuned neurons to leftward motion from the population are reduced, resulting in an imbalance in the overall response to the periodic stimulus. In Figure 4b, the unadapted response has six equal responses to three cycles of the input, an even multiple of the input frequency. In contrast, when a population is adapted, the response for the adapted direction is reduced (Figure 4b). This imbalanced response creates responses at odd multiples of the input frequency (Figure 4c).

The production of odd harmonics after adaptation, while consistent with direction-specific adaptation, does not directly show a difference in response for different directions of adaptation, as the odd harmonic ampli-

tude, which is a scalar quantity, cannot specify a direction. It is possible to use the other parameter of the SSVEP—its phase—to definitively identify direction-specific adaptation (Ales & Norcia, 2009). The imbalanced adapted response has a different temporal sequence, either strong/weak or weak/strong, depending on which of the adapting stimuli was presented (leftward vs. rightward in this example). The different temporal ordering results in a 180° phase difference in the odd harmonic components (e.g., a shift by one half of the period of the response; Figure 4d). The presence of odd harmonics that are 180° phase-shifted after adapting to two selected adapters is thus a strong diagnostic criterion—at the population level—of direction-selective cells. Adaptation can thus be used to reveal an underlying tuning property that is not apparent in the SSVEP recorded under unadapted conditions.

Generalizations of the pattern onset–offset VEP

If we adopt a more general definition of pattern, it is possible to extend the concepts of pattern reversal and pattern onset–offset VEPs to more complex stimuli. The first recorded pattern onset–offset VEPs modulated stimulus contrast: Pattern onset consisted of the replacement of a blank field with a high-contrast patterned field of the same mean luminance. Because the mean luminance was constant over time, the evoked response could be attributed specifically to mechanisms sensitive to spatial contrast (Spekreijse et al., 1973). The logic here is general and very useful in terms of controlling what aspect of visual processing is being measured by the SSVEP. The argument goes as follows: There is some lower level stimulus attribute—in this case luminance—that the experimenter wishes to control for in order to isolate responses to a higher level attribute, e.g., spatial contrast. In the original studies, because the blank field had the same mean luminance as the patterned field, any evoked response had to be the result of pattern- or contrast-specific mechanisms rather than luminance processes. This simple notion can be generalized to more complex stimuli by ensuring that the on and off phases of the stimulus are equivalent on some set of low-level features that the experimenter wishes to control for, but differ on some higher level "pattern" that does not need to be controlled for.

An early example of a higher level pattern onset–offset response is the so-called texture-segmentation VEP (Bach & Meigen, 1992; Lamme, Van Dijk, & Spekreijse, 1992). In a texture-segmentation VEP, a figure or pattern is created by texture rather than luminance discontinuities; this has been useful for studying image segmentation properties underlying object perception. A review of the older literature is available (Bach & Meigen, 1998).

A variant of the texture-segmentation paradigm is shown in Figure 5. Here pattern onset consisted of the appearance of a texture-defined disk region from an otherwise uniform texture field (Appelbaum, Ales, & Norcia, 2012). The off state consisted of a 13° field covered with static, one-dimensional contrast noise. The on state was created by rotating the texture by 180° at 1 Hz within a central 3° disk. This modulation caused the central disk to either mismatch with the background, creating a perceptually segmented state (Figure 5a, top left panel), or match exactly, blending into a perceptually uniform one-dimensional texture (Figure 5a, top right panel).

The responses to the segmented/uniform test condition are show in the frequency domain in Figure 5b and in the time domain in Figure 5c. The frequency spectrum for the uniform-segmented display consists of a series of narrow spikes at 1-Hz intervals, i.e., at 1*f*, 2*f*, 3*f*, 4*f*, etc. The gray bands indicate the responses at even harmonics of the 1-Hz stimulus frequency. The corresponding time-domain waveform shows a larger response at pattern onset (which occurred at 500 ms in the plot) than at pattern offset (at 0 ms). This asymmetry in the response (onset bigger than offset) manifests in the spectrum as the presence of odd harmonics.

To show that image segmentation rather than some other low-level cue is driving the odd harmonic responses, a control condition in which the local texture changes within the disk were the same was used. Critically, these image transients were not associated with changes in the segmentation state of the display. To produce equivalent local feature changes without a change in global organization, the texture inside the disk region was cut from a different random texture sample, and the disk region thus never matched the background after rotation by 180°. By comparing the responses in the top and bottom panels of Figure 5b, we can see that the even harmonic components are very similar in the two conditions, but that the uniform-segmented response contains multiple odd harmonic components that are absent from the segmented-segmented response. The odd harmonics are thus specific to the global segmentation state of the display. The even harmonics comprise responses due to local contrast changes within the central disk region, and these are equivalent in the two stimuli. The time-domain waveforms reflect these properties: The response to the segmented-segmented display consists of two nearly identical transient responses, consistent with the fact that the two image states are perceptually identical in this condition as well as being physically identical within the disk region. The figure- segmentation-specific activity can be measured directly from the

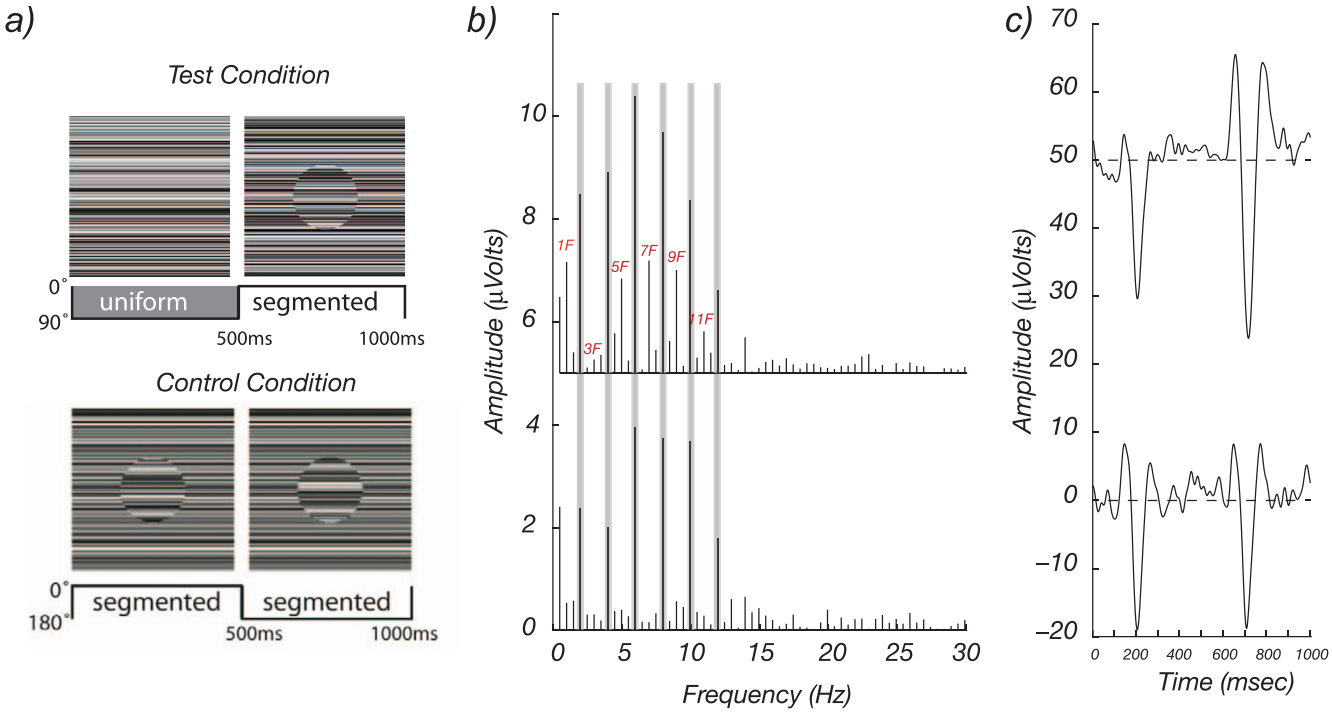

Figure 5. SSVEPs to higher level stimuli contain both figure-segmentation-related (odd harmonic) and nonfigure-related (even harmonic) responses. (a) Test condition: A spatially segmented display created by texture discontinuity cues was alternated with a spatially uniform field at 1 Hz. Control condition: The same local stimulus change, a 180° rotation of the texture within the disk region, does not change the segmentation state because the texture inside the disk never matches that of the background. (b) Top panel: The response spectrum from the test condition contains both odd and even harmonics. Bottom panel: The response spectrum from the control condition contains only even harmonics. (c) Top panel: The cycle average time course for the test condition shows larger responses to onset of the segmented image (at 500 ms) than to offset (0 ms). Bottom panel: Control-condition responses are equivalent after image transient at 500 and 0 ms.

odd harmonics of the test condition. In this example, the figure-segmentation related activity can be isolated from a single stimulus condition—the Test condition—rather than through a more time-consuming and error-prone process of subtracting test and control conditions.

Other examples of generalized pattern onset–offset responses come from the onset of twofold symmetry in random-dot patterns (Norcia et al., 2002), the onset of orientation structure in Glass patterns (Pei, Pettet, Vildavski, & Norcia, 2005), the onset of collinearity in arrays of Gabor patches (Norcia, Pei, et al., 2005; Norcia, Sampath, Hou, & Pettet, 2005), the onset of objects defined by binocular disparity (Cottereau et al., 2011; Cottereau, McKee, Ales, & Norcia, 2012; Cottereau, McKee, & Norcia, 2012), and the onset of phase correlations across orientation and scale in face or object images (Ales et al., 2012; Farzin, Hou, & Norcia, 2012). In each of these cases, it is possible to design a set of images in which the spatial structure of the local contrast elements is randomized (the off state of the pattern). These off images can be exchanged with a set of on images that have a comparable set of local elements but in which a higher level of structure has been imposed on the local elements. Through careful matching of the local contrast changes between on and off phases, responses to this level of structure are rendered symmetric for the two transitions, and thus these responses are projected onto the even harmonics of the stimulus frequency. By design, the higher order structure differs across stimulus phases, producing a difference between the two transitions (off to on and on to off), yielding odd harmonic responses.

SSVEP responses reflecting higher level visual processes

Historically, the primary applications of SSVEPs have been in studies of lower level visual processes, as just described, and attention (see Multiple temporal inputs for the study of visual attention). Some researchers have concluded that because an SSVEP response is often maximal over medial occipital electrode sites (typically Oz), it originates mainly from the primary visual cortex (Müller et al., 1997; Di Russo et al., 2007) and that "the" SSVEP is primarily a tool for studying sensory processes and low-level vision

(Regan, 1989). However, SSVEPs vary according to frequency and the type of stimuli presented (Alonso-Prieto et al., 2013), and as we discuss later, the SSVEP approach can be used to study higher level visual processes (i.e., object, face, or visual-scene perception). We will distinguish two approaches in which the SSVEP has been used to study higher level processes, one indirect and the other direct. An indirect approach is one in which the influence of a higher level process is revealed through its modulatory effect on an SSVEP generated by a low-level process, and measured over low-level visual areas. Direct approaches frequency-tag the high-level process itself.

Indirect approaches

Silberstein et al. (1990) have developed an indirect SSVEP approach to study high-level (visual) processes such as vigilance. This approach consists of the superimposition of a rapid (13-Hz) sinusoidal contrast modulation (45%) on a static visual stimulus that engages the participant in a cognitive task. Using this approach, a frontal SSVEP amplitude increase associated with the hold period of a working-memory task has been identified (Ellis, Silberstein, & Nathan, 2006; Perlstein et al., 2003; Silberstein, Nunez, Pipingas, Harris, & Danieli, 2001). Similarly, Peterson et al. (2014) have recently used the SSVEP approach to tag individual stimulus elements as they are encoded into working memory. By demonstrating that SSVEP amplitudes are larger for remembered items, relative to those that were forgotten, this finding illustrates how neural resources allocated during memory encoding directly contribute to working-memory capacity limits.

In another study, a 13-Hz flicker was superimposed on static, dynamic, and scrambled images of faces, and the SSVEP response was shown to be different across these three conditions (Mayes, Pipingas, Silberstein, & Johnston, 2009). This approach is indirect because the visual stimulus of interest is always present and unmodulated, but the stimulus modulation that actually generates the SSVEP is of a low-level feature (45% contrast modulation). The measured alterations of this low-level response are presumably due to diversion of attention towards the high-level feature (Hindi Attar, Andersen, & Muller, 2010). In another indirect approach, complex visual stimuli have been presented at periodic rates of 10 Hz or more (Gruss, Wieser, Schweinberger, & Keil, 2012; Kaspar, Hassler, Martens, Trujillo-Barreto, & Gruber, 2010; Keil et al., 2003; McTeague, Shumen, Wieser, Lang, & Keil, 2011; Moratti, Keil, & Stolarova, 2004). In these studies, the exact same image—namely a visual scene, an isolated object, or a face—appears and disappears at a fixed rate in a given trial of a few seconds. The SSVEP response obtained is compared across different kinds of stimuli flickering at the same rate in other trials (for instance, by comparing the SSVEP obtained to affective and nonaffective pictures). In this approach, the visual stimulus appears and disappears at a periodic rate from a background that is not equalized for low-level features (e.g., contrast). Thus the SSVEP response contains a mixture of low-level (e.g., populations of neurons responding to the change of contrast) and high-level (e.g., populations of shape-related neurons) visual responses. Moreover, in these studies the SSVEP is typically observed and recorded on medial occipital sites (around electrode Oz), suggesting that it essentially reflects low-level visual processes. The *modulation* of the periodic responses at Oz, by affective content for instance, may be secondary to sustained/unmodulated feedback from higher level areas that code the high-level content rather than being a direct time-locking to the high-level stimulus information.

Direct approaches

We consider an approach to higher level processing to be direct when the paradigm triggers the higher level process at the tagging frequency and when this higher level activity can be isolated from low-level visual processes either in the design or in the analysis. For instance, the sweep VEP described earlier has been extended to higher level vision by generalizing the pattern onset/offset VEP (Ales et al., 2012). In that study, a face-containing image was alternated at 3 Hz with an image whose phase spectrum had been randomized (Figure 6a). This process leaves the power spectrum the same between the two images, and thus mechanisms such as local filters that only measure power spectral content cannot distinguish the two stimulus states. Figure 6b shows a portion of the amplitude spectrum of the response to the alternation between intact and scrambled face images. The left panel shows the spectrum at Oz. Here the response is dominated by the second harmonic at 6 Hz. By contrast, the response over the right occipitotemporal cortex is dominated by the first harmonic (3 Hz). This is consistent with the face-selective responses observed over the right occipitotemporal cortex in standard ERP studies of the N170 component (Rossion & Jacques, 2011; for reviews, see Bentin, Allison, Puce, Perez, & McCarthy, 1996).

The visibility of the face images was then varied by progressive undoing of the phase scrambling over a series of 20 equally spaced steps during a 20-s sweep sequence. At the beginning of the sequence, a scrambled image alternated with another scrambled image at 3 Hz, leading to a symmetrical response at 6 Hz only (second harmonic) on medial occipital sites. After a certain level of descrambling, the face is perceived and the spatial asymmetry of the stimulus

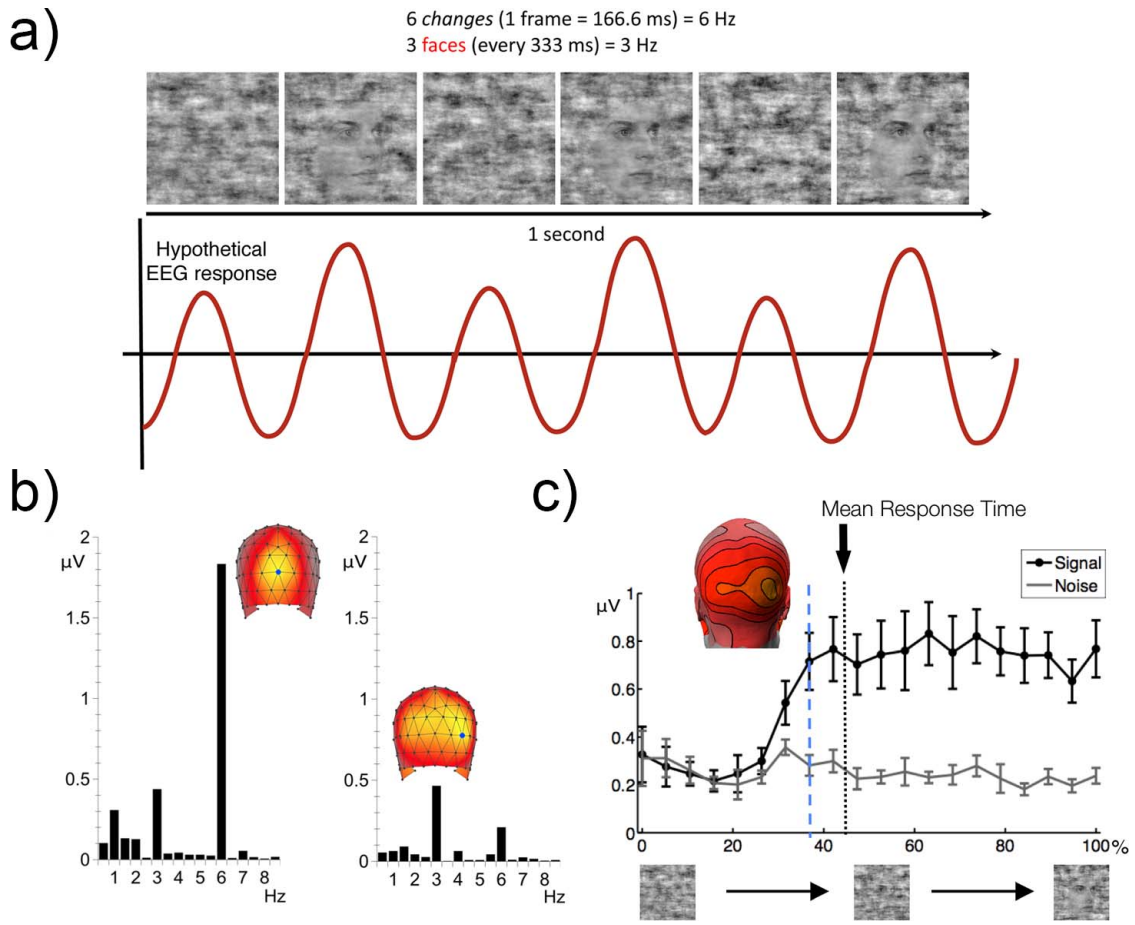

Figure 6. Face-detection sweep VEP (adapted from Ales et al., 2012). (a) Six images are presented per second, with every other image being (partially) intact and the others scrambled. Over a 20-s trial, a new level of phase randomization is presented over a series of 20 equal steps of phase coherence. The power spectrum is constant during the stimulation. Populations of neurons coding for faces independent of low-level information should respond exactly 3 times/s, the rate at which partially intact faces are presented. (b) Grand-averaged ($N = 10$) EEG spectrum elicited by the stimulation depicted in (a). This stimulation leads to a response dominated by 6 Hz (2*f*) at medial occipital sites (left panel). A 3-Hz (1*f*) response dominates the recording over right occipitotemporal sites, reflecting face perception (right panel). (c) SSVEP voltage versus stimulus coherence (0% to 100%) at 3 Hz (filled squares). The 3-Hz signal is compared to the activity in the neighboring frequency bins of the spectrum (e.g., 2.5 and 3.5 Hz), which serve as a noise baseline during the stimulus sequence that evolves from a fully phase-scrambled face to a clearly visible face stimulus. Face detection emerges in the EEG at about 35% of phase coherence, before the behavioral report of face detection (arrow). The topographical map is extracted at the level of the blue dotted line (about 35% of phase coherence), indicating the emergence of face detection over right occipitotemporal electrode sites.

alternation leads to a robust 3-Hz (first harmonic) response, which can be taken as an objective signature of face detection (see Figure 6c). The first harmonic (3 Hz) emerged abruptly between 30% and 35% phase coherence of the face and was most prominent on right occipitotemporal sites. Thresholds for face detection were estimated reliably in single participants from 15 trials, or on each of the 15 individual face trials. The SSVEP-derived thresholds correlated with (i.e., predicted) the concurrently measured perceptual face-detection thresholds. This first application of the sweep VEP approach to high-level vision provides a sensitive and objective method that could be used to measure and compare visual perception thresholds for various object shapes and levels of categorization in different human populations, including infants and individuals with developmental delay.

Another example of temporally modulating high-order image structure comes from a study of visual processing of 3-D pictorial cues that arise from shading relationships in images (Hou, Pettet, Vildavski, & Norcia, 2006). The researchers developed a stimulus paradigm in which the spatial relationships between shading information could be made to be consistent with either a 3-D interpretation in which the perceived structure varied in apparent depth across the image in one state or a flat plane in another. This stimulus thus comprised a generalized onset/

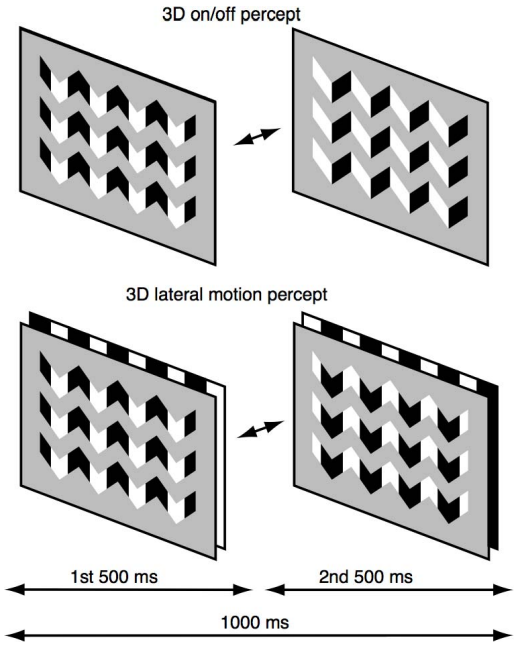

Figure 7. Bistable display creating two different depth interpretations of the same image. The top image depicts the perceptual state during which the observer perceives a change in depth structure. In this state, the display alternates between a surface that appears to be undulating in depth and another surface that is flat. In the second perceptual state (bottom panel), the display is organized into two layers—an aperture through which a grating is seen moving left and right in a fixed depth plane located behind the aperture.

offset stimulus in which the on state had a different perceived depth structure than the off state: The on state appeared 3-D and the off state appeared flat. This perceptual interpretation of the stimulus is illustrated in the top panels of Figure 7. Critically for the study, after viewing the display for a long period of time, a second percept became apparent—one in which the two states of the display had equivalent depth interpretations. Instead of the appearance of the display alternating between flat and undulating in depth, the display appeared to consist of a symmetric left/right movement of a flat pattern seen through a set of cutout apertures (illustrated schematically in the bottom panels of Figure 7).

In order to characterize the properties of the SSVEP corresponding to the two perceptual interpretations, the observers were given a button to indicate which state was dominant. These perceptual labels were then use to form separate data sets that were spectrum analyzed. Due to the asymmetric perceptual interpretation, alternations between the on and off stimulus states at $F = 1$ Hz led to the generation of strong odd harmonic responses (i.e., $1f$ [1 Hz] and $3f$ [3 Hz]). When the display was perceived as a flat plane moving left and right, the relative amplitude of the odd and even harmonics shifted towards being more dominated by the even harmonics. The conclusion from this experiment is that the SSVEP reads out a perceptually relevant population response, including whether states of the stimulus generate responses in the same or different populations. It should also be noted here that the SSVEP to this higher level stimulus was recorded at a very low stimulus frequency (1 Hz).

Higher level processes can also be investigated by periodic onset and offset of the visual stimulus against its background, by changing the higher level content of the stimulus at every cycle. Rossion and Boremanse (2011) presented different face pictures to human observers for about 1 min at a fixed rate of 3.5 Hz (Figure 8a). High-SNR EEG responses were confined to 3.5 Hz and its harmonics (Figure 8b). Although this response contains a mixture of low- and high-level visual processes, contrasting it to the response obtained when the exact same face picture was repeated at the same rate allowed the isolation of the higher level process of interest—individual face discrimination. A large repetition suppression effect—i.e., reduction of the SSVEP when the exact same face is repeated—is illustrated in Figure 8b. The differential SSVEP response was obtained despite significant changes of stimulus size at every stimulation cycle and was maximal over the right occipitotemporal cortex rather than medial occipital sites (i.e., Oz). In a subsequent study, this differential SSVEP was reduced when the face stimuli were presented upside down or contrast reversed (Rossion, Prieto, Boremanse, Kuefner, & Van Belle, 2012), two manipulations known to reduce the efficiency of individual face discrimination (e.g., Freire, Lee, & Symons, 2000; Russell, Sinha, Biederman, & Nederhouser, 2006). The advantage of the SSVEP approach in this paradigm is that it provides a robust implicit measure of individual face discrimination in a few minutes (Rossion, 2014). Interestingly, in order to provide this high-level visual discrimination measure, not only must the high- level content of the stimulus change at every cycle, but the response has to be measured over high-level visual areas. The frequency also matters: The SSVEP response decreases significantly over the occipitotemporal cortex at rates above 8 Hz, and the differential response cannot be obtained at such high frequencies (Alonso-Prieto et al., 2013).

This section has introduced several general principles that underlie the SSVEP paradigm. The first general principle is that a temporally periodic stimulus leads to a narrowband response in the frequency domain. The second is that because the visual system is nonlinear, responses will often be present at multiple harmonics of the stimulus frequency. The third is that considerations of sym-

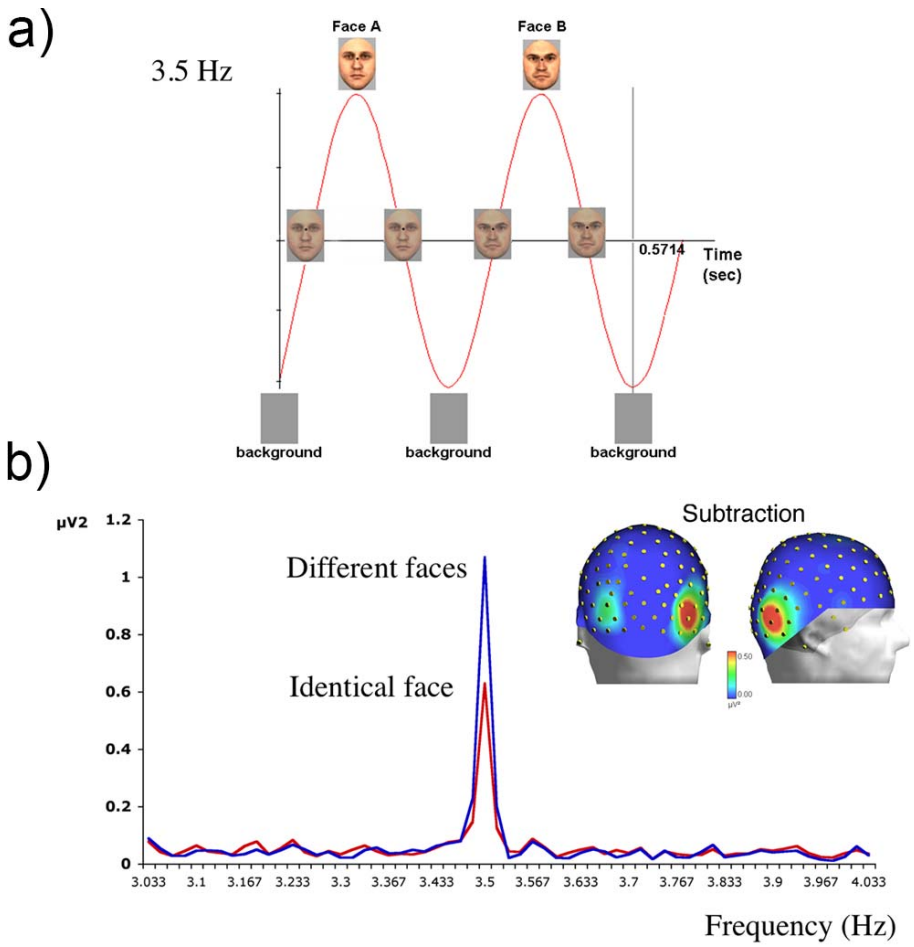

Figure 8. (a) Sinusoidal contrast modulation (0%–100%) of different face identities at a periodic rate of 3.5 Hz (Rossion & Boremanse, 2011). A new face appears every stimulus cycle. (b) EEG power spectrum and topographical maps of the difference between different-faces and same-face conditions, as obtained following a single trial of 70 s of stimulation at 3.5 Hz (grand-averaged data over 12 participants; Rossion & Boremanse, 2011). Stimulation with mixed-identity faces leads to a larger response than does repetitive stimulation with the same identity.

metry in stimuli reflect themselves in the particular set of harmonic responses that are observed in the recorded spectrum. Asymmetric stimuli are expected to generate responses with strong odd harmonic components, while symmetric stimuli, in most cases, will lead to responses that are dominated by even harmonics. These symmetry relationships are reflected in pattern onset/offset stimuli, which are asymmetric, and pattern reversal stimuli, which are symmetric. As a rule, asymmetric stimuli lead to asymmetric responses and symmetric stimuli lead to symmetric responses, with corresponding reflections in the relative strength of odd and even harmonics in the response spectrum. These normal relationships can be perturbed by adaptation and perceptual interpretation in ways that usefully relate to the underlying encoding mechanisms. Finally, the notion of pattern onset and offset can be generalized to higher order stimuli.

Multiple periodic visual inputs

In the previous section we described studies that have used EEG to track the neural responses to a single periodic visual input. In this section, we will describe one of the most important virtues of the SSVEP approach: its ability to measure responses from different visual processes simultaneously through the use of multiple stimulation frequencies. The fundamental insight here is that because the stimulus input frequencies strictly determine the response frequencies, it is possible to recover responses to several simultaneously presented stimuli via spectrum analysis if each one has a distinct frequency. This method was introduced by Regan (Regan & Cartwright, 1970; Regan & Heron, 1969) in the context of visual field mapping (i.e., perimetry) and was dubbed frequency tagging by Tononi, Srinivasan, Russell, and Edelman (1998). By careful choice of stimulation frequencies,

this form of multi-input stimulation allows an experimenter to assign tags to different stimuli and recover the respective responses in the frequency bins that correspond to each of the stimulation frequencies. Conceptually, this allows for the extraction of evoked responses from populations of cells that are selective to each of the unique input frequencies, even if they are spatially overlapping or embedded within the same stimulus element.

This section will cover applications of multiple-input frequency tagging in studies using multiple frequency inputs embedded in the same time sequence, multiple stimuli presented simultaneously, or stimuli comprising more than one "part," as well as important applications of the tagging approach to the study of attention. Multi-input interactions as an objective measurement of system nonlinearities and neural convergence will cover a second and very fundamental advantage of the multi-input approach: the ability to model the dynamic properties of the nonlinear processes through measurement of the nonlinear interactions between multiple input frequencies.

Multiple temporal inputs: Embedded frequency paradigms

Local/global processing in hierarchical stimuli

Many visual stimuli contain structure at multiple levels of complexity, and visual analysis of these patterns may reflect this feature hierarchy. A powerful way of separating responses driven by global structure from those driven by local structure is to dissociate the rates at which global and local structures are updated in the stimulus. The first example of this approach was the VEP generated by dynamic random-dot correllograms and stereograms (Julesz & Kropfl, 1982; Julesz, Kropfl, & Petrig, 1980). In these studies, the researchers wished to separate evoked responses to a higher level feature (binocular correlation or binocular disparity) from those to a lower level one (monocular image cues). To accomplish this goal, a binocularly matched set of dots was presented to each eye on a given display frame. Several frames later, a new set of matching dots was presented that portrayed the same global image. After several more updates of the monocular images, the global structure was changed (e.g., from uncorrelated to correlated or from crossed to uncrossed disparity). Purely monocular responses were generated at the rapid rate of monocular image updating. Because the successive monocular updates were temporally uncorrelated within an eye, there was no information coding the binocular state of the image at this frequency. By contrast, a purely binocular response was recorded at the frequency at which the binocular (global) status of the image was changed.

Subsequent researchers used this two-frequency tagging of local and global structure to measure orientation and direction selectivity in infants (Braddick, Atkinson, & Wattam-Bell, 1986; Wattam-Bell, 1991). For instance, Braddick et al. (1986) isolated an orientation-specific response by using two embedded frequency rates of stimulus change in a sequence. The phase of a grating changed at a fast rate of 25 Hz, generating a 25-Hz SSVEP (in adults subjects who participated in that experiment), and the orientation of the grating changed every three stimuli, i.e., at a rate of 8.3 Hz. While the orientation response was present in adults and in infants a few weeks old, it was absent in newborns, showing that orientation-specific cortical activity is not present at birth but develops early in infancy (see Braddick, Birtles, Wattam-Bell, & Atkinson, 2005, for more recent work on motion- and orientation-specific cortical responses in infancy).

An advantage of this approach is that the processes of interest, e.g., contrast change and orientation selectivity, can be assessed simultaneously by referring to the distinct frequency rates associated with their different update rates (i.e., tags). By measuring these processes simultaneously, it is possible to both shorten the overall duration of the experiment and, importantly, avoid complications that arise from attentional fluctuations or other types of state changes that arise when comparing responses from separate processes measured at different times (i.e., subtraction).

More recently, similar embedded-frequency designs have been used to study coherent-motion responses (Aspell, Tanskanen, & Hurlbert, 2005; Handel, Lutzenberger, Thier, & Haarmeier, 2007; Hou, Pettet, & Norcia, 2008; Lam et al., 2000; Nakamura et al., 2003; Niedeggen & Wist, 1999; Wattam-Bell et al., 2010), responses to global orientation structure in dynamic Glass and line patterns (Palomares, Ales, Wade, Cottereau, & Norcia, 2012; Wattam-Bell et al., 2010), texture segmentation (Ales, Appelbaum, Cottereau, & Norcia, 2013), and binocular disparity processing (Cottereau, Ales, & Norcia, 2014b; Cottereau et al., 2011; Cottereau, McKee, Ales, et al., 2012; Cottereau, McKee, & Norcia, 2012).

Figure 9 illustrates the embedded-frequency paradigm with a coherent-motion- processing example. In displays of this type, many small dots are presented on a given stimulus frame. The trajectory of the dots is subject to a rule that is applied to all dots. Because the rule is applied to all of the dots, the motion is *coherent* across the display. In this example, the coherently moving dots were constrained to move in trajectories along concentric arcs around fixation (see Figure 9a for a schematic illustration). In the first 500 ms of the 1-Hz display cycle, the dots all moved either clockwise or counterclockwise (e.g., CW, CCW, CW, CCW, . . .), jumping 17 arcmin in the prescribed direction every 33

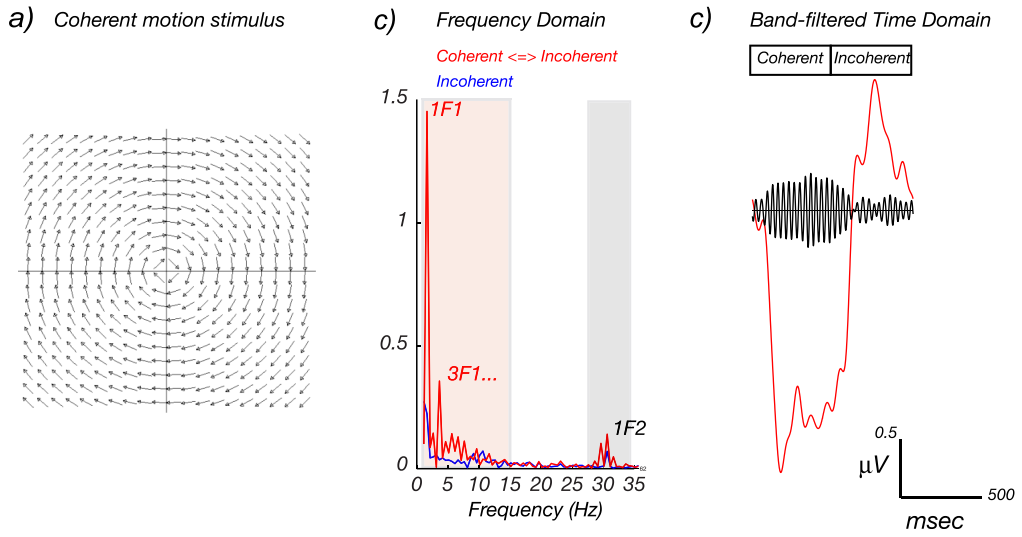

Figure 9. Hierarchical SSVEPs to a coherent-motion stimulus. (a) Schematic illustration of the coherent-motion onset/offset VEP stimulus in the coherent-motion phase. The position of a large number of bright dots is shifted, either in a consistent fashion for each dot (coherent global motion) or in a random fashion (incoherent local motion), at a rapid rate ($F2 = 30$ Hz). The display also alternates between coherent and incoherent states, but at a much lower frequency ($F1 = 1$ Hz). (b) In the frequency domain, a response is visible at the rapid 30-Hz update rate of the individual dots ($f2$) and at 1 Hz and its harmonics ($1f1$, $2f1$, $3f1$, . . .), which is the rate at which the global motion structure changes. Responses are also visible at $1f1 \pm 1f2$ (see Multi-input interactions as an objective measurement of system nonlinearities and neural convergence). (c) The cycle average of the coherent-motion onset/offset response in the time domain shows a mixture of long- and short-period fluctuations. The red curve is synthesized from the signals at $nf1$, where n ranges up to 15; see red shading in (b). The black curve is synthesized from responses over a band of frequencies centered on $1f2$, as indicated by the gray shading in (b). Figure derived from Hou et al. (2008).

ms (30 Hz). In the second 500 ms of the display cycle, the position of each dot was shifted by 17 arcmin in a random direction. Coherent motion thus appeared and disappeared at 1 Hz; this is the first frequency in the display ($F1$). Because the display also contained local contrast and motion transients at 30 Hz, there is a second frequency ($F2$) in the display. The spectrum of the response (Figure 9b) contains several narrowband peaks that are harmonics of the 1-Hz global motion-update rate. The first harmonic of the global update frequency is labeled $1f1$ and is by far the largest evoked response component in the data. A higher harmonic response associated with the global update frequency $F1$ occurs at $3f1$. The blue curve shows data for a control condition in which the dots were moving randomly in both halves of the 1-s stimulus cycle. Because of this, no coherent motion was seen, but locally random motion was visible. In this case, there are no peaks at the harmonics of $F1$, but there is a spike in the spectrum at the dot-update frequency ($1f2$, or 30 Hz).

Figure 9c shows time-domain reconstructions of the coherent-motion response. The red time course was created by inverse-Fourier transforming the response components between 1 and 15 Hz of data from the coherent-motion onset-offset VEP (red-shaded region of Figure 9b) and setting all other response frequencies to zero. The time course of the response resembles a 1-Hz sine wave, consistent with the dominance of the $1f1$ component in the spectrum. The black curve was reconstructed from frequencies around the local motion-update rate of the stimulus (gray-shaded region of Figure 9b). A rapidly oscillating response (30 Hz) can be seen that is maximal during the period of coherent motion (the first 500 ms of the display).

In studies of this type, the frequencies of the local and global update rates can differ by a factor of 10 or more. Because of this wide separation between stimulation frequencies, and because of the relative sluggishness of global evoked responses, both the odd and even harmonics of the global update response rate are interpretable as being due to the modulation of global structure. The responses to the local structure are generated at a much higher frequency and do not overlap with the global responses that are generated at low frequencies. There is thus a clear separation of brain responses to these attributes of the stimulus.

In paradigms of this type, the frequency tags are associated with stimulus attributes that exist at conceptually different hierarchical levels (e.g., high-frequency tags are associated with local attributes and low-frequency tags with global attributes). The level of analysis done by the brain on the stimulus is thus tagged by frequency, and one can then ask how different brain regions process the different stimulus

attributes (for an example of this approach, see Palomares et al., 2012).

Temporally embedded frequency rates and periodic oddball paradigms

Embedding an infrequent stimulus of one type at random within a stream of frequent stimuli of another type has been used extensively to study feature discrimination in the auditory and visual domains (Naatanen, 1990; Pazo-Alvarez, Cadaveira, & Amenedo, 2003), as well as target selection (P3) mechanisms (the P3 response; Sutton, Braren, Zubin, & John, 1965). In the mismatch negativity (MMN) paradigm, averaged responses to the frequent and infrequent stimuli are subtracted from one another, and the difference potential is used to indicate that the two stimulus classes represented by the frequent and infrequent stimuli have been discriminated. A similar set of questions can be addressed with the SSVEP by embedding the rare oddball stimulus in a rapid periodic train of standards, with the oddball frequency being a submultiple of the faster rate of the standard (Heinrich, Mell, & Bach, 2009). This approach has been used to study face individuation—the ability to discriminate one individual from another. Liu-Shuang, Norcia, and Rossion (2014) presented their participants with 60-s sequences containing a base face (A) presented at a 5.8-Hz frequency rate. Different oddball faces (B, C, D, ...) were introduced at fixed intervals (every fifth stimuli = 5.88 Hz/5 = 1.18 Hz: AAAABAAAACAAAAD...; see Figure10a). Significant responses were found in the EEG spectrum at 1.18 Hz and harmonics (e.g., $2f1/5 = 2.35$ Hz) over the right occipitotemporal cortex (Figure 10b). This high-level discrimination response was present in all participants after a few minutes of recording, for both color and grayscale faces, providing a robust neural measure of face discrimination in individual brains. Face inversion or contrast reversal did not affect the basic 5.88-Hz periodic response over medial occipital channels. However, these manipulations substantially reduced the 1.18-Hz oddball discrimination response over the right occipitotemporal region, indicating that this response reflects high-level processes that are partly face specific. The oddball response obtained with fast periodic visual stimulation has several advantages over a traditional visual MMN paradigm with faces (e.g., Kimura, Kondo, Ohira, & Schroger, 2012): (a) It is identified objectively at the frequency of the oddball and its harmonics, (b) the response can be measured in only a few minutes thanks to the high SNR of the approach, and (c) there is no need for a subtraction between two conditions (targets and standards) to isolate the discrimination response. This approach has been most recently extended to the categorization of natural face images (Rossion et al., 2015) and word/nonword discrimination (Lochy, Van Belle, & Rossion, 2014). It should prove useful in future studies that seek to identify visual discrimination responses in patient populations and infants.

Multiple temporal inputs and the tagging of spatial locations and perceptual organizations

Vision is inherently a spatial sense, and therefore many of the questions at the core of visual neuroscience address the representation and manipulation of visual space in the nervous system. The multi-input SSVEP approach is particularly well suited for addressing these questions and was, in fact, first applied to questions of spatial-location processing (Regan & Cartwright, 1970; Regan & Heron, 1969). The fundamental insight here is that because the stimulus input frequencies strictly determine the response frequencies, it is possible to recover responses to several simultaneously presented stimuli via spectrum analysis if each one has a distinct frequency. In the following section we will discuss research that has used the multi-input approach to study neural mechanisms that underlie spatial vision, scene perception, and perceptual organization.

Locations/perimetry

Visual function can vary over the spatial extent of the visual field as a result of normal aging or various medical conditions, such as glaucoma, stroke, or brain tumors. Visual field testing is therefore widely used by clinicians and researchers to diagnose and study the spatial characteristics of human vision. The multi-input SSVEP approach has long served as an important tool in this pursuit. The first use of multiple frequency-tagged inputs was to record responses generated by the left and right visual hemifields simultaneously, rather than sequentially as in traditional clinical perimetry (Regan & Cartwright, 1970; Regan & Heron, 1969). Modern versions have included up to 17 regions (Abdullah et al., 2012). The approach has been successful in dramatically reducing the time needed for visual field assessment. The primary limitation of this approach is that as the number of tagged locations goes up, either the range of temporal frequencies in the display must increase or the bandwidth of the recording must decrease. The disadvantage of increasing the range of frequencies is that sensitivity of the different parts of the visual field may itself depend on temporal frequency, and thus temporal-frequency differences are confounded with spatial position. The disadvantage of decreasing the frequency bandwidth to accommodate more stimuli in a given range of temporal frequency is that the

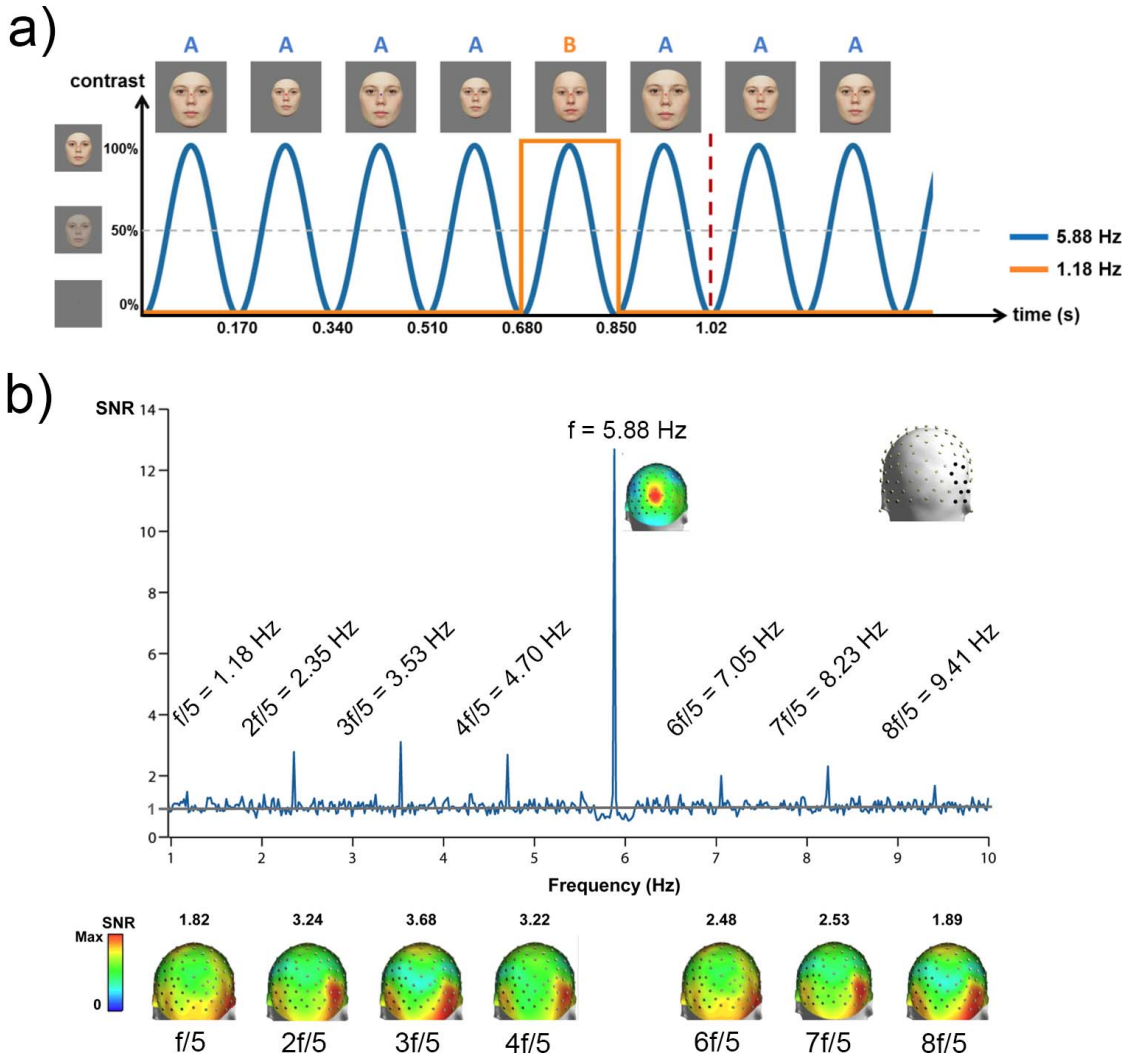

Figure 10. The periodic oddball paradigm (Heinrich et al., 2009) extended to face stimuli by Liu-Shuang et al. (2014). (a) Faces are presented by sinusoidal contrast modulation at a rate of 5.88 Hz. At fixed intervals of every fifth base face of a single individual (5.88/5 Hz = 1.18 Hz), a set of different-identity oddball faces are presented. (b) SNR spectrum of the right occipitotemporal ROI for faces (grand average, four sequences of 60 s for each of 12 participants). The channels composing this ROI are indicated with black dots on the 3-D head in the upper right. On the SNR spectrum, only significant oddball responses are labeled. Note that while the 1.18-Hz response appears small, it has an SNR of 1.49, corresponding to a 49% response increase. Below the spectrum, 3-D topographies of each harmonic response are displayed. The largest oddball response is observed over the occipitotemporal regions, with a clear right hemisphere lateralization.

recording time must be increased commensurately. This approach, in addition to being useful for perimetry, has been a major focus of brain–computer interface research (Vialatte, Maurice, Dauwels, & Cichocki, 2010; Zhu, Bieger, Garcia Molina, & Aarts, 2010). Tagging of locations for studying spatial attention will be described in detail in Multiple temporal inputs for the study of visual attention.

Figure–ground segregation networks

Visual-scene perception relies on the segregation of objects from their supporting backgrounds—so-called figure–ground segmentation. The multi-input SSVEP approach lends itself favorably to the study of scene segmentation because different regions of the scene can be tagged with different temporal frequencies. In such designs, the response spectrum can be evaluated at harmonics of the various region frequency tags to isolate the cortical activity that is specific to figure versus background processing. Researchers have used this approach to achieve a very precise experimental control of visual space and test the spatial dependency of cortical networks underlying figure–ground segmentation.

Using this two-input approach, Appelbaum and colleagues carried out a series of studies identifying and

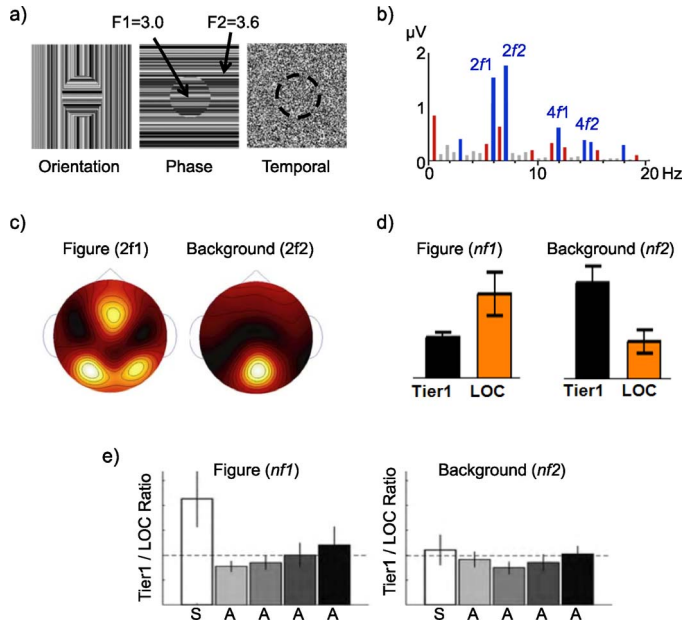

Figure 11. Figure–ground segmentation studies of Appelbaum and colleagues (Appelbaum et al., 2010; Appelbaum et al., 2006, 2008). (a) Stimuli in these studies were comprised of two-frequency textures in which a central circular figure alternated at 3.0 Hz (*f*1) and the surround alternated at 3.6 Hz (*f*2). These stimuli were composed of three different texture cues: orientation modulation of one-dimensional textures, phase modulation of one-dimensional textures, and white noise. (b) Example EEG response spectra, with significant responses colored (blue are harmonics of the figure and background, red are IM terms). (c) Topographic response distributions of second harmonics show distinct patterns. (d) Source-localized ROI profiles show a double dissociation, wherein the figure response (summed over harmonics) is large in the LOC and the background response is larger in first-tier retinotopic areas V1–V3. This pattern is present for all three cues, figure sizes of 2° and 5°, and figures presented at different retinal eccentricities. (e) Figure selectivity, as a ratio of retinotopic to LOC response, is only present for the surrounded stimulus (S), which shows a figure surrounded by a background, not for ambiguous (A) stimuli that do not have this Gestalt arrangement.

investigating distinct cortical networks responsible for the processing of both figure and background regions. In the first of these studies (Appelbaum, Wade, Vildavski, Pettet, & Norcia, 2006) texture cues were modulated such that a central circular region alternated at 3.0 Hz while the surrounding texture alternated at 3.6 Hz (Figure 11a). Using different orientation, phase, and temporally defined white-noise texture cues, the researchers found that the evoked responses (Figure 11b) attributed to the background produced a single medial occipital response, but the figure regions consistently produced bilateral occipital responses (Figure 11c).

To define which cortical areas were involved in these two networks, a source-imaging approach based on functional MRI (fMRI) was used to show that activity related to the figure region, but not the background region, was preferentially routed between first-tier visual areas (V1–V3) and the lateral occipital cortex (LOC), a visual brain area known from fMRI studies to demonstrate strong object selectivity (Malach et al., 1995). Here, separate fMRI mapping sessions were used to define the visual areas and a minimum-norm, distributed-source model was used to estimate each participant's SSVEP in these regions of interest (ROIs; for a summary of the technique, see Cottereau, Ales, & Norcia, 2014a). A separate network, extending from the first tier through more dorsal areas, responded preferentially to the background region (Figure 11d).

In a subsequent study, Appelbaum, Ales, Cottereau, and Norcia (2010) extended the analysis of the stimulus preferences of the LOC by including several ambiguous figure–ground arrangements in order to determine whether the Gestalt property of surroundedness (i.e., a smaller figure on a larger background) was necessary to selectively activate the LOC. For this purpose they compared the magnitude of frequency-tagged activity in the object-selective LOC across several different spatial arrangements that portrayed surrounded figure–ground arrangements (S) or contained two spatially symmetric, temporally modulating regions that were ambiguous (A) in their figure–ground arrangement. Using this approach, they found that replacing the classic surrounded figure–ground organization with a symmetric one greatly reduced the specificity of the LOC response to the different image regions (i.e., produced a Tier1/LOC ratio near 1; Figure 11e). They concluded that the surrounded Gestalt organization therefore exerts a powerful controlling effect on the routing of information about image regions through first-tier areas and object-selective cortex. Collectively, these studies illustrate how the multi-input SSVEP can be used to investigate the mechanisms supporting the early stages of visual-scene processing. As discussed in subsequent sections, these multi-input, figure–ground designs can also be used to study spatial interactions (Appelbaum et al., 2008) and spatial attention (Appelbaum & Norcia, 2009).

Perceptual bistability and perceptual organization

A particularly powerful means of studying the relationship between perception and neural activity involves the use of a physical stimulus that has more than one perceptual interpretation. A hallmark feature of such stimuli is perceptual bistability: The perceptual interpretations alternate stochastically over time. Binocular rivalry, the fluctuation in perception that occurs when different images are presented to the two eyes, is

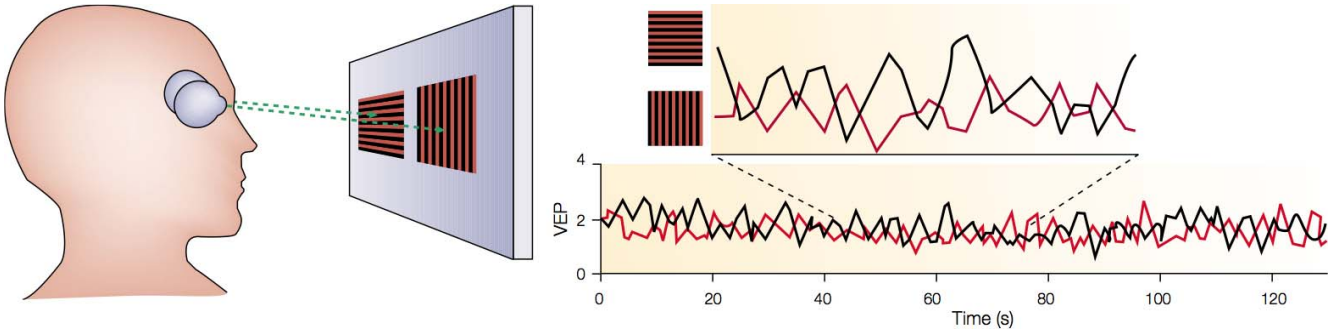

Figure 12. Frequency tagging used to measure rivalry in real time. The participant viewed a vertical grating oscillating at 5 Hz in one eye and a horizontal grating oscillating at 6 Hz in the other eye. Because the two stimuli were not binocularly fusable, they alternated in perceptual dominance. The curves on the right plot the time course of the evoked responses at the separate eye-tagging frequencies. The two time courses alternate in counterphase in sync with the perceptual alterations. From Blake and Logothetis (2002).

probably the best-studied bistable percept (for a review, see Blake & Logothetis, 2002). SSVEPs provide a very powerful way to determine *in real time* the alternations in perceptual dominance across the eyes. As early as 1964, Lansing reported an intermittent suppression of the SSVEP under conditions promoting rivalry. That work established that the amplitude at the flicker frequency of a monocular grating was sometimes suppressed during the presentation of a constant grating in the other eye. This intermittent suppression coincided well with the subject's perceived suppression of the flickering grating by the constant pattern. Building on this approach, Brown and Norcia (1997) developed a gold-standard technique to detect perceptual fluctuations in binocular rivalry. In that study, observers viewed dichoptically two differently oriented gratings that oscillated in counterphase at distinct frequencies ($F1 = 5.5$ Hz for the grating viewed by the left eye and $F2 = 6.6$ Hz for the grating viewed by the right eye; see Figure 12).

This stimulus produced strong SSVEPs over occipital electrodes at frequencies that were twice the two input frequencies ($2f1$ and $2f2$). Fourier analysis revealed that the amplitudes at these frequencies were negatively correlated between the two eyes (i.e., when the amplitude at the frequency associated with one grating was large, the response associated with the other grating was invariably small). Moreover, these modulations were tightly phase-locked to the observers' perceptual reports of dominance and suppression (i.e., the grating associated with the frequency of the highest amplitude was the one that was perceived). This approach therefore permits a determination of which image a subject perceives without a behavioral report and can thus be used to measure rivalry in various populations such as infants and animal subjects. The Brown and Norcia (1997) study had several follow-ups that aimed at investigating the neural correlates of perceptual dominance (Cosmelli et al., 2004; Srinivasan, Russell, Edelman, & Tononi, 1999; Sutoyo & Srinivasan, 2009; Tononi et al., 1998), the influence of emotional stimuli on rivalry (Alpers, Ruhleder, Walz, Muhlberger, & Pauli, 2005), and the relationship between attention and binocular rivalry (Zhang, Jamison, Engel, He, & He, 2011).

Beyond binocular rivalry, other types of multistable stimuli have been used in SSVEP designs in order to relate neural activity to perception. Most notably, Parkkonen, Andersson, Hamalainen, and Hari (2008) used a modified Rubin face–vase illusion in which the face and vase regions were tagged with dynamic white noise at two different frequencies. Using this design and magnetoencephalographic (MEG) recording, they demonstrated that activity in the early visual cortex covaried with the perceptual states reported by the observers, indicating cortical loci which the visual system uses to achieve object-level representations.

Multiple temporal inputs for the study of visual attention

Attention is an essential neurobiological function that allows an organism to select the most important stimuli in the environment for enhanced neural processing. Because at any moment there is more information in the environment than can be processed, efficient attentional control is regarded as a critical cognitive faculty by which to filter out irrelevant distractions and focus on the stimuli that are most likely to lead to successful behaviors. Attention is not, however, a unitary construct or mechanism, but rather a set of interrelated processing schemas that are applied to many perceptual and cognitive operations (Chun, Golomb, & Turk-Browne, 2011). A major goal of vision science has been to identify the core behavioral processes and neural mechanisms that constitute the diverse taxonomy of internal (endogenous) and exter-

nal (exogenous) attention. Over the last two decades, the use of SSVEP designs has provided substantial insight.

The SSVEP is particularly well suited to attention-research questions, as it provides a high-SNR measure of neural activity that can be unambiguously associated with specific external stimuli, even when multiple stimuli are present at the same time. Importantly, it allows monitoring of responses made to stimuli that are outside of the focus of attention, something that is difficult to do with behavioral methods. Moreover, the SSVEP can be flexibly deployed over a number of configurations, including the tagging of both spatially distinct and spatially overlapping stimuli. In light of these attributes, the SSVEP approach has gained possibly its greatest utility in studies that have addressed the cognitive and neural mechanisms underlying volitional attention in human beings.

In the following section we review some of the major contributions that SSVEP studies have made to the understanding the cognitive and neural mechanisms of selective attention. Additional descriptions of several of these studies can also be found elsewhere (Andersen, Muller, & Hillyard, 2012).

Frequency tagging as a means to study processes inside and outside of the focus of spatial attention

Frequency tagging makes it possible to monitor the response to multiple stimuli that are simultaneously visible. This feature of the SSVEP makes it possible to measure the effects of allocating attention to spatial location even for stimuli that are outside of the focus of conscious attention. In the first application of the SSVEP to spatial attention (Morgan, Hansen, & Hillyard, 1996), two strings of alphanumeric characters were presented in the left and right visual hemifields (Figure 13). The participants' task was to fixate a central marker and to report the presence of a single digit among a series of letters in one or the other string as indicated by a spatial cue. The character strings were displayed on top of a small flickering rectangle presented at 8.6 Hz in one hemifield and 12 Hz in the other. The flickering rectangles were irrelevant to the task but were used to generate SSVEPs that reported the effect of spatial attention to the cued and uncued streams. The SSVEP was larger to the attended location than to the simultaneously recorded unattended location. A follow-up study linked this SSVEP effect to blood-oxygen-level dependent activations in fusiform and lateral occipital/temporal areas (Hillyard et al., 1997).

Following this early work, Muller, Picton, et al. (1998) showed selective amplitude enhancements for task-relevant, frequency-tagged features (color changes) at spatially cued locations. Since these initial reports, there have been many applications of and variations on this basic design. While an enhancement of SSVEP amplitude with spatial attention is the most common result, there have been exceptions (Ding, Sperling, & Srinivasan, 2006; see discussions in Andersen, Muller, & Hillyard, 2012; Toffanin, de Jong, Johnson, & Martens, 2009).

The spatial distribution of attention

Frequency tagging also provides a useful means to study the spatial distribution of attention. One of the first questions addressed in SSVEP spatial-attention studies was whether the focus of attention comprised a unitary spotlight. The first test of this idea used a concentric organization of tags, with one tag being centrally fixated and the other tag extending concentrically around it (Muller & Hubner, 2002). A series of small capital letters was presented over the central tag (frequency $F1 = 7$ or 11.67 Hz), and a series of large capital letters was present for the surrounding tag (frequency $F2 = 11.67$ or 7 Hz). Participants were asked to detect targets within one or the other stream. The response to the central tag was not enhanced by attention to the concentric surround, suggesting that the focus of attention could be shaped like a doughnut. This work was extended and confirmed (Muller, Malinowski, Gruber, & Hillyard, 2003) using a display with four independently tagged locations arranged on a line. The participants were cued to attend to the end locations. The SSVEP recorded at the intervening locations was no larger than that recorded for unattended locations in the opposite hemifield, indicating that the focus of attention can be split to at least two locations.

Subsequently, SSVEPs have been used to study how attention serves to modulate processing when the focus of attention is concentrated on items within the same visual hemifield versus when it is split between hemifields. First, as shown by Malinowski, Fuchs, and Muller (2007), SSVEP amplitudes and behavioral effects are reduced, but still present, when all stimuli are displayed within the same hemifield. More recently, Stormer, Alvarez, and Cavanagh (2014) used a hybrid SSVEP and P3 design to show that attention primarily serves to modulate early visual processing when it is divided across hemifields (yielding virtually no within-hemifield attentional effect), whereas higher level processes indexed by the P3 ERP component are not limited by such visual-hemifield constraints. Together, these studies illustrate that the nature of spatial attention is imposed by competition within and between hemifield cortical maps that occur at various stages of the visual processing hierarchy.

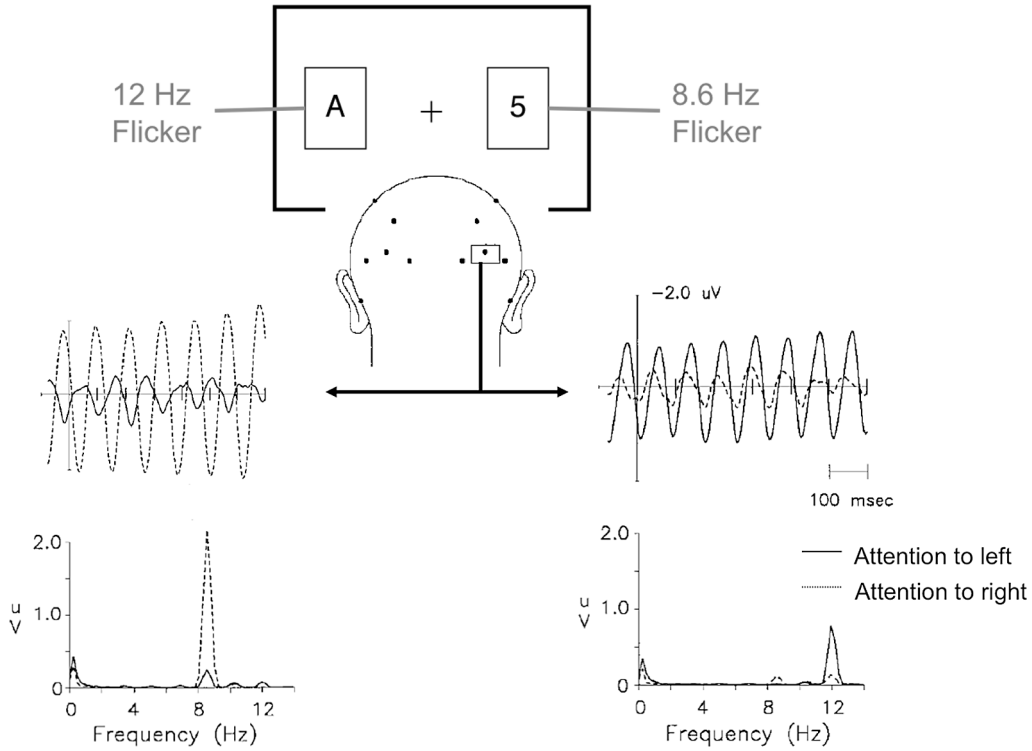

Figure 13. Figure adapted from the first SSVEP spatial-attention study (Morgan et al., 1996). Two strings of alphanumeric characters are presented in the left and right visual hemifields. The participants' task is to fixate a central marker and to report the presence of a single digit among a series of letters in one or the other string, as indicated by a spatial cue. The character strings are displayed on top of a small flickering rectangle presented at 8.6 Hz in one hemifield and 12 Hz in the other. The flickering rectangles are irrelevant to the task but were used to generate SSVEPs that reported the effect of spatial attention to the cued and uncued streams. The SSVEP, represented here in the time domain and in the frequency domain, was larger to the attended location than to the simultaneously recorded unattended location. Left bottom spectrum: Paying attention to the right increases the 8.6-Hz response, as compared to the condition where attention is on the left. Right bottom panel: Paying attention to the left increases the 12-Hz response, as compared to the condition where attention is on the right. Note that the responses are not presented on a single spectrum, since the analysis is performed on time windows that are integers of 8.6 Hz (displayed on the left) or 12 Hz (on the right).

The time course of spatial attention

Due to the high SNR of the SSVEP, it is possible to measure reliable frequency-tagged responses over short time windows (e.g., 500–1000 ms). Through sliding these windows progressively in time over successive portions of a data record, as in the sweep VEP (see earlier), it has been possible to study the temporal evolution of cued spatial attention. Using this approach, Muller, Teder-Salejarvi, and Hillyard (1998) linked the time course of spatially cued attention to a contemporaneous emergence of accurate target discrimination at newly cued locations. Moreover, observers who could switch attention more quickly had faster amplitude changes in the SSVEP (Belmonte, 1998), indicating a strong functional link between behavioral outcomes and neural signals measured by the SSVEP.

The underlying mechanism by which the SSVEP is modified by spatial attention has been addressed in several studies. Di Russo, Spinelli, and Morrone (2001) reported that spatial attention increased the slope of the SSVEP contrast response function, an effect known as response gain. A similar effect was also reported by Kim, Grabowecky, Paller, Muthu, and Suzuki (2007). Lauritzen, Ales, and Wade (2010) used fMRI to define a set of visual-area ROIs and combined this with cortical source-modeling techniques to show that spatial attention produced a response gain effect in V1, human middle temporal (hMT), and intraparietal sulcus ROIs, but a contrast gain effect (leftward shift of the contrast response function) in the V4 ROI. In that study, behavioral sensitivity correlated with activity in V1, hMT, and intraparietal sulcus ROIs, where response gain effects were found, but not in the V4 ROI, where the contrast gain effect occurred. Many SSVEP studies of spatial attention have compared responses from attended and unattended stimuli. However, the effect of spatial attention on the SSVEP is not inherently all-or-nothing—the magnitude of attentional modulation of the frequency-tagged SSVEP scales with the amount of attention paid to competing items (Toffanin et al., 2009).

Spatial attention has also been reported to increase the trial-by-trial synchrony of the SSVEP (Kim et al., 2007). However, because the increased synchrony in that study was also accompanied by an increase in response amplitude, it is not clear whether the increase in synchrony was due to a genuine increase in synchronous neuronal firing or was due to the higher SNR of the evoked response in the attended conditions (Andersen, Muller, & Hillyard, 2012). Increased SNR would cause the phase of the evoked response to be determined more by the evoked response and less by additive EEG background noise. A more recent study (Kashiwase, Matsumiya, Kuriki, & Shioiri, 2012) found that increases in intratrial phase coherence can occur earlier in time than increases in response amplitude, which is stronger evidence that spatial attention can effect response synchronization or reliability independent of changes in response amplitude. A puzzling aspect of that study, however, is that the measured effects on response synchrony and amplitude occurred after a significant fraction of the behavioral responses were executed, and thus the functional significance of this effect remains unclear.

Nonspatial attention

The multi-input SSVEP studies already discussed provide compelling evidence that volitional attention operates on spatially distinct regions of a scene to modulate neural processing in an adaptive, goal-oriented manner. Ample evidence also exists that attention can operate in a nonspatial manner to enhance processing of particular visual features such as color, orientation, or direction of motion. Because the SSVEP can be obtained from multiple overlapping stimuli, this method has been particularly useful in elucidating the neural mechanisms underlying such feature-based attention.

Pei, Pettet, and Norcia (2002) were the first to demonstrate nonspatial attentional effects with the SSVEP. In their study, a series of 16 crosses were formed out of vertical and horizontal bars (see Figure 14, top). Because the question here was about feature processing rather than spatial-location processing, it was important to use temporal frequencies that were low enough for the features to be seen distinctly and not blurred. Therefore, the vertical and horizontal bars were made to oscillate locally at two different, but very close temporal frequencies (counterbalanced at 2.4 and 3.0 Hz). By using bars of differing luminance that generated occlusion cues, the researchers were able to assign different depth orders (in front or behind), such that attentional selection could be made based on these depth cues but not on spatial location. Using this design, they found that attention increased the amplitude of the second harmonic of the response, and that the amplitude of this harmonic coded the depth order of the stimuli. The fourth harmonic was indifferent to the depth-order cue and was not affected by attention (see Figure 14, bottom panels). These results suggested that attention operated after depth-order relationships, such as those used to parse overlapping objects on the basis of their surface relationships, had been extracted. The study showed not only that attention can modulate neural processing in a spatially nonspecific manner but that this modulation acts after a 3-D interpretation of the scene has been made.

Following this work, Chen, Seth, Gally, and Edelman (2003) recorded steady-state MEG responses to superimposed counterphase-flickering red and green, vertical and horizontal gratings. In this design, participants were asked to maintain sustained attention to either the vertical or horizontal grating and to detect a brief, transient change in the width of the central bars. The authors found that when participants were instructed to report changes in the width of the central three bars, the SSVEP at the corresponding stimulus frequency was enhanced relative to that of the unattended grating. However, when the participants were instructed to report changes to just the center bar, the attended SSVEP was suppressed. This study provided further evidence for the modulatory role of nonspatial attention.

Beginning in 2006, Muller, Andersen, and Hillyard conducted a series of elegant studies aimed at dissociating the influence of attention to features and feature conjunctions from the influence of spatial attention. These studies utilized overlapping fields of randomly moving red and blue colored (or in some cases achromatic) dots that were modulated at distinct frequencies (Figure 15). In the first of these studies (Muller et al., 2006), participants were cued to attend one of the colored dot fields to detect the occurrence of a brief period of coherent motion, while ignoring similar events in the other, unattended stream. Using this design revealed a robust enhancement of the SSVEP amplitude for the attended stream that was maximal over occipital recording sites, localized to early visual areas V1–V3, and not attributable to selection of either the motion transient or the different flicker frequencies. Following from this initial study, the researchers next set out to chart the time course of these feature-based attention effects. Using a similar design, Andersen and Muller (2010) introduced a brief cue that oriented the participants to attend either the red or the blue dot fields and detect a transient motion change in the newly attended stream. They observed an initial enhancement of the SSVEP amplitude to the attended stimulus stream, beginning at about 220 ms after the attention-directing cue. This modulation was followed by a subsequent suppression of the SSVEP to the unattended stimulus, beginning at roughly 360 ms.

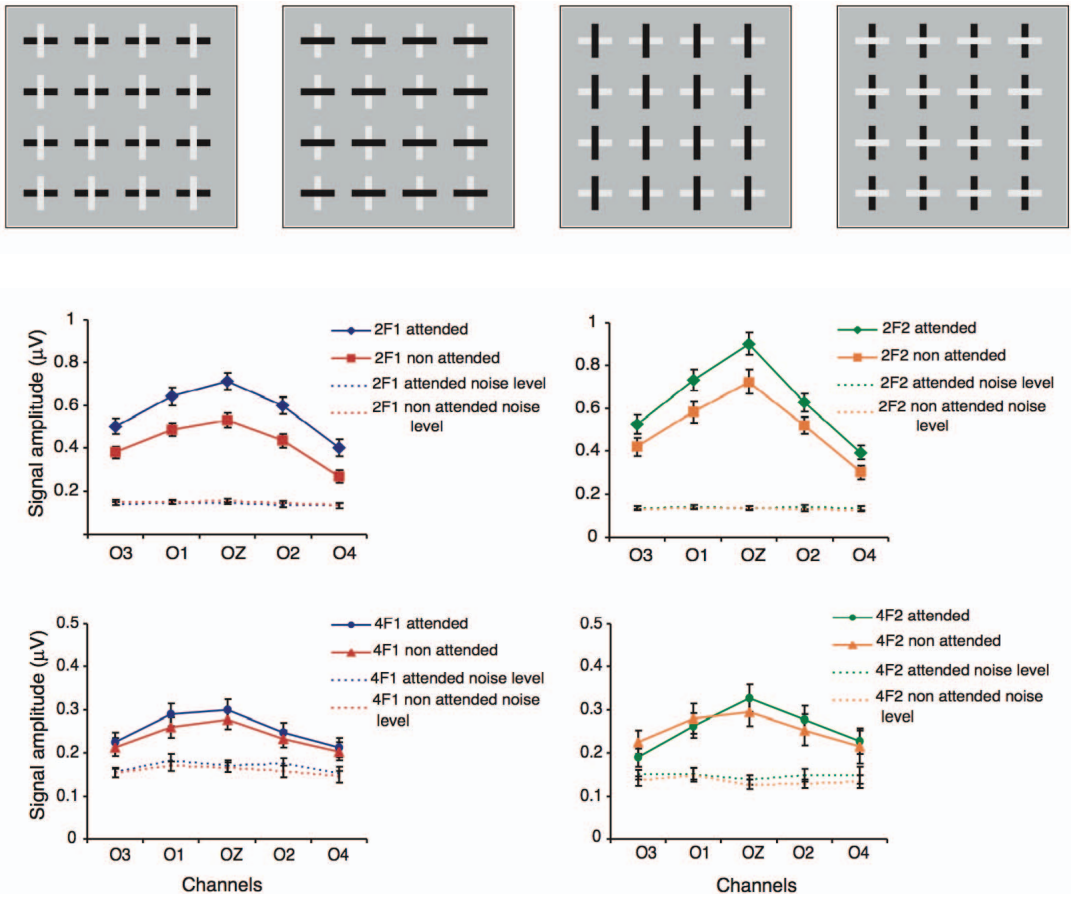

Figure 14. Frequency tagging used to study feature-based attention. Top panel: schematic illustration of moving-bar stimuli. The horizontal and vertical bars oscillated at slightly different frequencies. Occlusion cues were used to cause one set of bars to be seen in front of the other set. Lower panel: The stimulus to which attention was directed resulted in a higher amplitude response at the second but not the fourth harmonic. Figure composed from Pei et al. (2002).

Importantly, these SSVEP effects were strongly correlated with the response times for detecting the transient-motion target, such that larger enhancement and suppression effects were associated with shorter response times.

Subsequent studies from this group of authors have approached a number of other important aspects of feature-based attention. For example, by randomizing the spatial movement of the colored dots, they have shown that the selection of color is achieved without mediation of spatial attention (Andersen et al., 2009). Further, by manipulating the contrast ratio of achromatic versions of these random-dot kinematograms relative to the background, they were able to bring the bottom-up saliency of these stimuli under experimental control (Andersen, Muller, & Martinovic, 2012). This manipulation produced separable effects of gain enhancement and inhibitory stimulus competition at different levels of the visual processing hierarchy. In particular, the researchers observed that attention resulted in multiplicative enhancement in the SSVEP amplitude at midline-occipital sites but an additive influence at parietal sites, thereby indicating different competitive interactions at different levels of visual processing.

Having observed distinct influences of nonspatial attention on single feature attributes, Andersen, Hillyard, and Muller (2008) set out to explore how attention for multiple feature conjunctions was carried out in the human brain. In that study, frequency-tagged SSVEPs were recorded from four types of bars that each flickered at different a frequency. These bars were either horizontal and blue (10 Hz), vertical and red (12 Hz), horizontal and red (15 Hz), or vertical and blue (17 Hz). Participants were instructed to attend a particular combination of these shared visual features and to detect a brief period of coherent motion in the attended field. From this task, the authors observed that the SSVEP amplitudes showed parallel and additive facilitation. Namely, the attended color and the attended orientation were both facilitated individually, while the conjunction of the attended color and the attended orientation received the sum of each of the two individual feature enhancements. This important

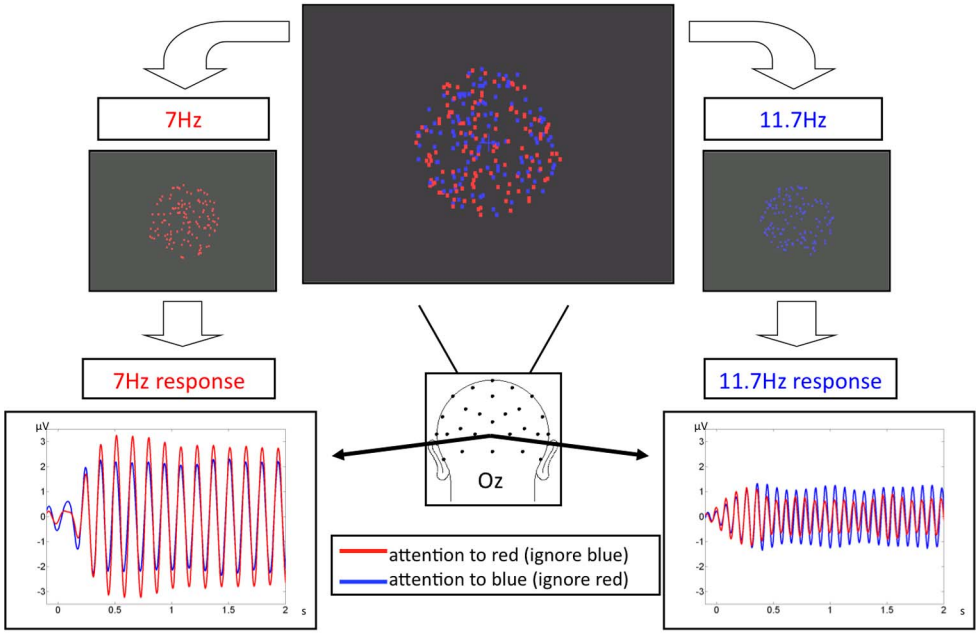

Figure 15. The effect of selective attention on the SSVEP (Muller et al., 2006). In this study, participants were cued to attend to one of the colored dot fields to detect the occurrence of a brief period of coherent motion while ignoring similar events in the other, unattended stream. There was a robust enhancement of the SSVEP amplitude for the attended stream that was maximal over occipital recording sites. Compared to the study of Morgan et al. (1996), the study illustrated here shows that attention can selectively enhance and suppress the representation of visual stimuli that spatially overlap.

finding suggests a specific means by which attention enables rapid guided visual search, and provides a broader platform for understanding the mechanisms of sustained nonspatial attention (Painter, Dux, Travis, & Mattingley, 2014).

A number of other researchers have applied the multi-input SSVEP technique to study other important aspects of nonspatial and object-based attention. For example, Appelbaum and Norcia (2009) have shown that directed versus divided attention to an object's shape modulates the amplitude and phase of SSVEP responses over a widely distributed network of brain areas including occipital visual areas and frontal control areas. Using the fMRI-defined ROI analyses described earlier (in Figure–ground segregation networks), Palomares et al. (2012) contrasted the influence of attention to global (0.83 Hz) and local (30 Hz) features of both coherent-motion and Glass-pattern stimuli. Attention to global motion, or dynamic global form in Glass patterns, modulated responses that were harmonics of the global update rate but not the local update rate. Attentional modulation was largest in an hMT ROI for the motion task but in the LOC for the dynamic-form task. Importantly, the local element response ($1F2$; 30 Hz) was not modulated by attention in the LOC, while the response to the global update was. This indicates that it is the hierarchical level of the stimulus that determined the attention effect, not the location of the responding brain area in the cortical hierarchy.

Using an adapted multiple-object tracking task, Stormer, Winther, Li, and Andersen (2013) investigated the neural mechanisms by which the visual system is able to simultaneously track multiple moving objects. In that task, participants were instructed to track five or seven randomly moving, frequency-modulating targets among a large number of nontargets modulating at a distinct frequency. The authors observed that sustained attention to the tracked objects enhanced the corresponding target SSVEP amplitude and that the magnitude of this enhancement predicted faster correct identification at the end of the trial. The cortical sources of these effects were located in the early visual cortex V1–V3 as well as the motion-sensitive area hMT, indicating that sustained multifocal attention can operate at early stages of visual processing. Related work by Verghese, Kim, and Wade (2012) focused on area V1 to show that the nature of attentional modulation in this area is dependent on the task being performed. In that study, contrast and orientation discrimination tasks produced differing narrow- and broadband SSVEP tuning functions that each aligned with psychometric performance. In a similar vein, Stormer and Alvarez (2014) recently used a color-feature SSVEP design in which differences in target and distractor color hue were parameterized in CIELAB color space to show that attention not only facilitates

target processing but also actively inhibits processing of similar color hues across the visual field. These findings indicate that attention acts to select the most informative neural population, that these populations change depending on the nature of the task, and that these selection mechanisms can operate on features much as has been shown for location-based attention. Other SSVEP findings from Wieser and Keil (2011) have illustrated the temporal dependence of activity in these attention-selective networks.

Recently, Garcia, Srinivasan, and Serences (2013) tracked the time course of feature selectivity by generating orientation-selective response profiles based on the spatial distribution of the SSVEP response. Using a linear discriminant classification approach to dynamically track the temporal evolution of orientation-selective responses, they found that feature attention produced a multiplicative modulation of the SSVEP. Importantly, they showed that behavioral performance on the orientation discrimination task could be predicted based on the amplitude of these temporally precise feature-selective response profiles.

Finally, in an elegant recent study, Baldauf and Desimone (2014) combined steady-state MEG with fMRI and diffusion tensor imaging (DTI) to characterize the circuits and timing of object-based attention. By using stimuli in which the phase coherence of overlapping face and house images was modulated periodically, they were able to create stimuli that did not change in luminance or contrast but could be still tracked via separate frequency tags. Brain responses to these stimuli were monitored using MEG as participants attended to the overlapping streams for cued targets. By combining the SSVEP with functional ROIs defined from fMRI, the researchers found that attention to faces resulted in enhanced sensory responses in the fusiform face area, whereas attention to houses increased responses in the parahippocampal place area.

Collectively, these studies provide compelling evidence of the power of the multi-input SSVEP method for tracking and disentangling the mechanisms involved in spatial, nonspatial, and object-based attention. They indicate that attention controls interactions between hierarchically arranged brain areas, with frontal control areas providing top-down biasing signals and specific sensory and occulomotor regions being uniquely involved in different aspects of attentional control and depending heavily on the nature of the task. Given that these important findings have manifested in a relatively short number of years, it is encouraging to think about the future of the SSVEP methodology in research and applied techniques that can uncover brain adjustments in real time as needed for dynamic attentional control.

Multi-input interactions as an objective measurement of system nonlinearities and neural convergence

A central goal of the visual system is to combine the diversity of afferent information coming from the eyes into a meaningful representation of the world. Much prior work with animal physiology has shown that the nature of processing and information convergence in the visual system is manifestly nonlinear. Most human neuroimaging approaches rely on subtractions and are therefore not well suited for studying these nonlinear processes, because the residual of a subtraction can represent linear or nonlinear processes or a mixture of both. The multi-input SSVEP, however, is better suited to this task, because the specific output frequencies present in the recording provide direct evidence for both the presence of nonlinearity in the system and information about the form of the nonlinearity.

Nonlinear systems produce a more complex output than linear systems: Their outputs consist of multiple harmonics for a single input, while linear systems produce only an output at the stimulus frequency, possibly scaled in amplitude or shifted in phase. When more that one temporal input is used, additional components known as intermodulation (IM) terms are produced by a nonlinear system. These responses occur at frequencies that are directly related to the input frequencies as sums and differences of the different harmonics of the stimulus frequencies. Each type of nonlinear process has its own pattern of output frequencies, and from this pattern one can deduce much about the type of nonlinearity present in the system (Regan & Regan, 1989), allowing researchers to build and test models of neural convergence. An important converse is that in order to characterize a nonlinear system, multiple inputs must be used. In the frequency domain, the number of input frequencies needed to fully characterize a nonlinear system scales directly with the nonlinear order, or complexity, of the system (Chua & Liao, 1991).

The nonlinearity of the system is important because, unlike in a linear system, the order of operations matters. In a nonlinear system, the input is qualitatively transformed after each transit of a nonlinear stage. Consequently, the order of nonlinear operations leaves distinct traces that can be used to deduce what the nonlinear operations were and in what order they occurred. Formal nonlinear analysis of the SSVEP and the concept called sequential analysis were first introduced to the field by Spekreijse and colleagues (Spekreijse & Oosting, 1970; Spekreijse & Reits, 1982).

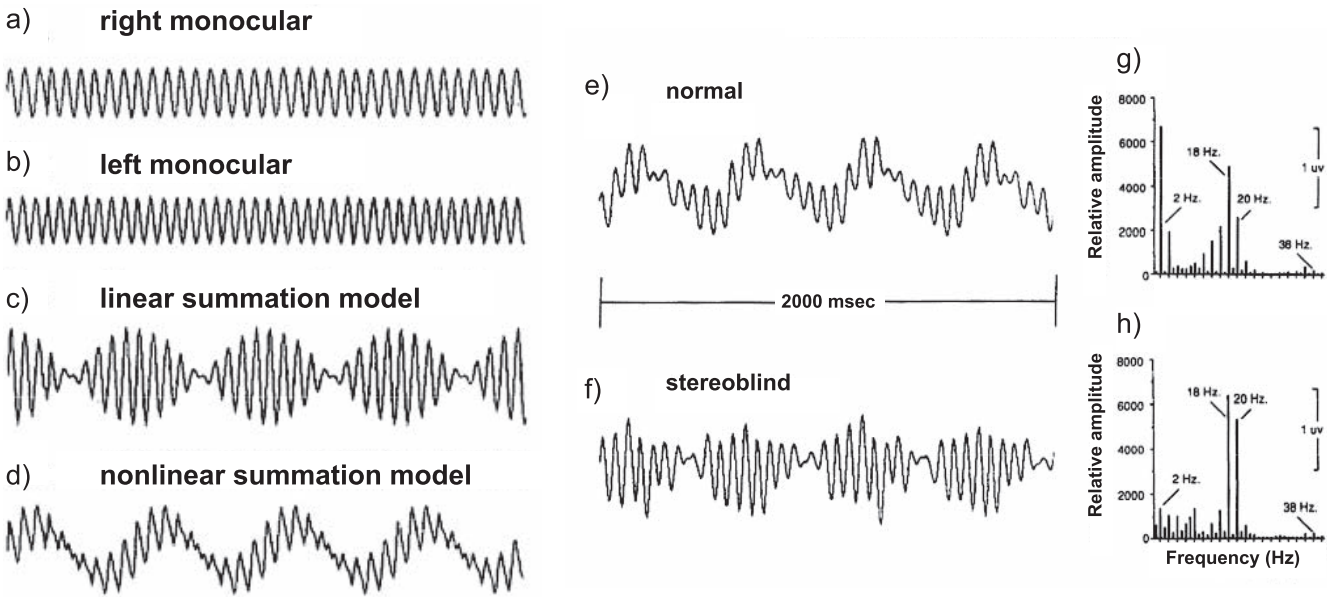

Figure 16. Objective detection of binocular convergence through measurement of intermodulation responses. (a–b) Hypothetical frequency tagged inputs presented to each eye. (c) Hypothetical response waveform for linear (nonbinocular) summation. (d) Hypothetical response waveform for nonlinear (binocular) summation. (e, g) Measured responses from an observer with normal binocular vision. (f, h) Measured responses from an observer with stereo-blindness. See text for details. Redrawn from Baitch and Levi (1988).

In the following sections we describe two of the most common areas where nonlinear approaches towards multi-input SSVEP have yielded particular gains: binocular summation and spatial interactions.

Binocular summation and normal binocular vision

The most intuitive example of how the SSVEP can be used to study neural convergence is the case of binocular summation. Stimuli presented separately to each eye make their way via separate pathways from the retina into cortex, where they are first combined in binocular cells. Whether and how this combination is accomplished is of interest both to clinicians who treat disorders of binocular vision and to computational neuroscientists who are interested in the nature of the nonlinear processes underlying different aspects of binocular vision.

Nonlinear summation is illustrated schematically in the context of binocular inputs in Figure 16, which is redrawn from Baitch and Levi (1988). In this study, a periodic input at $F1 = 18$ Hz was delivered to the right eye and another, nonharmonically related stimulus at $F2 = 20$ Hz was delivered to the left eye. These inputs are illustrated schematically in Figure 16a and b. If binocular summation is linear, the SSVEP response will be the simple sum of the two stimulus frequencies (see Figure 16c). If summation is nonlinear, the response waveform differs substantially from linear summation. Baitch and Levi modeled the binocular combination process as summation followed by rectification; the resulting theoretical response is shown in Figure 16d. In comparing Figure 16c and d, it is clear that linear and nonlinear models predict very different responses.

To manipulate the status of binocular convergence mechanisms experimentally, Baitch and Levi presented their stimuli to observers with normal binocular vision and to observers with stereo-blindness. The time-domain responses of the observers with normal vision resembled the nonlinear summation model (compare Figure 16e to d), but those of the observers with stereo-blindness resembled the linear model (compare Figure 16f to c). In the binocular model, the inputs of the two eyes are summed before convergence and the model is thus inherently a binocular model. In the linear model, the two eye responses are generated independently and do not depend on one another. The linear model is inherently monocular. Consistent with the manipulation, participants with normal binocular vision have responses that resemble those of the binocular model, while participants with stereo-blindness have responses that resemble the monocular model.

Figure 16g shows the response spectra for an observer with normal vision, while Figure 16h shows the response from an observer with stereo-blindness. As mentioned already, nonlinear processing mechanisms generate responses at frequencies that are low-order sums and differences of the input frequencies. If the

first input is labeled $F1$ and a second input is labeled $F2$, a nonlinear process will generate outputs at harmonics of the two input frequencies ($1f1$, $2f1$, $3f1$, $1f2$, $2f2$, $3f2$, etc.) and at frequencies equal to $1f1 + 1f2$ (the sum frequency), $1f1 - 1f2$ (the difference frequency), and possibly others (e.g., $2f1 + 2f2$). Responses at these combination frequencies, the IM responses, were first measured in the visual domain in the context of lateral spatial interactions (Ratliff & Zemon, 1982). The frequencies at which these responses occur are specific to the underlying nonlinearity (Regan & Regan, 1988). The spectrum recorded from an observer with normal binocular vision has robust responses at $1f1$ (20 Hz) and $1f2$ (18 Hz), and there are also responses at 2 Hz (the difference frequency, $1f1 - 1f2$) and other nonlinear combination frequencies (Figure 16g). Observers who do not have normal binocular vision show strong reductions of the IM (inherently binocular) responses (Figure 16h). Nonfusable dichoptic inputs such as cross-oriented gratings in the two eyes do not lead to IM responses (Brown, Candy, & Norcia, 1999; Sutoyo & Srinivasan, 2009). Taken together, these results demonstrate that IM response components directly reflect the dynamics of nonlinear summation and convergence processes.

Nonlinear spatiotemporal interactions

The multi-input nonlinear analysis approach can also be used to study the properties of receptive fields, a central construct in visual neuroscience. The basic elements of receptive fields are the regions of space over which neurons pool inputs and the pooling operation that is used to combine over both space and time. Receptive fields of single neurons are inaccessible at the scalp, but it is possible to study spatiotemporal pooling at the population level using multi-input SSVEPs. The requirements for such measurements are simple: At least two spatial locations must be driven by distinct temporal frequencies. The spatiotemporal interaction is characterized by the set of nonlinear combination frequencies recorded at the output (Regan & Regan, 1989). Through manipulation of either spatial or temporal aspects of the input, the spatial and temporal properties of the population response can thus be studied at the scalp.

Image-segmentation mechanisms

The analysis of nonlinear spatiotemporal interactions in the SSVEP was pioneered in the late 1970s and early 1980s by Ratliff's group (Ratliff & Zemon, 1982; Zemon & Ratliff, 1982, 1984; Zemon, Victor, & Ratliff, 1986). In these early studies, a windmill-dartboard configuration was used. The paradigm is illustrated in a simplified form in Figure 17, with rectilinear gratings and checkerboards instead of the radial versions used in the original studies. In this illustration, alternate abutting sections of the pattern reverse in contrast at different temporal frequencies, F1 and F2. Figure 17a indicates the time sequence of the F1 and F2 pattern reversals, with a low value on the timeline indicating one spatial phase and a high value indicating the contrast-reversed phase (i.e., black elements turn to white and white turn to black). The first input reverses at 3.0 Hz and the second at 3.6 Hz in this example. Figure 17b shows the *spatial states* of the display, of which there are four distinct types (two aligned and two misaligned). Regions of the display modulated at $F1$ are highlighted in yellow, and those driven at $F2$ are highlighted in purple. As can be seen in Figure 17a, the transitions between these states occurs at variable times and the states are of varying durations. The arrows link the states coded in the time sequence of Figure 17a to the corresponding spatial configurations shown in Figure 17b for the beginning of the sequence. The gray bands indicating the times the display is in the segmented state (S) are of varying duration and spacing. It should be noted that the segmentation state does not change at a periodic temporal frequency that could drive a linear SSVEP at that frequency. In the example, the whole sequence repeats itself every 1.6 s, but there is no physical event in the display that repeats at 1.6 s, nor is there periodic change of the segmentation state. Importantly, Ratliff and colleagues observed that the SSVEP evoked for these stimuli contained robust responses not only at frequencies that were harmonics of the two input frequencies $F1$ and $F2$ but also at IM frequencies equal to the sum and difference between $F1$ and $F2$ (Zemon & Ratliff, 1982, 1984).

The logic of the paradigm in terms of what it reveals about spatial integration is illustrated in Figure 17c. In this example, potential receptive fields, or spatial pooling mechanisms, are illustrated by the colored disks. The response expected from small receptive fields that lie only on regions modulated at $F1$ will be only at harmonics of $F1$ (i.e., $nf1$); similarly, small receptive fields that only see regions of the pattern flickering at $F2$ will only generate responses at $mf2$ Hz, where n and m are small integers. By contrast, temporally nonlinear receptive fields that jointly process both regions and are sensitive to the spatial configuration (aligned versus misaligned) will generate responses at frequencies equal to sums and differences of the harmonics of the two driving frequencies ($nf1 \pm mf2$).

Zemon and Ratliff (1982, 1984) showed that the nonlinear mechanism generating the IM response was extremely selective. The introduction of gaps as small as 3 arcmin between the regions and slight misalignments of the relative phase of the pattern regions both strongly reduced the magnitude of the IM response (see

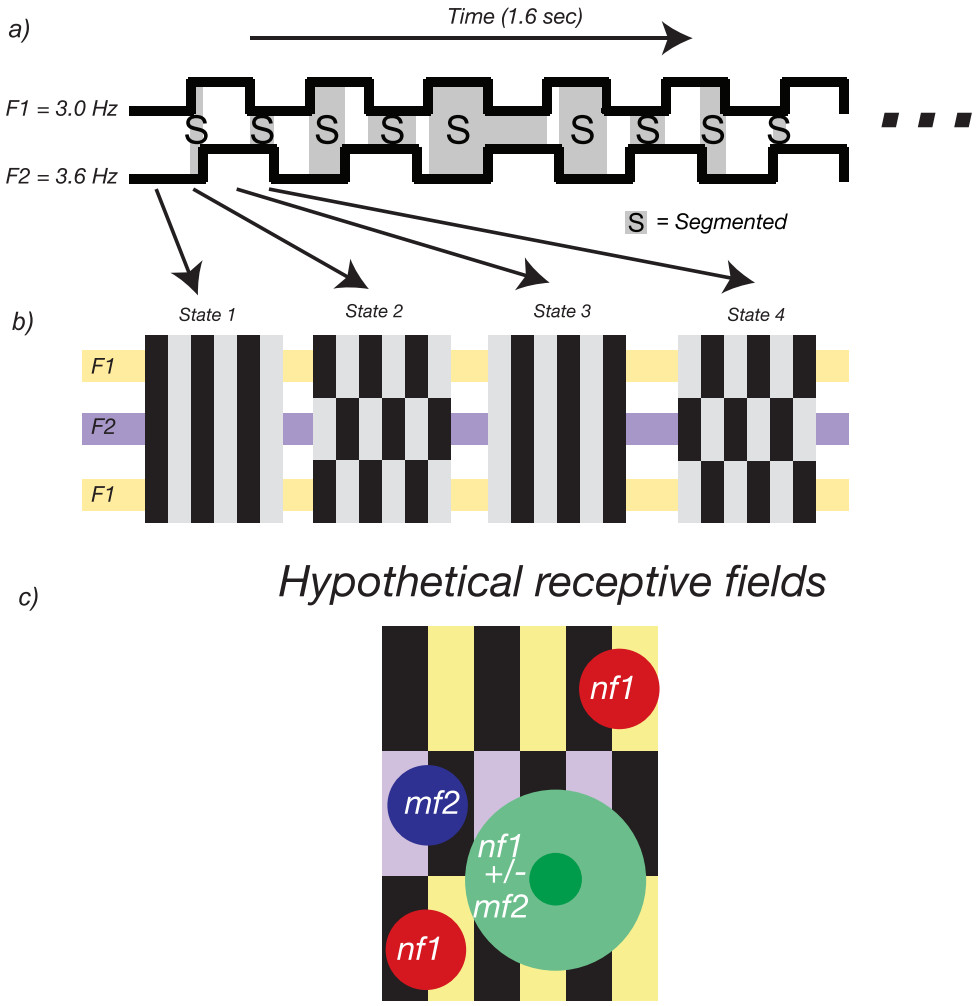

Figure 17. Multi-input SSVEP and neural-convergence receptive fields. (a) Temporal sequence of the multi-input stimulus. When both sequences have the same value, the pattern is aligned; when they have different values, the uniform field is segmented into different parts. The shaded regions labeled "S" show when the segmented states happen. (b) The four underlying spatial states of the stimulus created. (c) Hypothetical receptive fields that overlie different portions of the stimulus. The red receptive fields lie entirely within regions driven at F1, producing only harmonics of this frequency (*nf*1). The blue receptive field is entirely within the F2-driven region, producing only harmonics of F2 (*mf*2). The green receptive field spans the F1–F2 border. The receptive fields that span the two frequencies can produce responses exhibiting nonlinear interactions between the two driving frequencies (e.g., *nf*1 ± *mf*2 terms).

also Appelbaum et al., 2008; Hou, Good, & Norcia, 2007; Victor & Conte, 2000). The original interpretation of these results was that extremely small receptive fields spanning the border of the pattern were responsible for generating IM responses (e.g., the nominal receptive field corresponded to the smaller dark-green region rather that the larger light-green region). This interpretation is almost certainly an oversimplification, and more recent studies have shown that IM responses depend on both spatial separation and focused attention (Fuchs, Andersen, Gruber, & Muller, 2008), but the approach has nonetheless been very useful for describing the mechanisms of fine-grained processing of spatial position and the mechanisms of image segmentation.

Subsequent to these early studies, offset grating patterns have been used to convert the original windmill-dartboard paradigm into a test of vernier acuity—one of the most precise of all visual acuities (Hou et al., 2007; Norcia, Wesemann, & Manny, 1999). These studies and others (Victor & Conte, 2000) characterized both the spatial and temporal dynamics of a neural mechanism underlying the detection of subtle image discontinuities (breaks of collinearity), one of the primary cues for later stage object-segmentation processes. These studies showed that the IM response was well correlated with psychophysical vernier acuity both in central vision and in the periphery (Norcia et al., 1999), as well as in patients with amblyopia (Hou et al., 2007), a developmental disorder of spatial vision. The developmental sequence of this response differs from that for grating

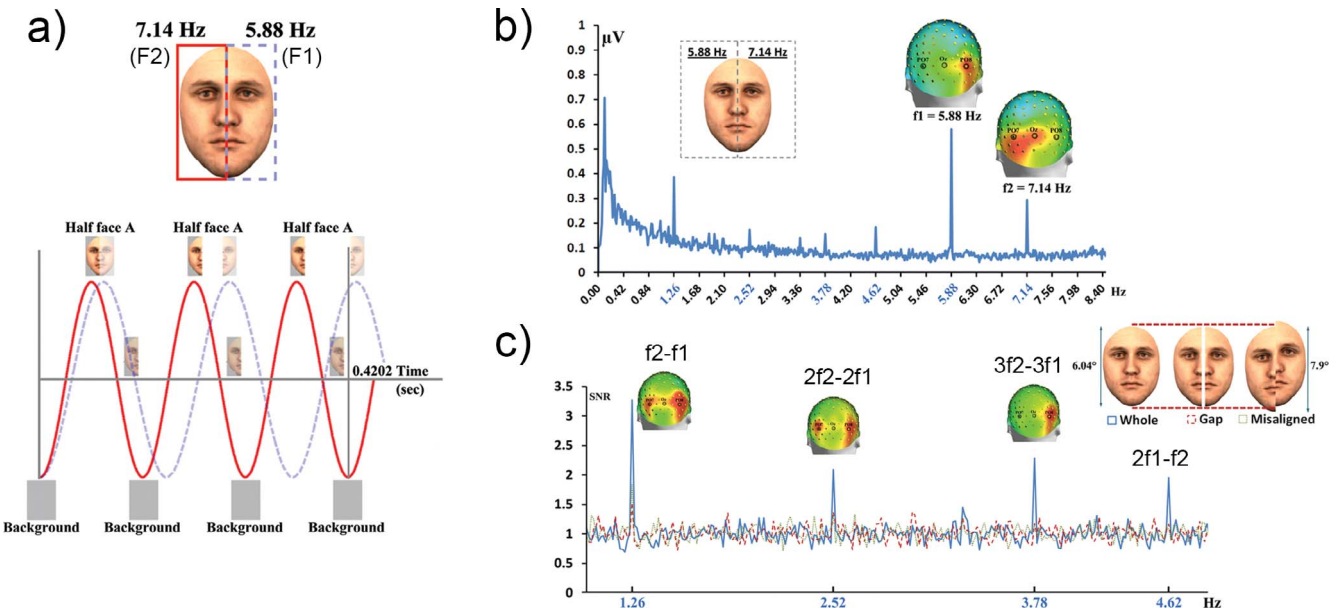

Figure 18. Objective evidence of integration between face parts from EEG frequency tagging (Boremanse et al., 2013, 2014). (a) The two halves of a face stimulus are contrast-modulated at different frequencies (5.88 and 7.14 Hz) for 60 s, and the frequency of stimulation is counterbalanced across faces halves in different trials. (b) The response to each face half can be identified objectively in the EEG spectrum and is contralateral to the side of stimulation. (c) IM response components at the exact differences between the two stimulation frequencies (e.g., $f2 - f1 = 1.26$ Hz; $2f2 - 2f1 = 2.52$ Hz; etc.). These IM responses are localized primarily over the right occipitotemporal cortex and only arise when a population of neurons in the system processes both frequency inputs. Contrary to the responses to each of the parts (5.88 and 7.14 Hz), these IM responses are specific to a condition where the two face halves form a whole integrated face: They disappear when the face halves are separated by a gap or spatially misaligned. Face inversion also specifically reduces the IM responses (Boremanse et al., 2013, 2014).

acuity, extending into late adolescence (Skoczenski & Norcia, 2002).

Spatiotemporal grouping

Spatiotemporal interaction within receptive fields can occur over multiple spatial scales and along many different stimulus dimensions. The flip side of the image- segmentation process, just described, are processes that are involved in the integration or grouping of features. Previous psychophysical research has shown that motion signals are grouped over space in a fashion that is highly specific in terms of the configurations that do or do not support perceptual grouping. The phenomenological appearance of the motion relationships and the apparent direction of motion are thus subject to a set of rules that may be driven by prior experience with natural images (Wagemans et al., 2012).

A particularly rich framework for studying motion grouping is the occluded-diamond paradigm (Lorenceau & Shiffrar, 1992). In the simplest version of this paradigm, four bars are presented, arranged to form the sides of a diamond. The bars do not extend fully to form a complete diamond-shaped contour. The bars that are parallel to each other are set in oscillatory motion, and in the original demonstration, the temporal phase of the motion differed by 90°. In this configuration, the bar pairs appear to oscillate independently (nonrigid motion). The simple introduction of set of visible occluders over the parts of the image where the bars would join, if they were continued to form a closed figure, results in a dramatic change in the appearance of the bar motion. Instead of moving independently, the bar pairs join together as a rigidly moving group. By setting the bar pairs in motion at two different temporal frequencies, Aissani, Cottereau, Dumas, Paradis, and Lorenceau (2011) were able to show that the IM components of the MEG depended on the perceptual grouping. A similar approach has been taken to study long-range integration of contour information (Gundlach & Muller, 2013).

IM responses as indicators of perceptual grouping can also be used to study very complex forms of spatial integration, such as those involved in face perception. In a recent study (Boremanse, Norcia, & Rossion, 2013), the left and right halves of a single face stimulus were contrast-modulated at different frequency rates ($F1 = 5.88$ Hz and $F2 = 7.14$ Hz; Figure 18a). This approach was used to identify objectively the neural representation of each half of a face when these two

halves are presented simultaneously and to attempt to identify an objective trace of the integration of these two halves into a unified representation, or a so-called holistic representation (Rossion, 2013; Tanaka & Farah, 1993).

Each input face half produced an SSVEP over posterior electrode sites exactly at the fundamental frequencies $f1$ and $f2$ (Figure 18b). These responses constitute unambiguous electrophysiological tags of each stimulated face part, so the frequency-tagging approach is able to cope with the challenge of presenting a whole face and measuring simultaneously the response to two of its parts. Most interestingly, specific responses corresponding to exact differences between the two input frequencies (e.g., $7.14 - 5.88 = 1.26$ Hz; Figure 18b and 18c) were found. These IM responses had a bilateral occipitotemporal topography, with a right hemispheric predominance, suggesting the presence of high-level integration processes specifically related to the perception of a face as an integrated unit (holistic face perception). Importantly, manipulations breaking the whole face into its constituent parts, such as spatial separation by a gap, misalignment, or inversion, reduced or abolished most of the IM responses, while leaving the responses to the face parts at the fundamental frequencies unaffected (Figure 18b). These findings were taken as objective evidence that an intact upright face is different from the sum of its parts (Boremanse et al., 2013), an important issue in face-perception research and high-level vision in general.

In a follow-up study (Boremanse, Norcia, & Rossion, 2014), a condition was introduced with face identity changing at every stimulation cycle. Compared to a contrast modulation of different face identities, SSVEP responses to each face half, at 5.88 and 7.14 Hz, decreased when the same face was presented. Contrary to repetition suppression effects for whole faces, which are usually found over the right occipitotemporal cortex (Rossion & Boremanse, 2011; Rossion et al., 2012), these part-based repetition suppression effects were found on all posterior electrode sites and were unchanged when the two face halves were manipulated by separation, lateral misalignment, or inversion. In contrast, IM components (e.g., 7.14 Hz − 5.88 Hz = 1.26 Hz) were significantly reduced following these manipulations. Additionally, the IM components decreased substantially for face halves belonging to different identities, which form a less coherent face than when they belong to the same face identity. These observations provide objective evidence for dissociation between part-based (fundamental frequencies) and integrated (intermodulation) responses to faces in the human brain, suggesting that only the integrated responses may reflect high-level, possibly face-specific, representations.

Testing of nonlinear models

The multi-input approach to the SSVEP provides a powerful way to test computational models of visual processing. As discussed before, each type of nonlinear mechanism has a characteristic signature of nonlinear response components (Regan & Regan, 1988). One approach to testing models is to compose a list of nonlinearities and their corresponding signatures that can be used for comparison with measured data (Regan & Regan, 1988). This approach was taken in the earliest studies of IM responses that were modeled by summation followed by squaring or rectification (Baitch & Levi, 1988; Zemon & Ratliff, 1984). Some simple nonlinearities can be fully described analytically (Regan & Regan, 1988; Victor & Conte, 2000). Other studies (Candy, Skoczenski, & Norcia, 2001; Tsai, Wade, & Norcia, 2012) have tested predictions of variations of the contrast normalization model (Geisler & Albrecht, 1992; Heeger, 1992; Robson, 1988). In the study by Tsai et al. (2012), model fitting to experimental data was used to reject two forms of the normalization model in favor of a third. Here the form of the IM responses was decisive in discriminating the different models. The fact that only the full nonlinear analysis could clearly favor one model over another shows the importance and utility of using all of the relevant response terms when developing mechanistic models.

Current status and future directions

Strengths and limitations of SSVEPs

Throughout this article, we have indicated that the SSVEP approach has the desirable property of *objective* definition of response components: The generation of the response components is constrained at the outset by the experimenter through the decision of which frequency or frequencies to use. This decision determines exactly which frequencies are relevant and which are irrelevant to the response analysis. Furthermore, different frequency components have qualitatively different and objective meaning in the experiment: In alternating between two stimulus states, odd harmonics indicate asymmetric processing and IM components indicate joint, nonlinear processing of inputs. Moreover, the response is *implicit*: It can be measured in the absence of an overt behavior and thus is not influenced by decision-criterion effects lying after sensory or perceptual encoding stages. Thus, the approach can be used similarly in typical human adults and in populations who are unable to provide overt behavioral responses, such as infants or certain patient populations.

One of the hallmark features of the SSVEP is its high SNR. This derives from the fact that the response itself is narrowband, while noise sources are broadband. This feature allows researchers to record subtle differences between visual stimuli in a relatively short amount of time and is what enabled the development of the sweep paradigm. Transient ERPs, by contrast, are influenced by the full range of frequency content allowed into the recording by the front-end amplifier filters. Movement artifacts and low-frequency noise arising from skin potentials are especially problematic with transient ERPs (Luck & Kapenmans, 2012), but they are much less of a problem with high-frequency SSVEPs.

The high SNR of the SSVEP, however, comes with a cost: The use of a single stimulus frequency (or even several frequencies) probes the system over only a limited range of temporal frequencies. Ideally one would like to know how the system responds to a given stimulus presented at an arbitrary rate, and whether the response depends qualitatively on the frequency chosen. To fully characterize the system involves recording the responses at many different frequencies—a slow process indeed. An alternative approach is to probe the system with temporally broadband stimuli (random or pseudorandom time sequences; Marmarelis, 2004; Sutter, 2001). The resulting responses are a more complete description of the system response because the stimulation process drives the system over its full temporal operation range. The completeness of description afforded by these approaches however comes at a price: Noise-based analysis methods have substantially lower SNR than SSVEP methods, and long recording times are often needed to make the desired measurements. This trade-off between the completeness of the characterization of the system response and the time to make the measurements is fundamental and inescapable. In practical terms, the question devolves into which temporal frequency is best for empirically describing the phenomenon one wishes to address. This frequency will depend on the nature of the task being investigated. As noted earlier, the relevant range of responses is not fixed but is related to the complexity of the stimulus being processed.

Whether a given evoked response component reflects a specific or a nonspecific process is a function of the design of the stimulus, the nature of the analysis of the response, and the use of control stimuli that can provide an independent test of the specificity of the paradigm. A very clear example of the effectiveness of stimulus design is the dynamic random-dot stereogram and related hierarchical stimuli (see Multiple temporal inputs: Embedded frequency paradigms). In the dynamic random-dot stereogram, by nature of the design of the stimulus, there are no monocular cues, and thus any evoked response measured to changes in binocular correlation or disparity are specifically due to binocular and not monocular processes. More generally, specificity in hierarchical stimuli, including the fast-oddball paradigm, comes from dissociating the rate of local contrast change from that of the more global property one wishes to study. The different kinds of responses can thus be isolated by frequency-specific analysis.

With more traditional contrast-modulated stimuli that contain only a single frequency, something more needs to be done to infer sensitivity to a specific stimulus attribute. Here one generally needs a control condition, because a harmonically related response could arise from a number of different processes. We illustrated this with our example of isolating face-individuation-related activity through the use of adaptation (Figure 8).

With proper stimulus design, one can directly interpret odd harmonics as being specific to the onset of a global feature (see Figure 5). Here the subtraction between a test and a control condition is effectively built into the spectral analysis. Differential activity specifically appears in the odd harmonics and may or may not appear in the even harmonics.

A distinctive advantage of the SSVEP approach is the ability it affords to record from multiple simultaneously presented stimuli. With frequency tagging, one can separate the response to the different stimulus parts via their specific tagged responses and directly measure nonlinear interactions between the inputs. This approach has strong implications for the design of experiments and makes certain analyses possible that are otherwise impossible. It also makes a step towards providing a more complete description of the system response, particularly when the IM components are analyzed. It should be noted that it is also possible to temporally tag stimuli using random or pseudorandom temporal sequences and thus measure tagged response waveforms and nonlinear interactions in the time domain (Sutter, 2001).

Despite a number of advantages stemming from the narrowband nature of the SSVEP, the corresponding periodic nature of steady-state stimuli makes it difficult to study the temporal sequence of activation, particularly when high rates of stimulation are used. This has been cited as a major limitation of the method (Luck, 2005). At high stimulation rates, there are significant delays in the visual pathway due to both integrative activity within the retina and cortex and propagation delays over fiber pathways between processing stages. If the delays are greater than the period of the stimulation, there is an uncertainty about which cycle of the response corresponds to the absolute latency. It is nonetheless possible to derive an estimate of temporal response delay from the SSVEP by measuring SSVEP phase at multiple stimulation frequencies (Lee, Birtles, Wattam-Bell, Atkinson, & Braddick, 2012; Lopes da Silva, van Rotterdam, Storm van Leeuwen, &

Tielen, 1970; Regan, 1966; Spekreijse, 1978; see Appendix 2 for details). The method relies on measuring the SSVEP phase at two or more temporal frequencies and thus at least doubles the recording time. Because the visual system is nonlinear, this approach is essentially an empirical one, as there has yet to be a theoretical generalization of the approach that includes all the harmonics of nonlinear SSVEP responses.

Directly relating parameters of the SSVEP to the temporal evolution of neural activity underlying different behavioral responses is also challenging. It is common in transient-ERP experiments to have participants respond behaviorally to discrete stimulus events and to use the behavioral data to generate a response-contingent analysis that can then be used to map out the time course of evoked potentials that are related to the generation of the response (Hillyard, Hink, Schwent, & Picton, 1973; Sutton et al., 1965). It is possible to create a similar SSVEP paradigm by embedding transient probe tasks in SSVEP paradigms (Ales, Appelbaum, & Norcia, 2010; Cottereau, Ales, et al., 2014b). The use of SSVEP to tag the ongoing stimulus presentation allows for a very clean subtraction of the evoked potential created by the stimulus. While this enables better discounting of the stimulus-related activity, the remaining response-related activity is no longer an SSVEP. One can still access decision-related activity using traditional ERP techniques (Luck & Kappenman, 2012), but it is no longer possible to tag this activity in the frequency domain.

Another common issue with SSVEPs is that because the stimulus is periodic, predictive or anticipatory activity can be generated if the participant learns the repetitive stimulus sequence. This concern led to the introduction of time-jittered event-related designs for the study of the earliest phases of attention via evoked potential methods (Hillyard et al., 1973; Naatanen, 1975). This limitation can be circumvented by steady-state stimulation with random temporal inputs (Sutter, 2001). Here the temporal order of processing can be determined in the absence of anticipatory responding, and responses to multiple inputs can be measured along with their spatiotemporal interactions. However, as noted before, these methods entail a significant cost in SNR.

As with any method that records neural activity at the scalp, the ability to localize the sources of the SSVEP to specific cortical areas or cell classes is limited by the blurring of the field by the head volume conductor (Dannhauer, Lanfer, Wolters, & Knosche, 2011; Hamalainen, Ilmoniemi, Knuutila, & Lounasmaa, 1993), by cancellation of activity from opposing sources such as those on opposite walls of a sulcus (Ahlfors et al., 2010), by cancellation due to opposing directions of current flow within the cortical laminae (Mitzdorf & Singer, 1979), and finally by the ill-posed nature of inverse modeling procedures (Grech et al., 2008). Nonetheless, the validity of source localization depends on the SNR, and the high SNR of the SSVEP provides an advantage over standard ERP approaches. Moreover, significant progress has been made in providing a useful level of spatial precision when detailed anatomical data from MRI are used to build accurate electrical models of the volume conductor and when sophisticated inverse methods with realistic constraints are used (Appelbaum et al., 2006; Bai, Towle, He, & He, 2007; Cottereau, Ales, & Norcia, 2012; Cottereau, Ales, et al., 2014a; Sharon, Hamalainen, Tootell, Halgren, & Belliveau, 2007).

Neural mechanisms and relationship to transient ERPs

Beyond the questions of source localization and source visibility, it is not well understood what the relative contributions are of presynaptic excitatory and inhibitory potentials versus spiking activity to surface activity (Buzsaki, Anastassiou, & Koch, 2012). This is not a problem specific to the SSVEP, but it is nonetheless a limitation of the EEG method. The frequency-domain approach can be readily applied in other recording modalities that have greater spatial resolution, such as electrocorticography (Winawer et al., 2013) or intracerebral recordings with depth electrodes (Jonas et al., 2014) local field potentials (Norcia, 1996), and single-unit recording (Bonds, 1989). Future studies that link these invasive measurements to surface activity will be particularly valuable in informing the interpretation of the SSVEP.

Another issue that is worth a brief discussion is the relationship between SSVEPs and transient ERPs. As noted at the beginning of this article, it is often assumed that SSVEPs are responses to very rapid (>8–10 Hz) trains of stimuli, in contrast to transient ERPs in which there is a long (and variable) delay between stimuli. We, on the other hand, consider the SSVEP to be a periodic response to a periodic stimulus, without making assumptions about the minimum rate of stimulation. Very slow stimulation rates can generate evoked-response time courses that look indistinguishable from those of traditional transient ERPs, even though their spectrum is composed of a series of narrowband frequency components (see Figures 5 and 9 for examples). If, however, as in traditional transient ERP paradigms, the stimulation has random intertrial intervals, the resulting spectrum is continuous over a broad band of frequencies. The difference in spectra

depends on whether or not the input is periodic (Regan, 2009).

In this context, the issue of whether the SSVEP reflects the linear summation of transient ERPs arises; this has been discussed by several authors (see Galambos, Makeig, & Talmachoff, 1981, in the auditory domain; Capilla, Pazo-Alvarez, Darriba, Campo, & Gross, 2011, in the visual domain; Regan, 1989 for a discussion of this issue). When transient ERPs measured from temporally isolated stimuli are used to predict the SSVEP, there is poor agreement (Capilla, Pazo-Alvarez, Darriba, Campo, & Gross, 2011). If, however, a different kind of transient-ERP waveform is generated from responses during a dense, temporally jittered stimulation sequence, high-frequency SSVEPs (~10 Hz) can be synthesized with good accuracy.

The main problem that confounds comparisons between transient and steady-state VEPs is the presence of both static and dynamic nonlinearities in the visual pathway. It is important to first make clear that the concept of linearity that was targeted by Capilla et al. (2011) is different from the static nonlinearity defined at the beginning of this article (Figures 1 and 2). A static nonlinearity distorts the input in exactly the same way, independent of the frequency of the inputs. However, when comparing between fast and slow stimulation rates, it is important to be aware of dynamic nonlinearities. The output of a system that has a dynamic nonlinearity will depend on the relative timing between successive stimulation events. Simple nonlinear models that have dynamic nonlinearities can be formed from cascades of linear filters and nonstatic nonlinearities such as squaring or rectification (Zemon & Ratliff, 1984).

The complexities introduced by dynamic nonlinearities are not limited to periodic stimulation. Fast *nonperiodic* stimulation reveals clear violations of linear temporal superposition (Sutter, 2001). The temporally dense, time-jittered stimulus that Capilla et al. (2011) used to generate ERPs engages dynamic nonlinearities in a different way than does a traditional ERP presentation mode composed of widely spaced events. The synthesis results of Capilla et al. are interesting, but it is unclear how useful this approach is for predicting other types of SSVEPs. Any future research comparing transient ERPs and SSVEP needs to address dynamic nonlinearities as a fundamental determinant of responses at different stimulation rates.

Another aspect of ERPs that is tightly related to dynamic nonlinearities is the nature of the underlying neural mechanisms that generate the measured evoked response. A dominant view of evoked-response generation is that they are the result of time-locked stimulus-evoked transients in cortex (Dawson, 1954). According to an alternative view, stimulus presentation generates an evoked potential by changing the ongoing dynamics, e.g., by phase-resetting ongoing oscillations (Makeig et al., 2002; Sayers, Beagley, & Henshall, 1974). This idea that evoked potentials are created by changing ongoing dynamics also applies to steady-state stimulation. Here the idea is that periodic stimulation, rather than being a (nonlinear) superimposition of stimulus-evoked transients, entrains oscillators to the stimulation phase. In the visual system, to take a concrete example, a 10-Hz stimulation rate would give rise to a large SSVEP response over the visual cortex because it entrains the prominent ongoing oscillatory rhythm in the alpha range (8–12 Hz), which is also large over visual cortex (Spaak, de Lange, & Jensen, 2014). However, it should be mentioned that the frequency rate giving the largest SSVEP response is not tied to the range of 8–12 Hz, but rather depends on the kind of stimulus property that is modulated. For individual face stimuli presented in pattern onset/offset mode, the stimulus frequency giving rise to the largest face-specific response over the higher level visual cortex appears to be at around 6 Hz (i.e., six faces/s), not 10 Hz (Alonso-Prieto et al., 2013). The exact nature of the underlying generators of the evoked potential is far from resolved and remains an active area of current research. The interested reader is referred to recent critical discussions of the issue of entrainment of endogenous rhythms (Capilla et al., 2011; Keitel, Quigley, & Ruhnau, 2014; Shah et al., 2004).

Prospects for the future of the SSVEP

While much has been learned from the SSVEP up to this point, there are many opportunities and challenges that lie ahead. Some of the opportunities involve extension of the technique to broader classes of visual stimulation and to studies of multisensory integration (Giani et al., 2012; Nozaradan, Peretz, & Mouraux, 2012; Regan, He, & Regan, 1995; Saupe, Schroger, Andersen, & Muller, 2009). In addition, through the continued innovation of more sophisticated experimental designs, researchers will be able to address questions relating to higher level cognitive processes, such as memory and decision making. Better signal-processing procedures, such as those being developed for brain–computer interfaces, could be applied to studies of visual processing (Davila, Srebro, & Ghaleb, 1998; Friman, Volosyak, & Graser, 2007; Garcia Molina & Zhu, 2011; Zhu et al., 2010). A particularly fruitful avenue for future study is parallel application of SSVEP protocols in studies with intracranial electrodes, either in animal models or in humans.

Parallel studies with voltage-sensitive dye imaging (Benucci, Frazor, & Carandini, 2007) or other imaging modalities with high temporal resolution will be particularly important for understanding the underlying nonlinear processes involved in generating the response and the extent to which activity recorded at the surface is representative of activity within different cortical areas. By combining these new technical approaches with formal computational modeling that links the underlying processing to their manifestations at the scalp, the SSVEP will become even more useful and its strengths and weaknesses will be better understood.

Keywords: visual evoked potentials, steady-state, spectrum analysis, vision, attention, perceptual organization

Acknowledgments

This work was supported by EY018875 and EY015790 (AMN, JMA, BRC) from the National Institutes of Health. BR is supported by the National Research Fund (FNRS, Belgium) and ERC grant facessvep 284025. LGA is supported by DARPA: D12AP00025-002.

Commercial relationships: none.
Corresponding author: Anthony M. Norcia.
Email: amnorcia@stanford.edu.
Address: Department of Psychology, Stanford University, Stanford, CA, USA.

References

Abdullah, S. Aldahlawi, N., Rosli, N., Vaegan, Y., Boon, M. Y., & Maddess, T. (2012). Effect of contrast, stimulus density, and viewing distance on multifocal steady-state visual evoked potentials (MSVs). *Investigative Ophthalmology & Visual Science, 53*(9), 5527–5535, http://www.iovs.org/content/53/9/5527. [PubMed] [Article]

Acunzo, D. J., Mackenzie, G., & van Rossum, M. C. (2012). Systematic biases in early ERP and ERF components as a result of high-pass filtering. *Journal of Neuroscience Methods, 209*(1), 212–218.

Adrian, E. D. (1944). Brain rhythms. *Nature, 153,* 360–362.

Adrian, E. D., & Matthews, B. H. C. (1934a). The Berger rhythm: Potential changes from the occipital lobes in man. *Brain, 4*(57), 355–385.

Adrian, E. D., & Matthews, B. H. (1934b). The interpretation of potential waves in the cortex. *Journal of Physiology, 81*(4), 440–471.

Ahlfors, S. P., Han, J., Lin, F. H., Witzel, T., Belliveau, J. W., Hamalainen, M. S., . . . Halgren, E. (2010). Cancellation of EEG and MEG signals generated by extended and distributed sources. *Human Brain Mapping, 31*(1), 140–149.

Aissani, C., Cottereau, B., Dumas, G., Paradis, A. L., & Lorenceau, J. (2011). Magnetoencephalographic signatures of visual form and motion binding. *Brain Research, 1408,* 27–40.

Ales, J. M., Appelbaum, L. G., Cottereau, B. R., & Norcia, A. M. (2013). The time course of shape discrimination in the human brain. *NeuroImage, 67,* 77–88.

Ales, J., Appelbaum, L., & Norcia, A. (2010). Neural signatures of shape discrimination decisions at threshold. *Journal of Vision, 10*(7): 106, http://www.journalofvision.org/content/10/7/106, doi:10.1167/10.7.106. [Abstract]

Ales, J. M., Farzin, F., Rossion, B., & Norcia, A. M. (2012). An objective method for measuring face detection thresholds using the sweep steady-state visual evoked response. *Journal of Vision, 12*(10): 18, 1–18, http://www.journalofvision.org/content/12/10/18, doi:10.1167/12.10.18. [PubMed] [Article]

Ales, J. M., & Norcia, A. M. (2009). Assessing direction-specific adaptation using the steady-state visual evoked potential: Results from EEG source imaging. *Journal of Vision, 9*(7):8, 1–13, http://www.journalofvision.org/content/9/7/8, doi:10.1167/9.7.8. [PubMed] [Article]

Allen, D., Norcia, A. M., & Tyler, C. W. (1986). Comparative study of electrophysiological and psychophysical measurement of the contrast sensitivity function in humans. *American Journal of Optometry Physiological Optics, 63*(6), 442–449.

Almoqbel, F., Leat, S. J., & Irving, E. (2008). The technique, validity and clinical use of the sweep VEP. *Ophthalmic and Physiological Optics, 28*(5), 393–403.

Alonso-Prieto, E., Belle, G. V., Liu-Shuang, J., Norcia, A. M., & Rossion, B. (2013). The 6 Hz fundamental stimulation frequency rate for individual face discrimination in the right occipito-temporal cortex. *Neuropsychologia, 51*(13), 2863–2875.

Alpers, G. W., Ruhleder, M., Walz, N., Muhlberger, A., & Pauli, P. (2005). Binocular rivalry between emotional and neutral stimuli: A validation using fear conditioning and EEG. *International Journal of Psychophysiology, 57*(1), 25–32.

Andersen, S. K., Hillyard, S. A., & Muller, M. M. (2008). Attention facilitates multiple stimulus fea-

tures in parallel in human visual cortex. *Current Biology, 18*(13), 1006–1009.

Andersen, S. K., & Muller, M. M. (2010). Behavioral performance follows the time course of neural facilitation and suppression during cued shifts of feature-selective attention. *Proceedings of the National Academy of Sciences, USA, 107*(31), 13878–13882.

Andersen, S. K., Muller, M. M., & Hillyard, S. A. (2009). Color-selective attention need not be mediated by spatial attention. *Journal of Vision, 9*(6):2, 1–7, http://www.journalofvision.org/content/9/6/2, doi:10.1167/9.6.2. [PubMed] [Article]

Andersen, S. K., Muller, M. M., & Hillyard, S. A. (2012). Tracking the allocation of attention in visual scenes with steady-state evoked potentials. In M. I. Posner (Ed.), *Cognitive neuroscience of attention* (pp. 197–218). New York: Guilford.

Andersen, S. K., Muller, M. M., & Martinovic, J. (2012). Bottom-up biases in feature-selective attention. *Journal of Neuroscience, 32*(47), 16953–16958.

Appelbaum, L. G., Ales, J. M., Cottereau, B., & Norcia, A. M. (2010). Configural specificity of the lateral occipital cortex. *Neuropsychologia, 48*(11), 3323–3328.

Appelbaum, L. G., Ales, J. M., & Norcia, A. M. (2012). The time course of segmentation and cue-selectivity in the human visual cortex. *PLoS One, 7*(3), e34205.

Appelbaum, L. G., & Norcia, A. M. (2009). Attentive and pre-attentive aspects of figural processing. *Journal of Vision, 9*(11):18, 1–12, http://www.journalofvision.org/content/9/11/18, doi:10.1167/9.11.18. [PubMed] [Article]

Appelbaum, L. G., Wade, A. R., Vildavski, V. Y., Pettet, M. W., & Norcia, A. M. (2006). Cue-invariant networks for figure and background processing in human visual cortex. *Journal of Neuroscience, 26*(45), 11695–11708.

Appelbaum, L. G., Wade, A. R., Vildavski, V. Y., Pettet, M. W., & Norcia, A. M. (2008). Figure/ground interaction in human visual cortex. *Journal of Vision, 8*(9):8, 1–19, http://www.journalofvision.org/content/8/9/8, doi:10.1167/8.9.8. [PubMed] [Article]

Aspell, J. E., Tanskanen, T., & Hurlbert, A. C. (2005). Neuromagnetic correlates of visual motion coherence. *European Journal of Neuroscience, 22*(11), 2937–2945.

Bach, M., & Meigen, T. (1992). Electrophysiological correlates of texture segregation in the human visual evoked potential. *Vision Research, 32*(3), 417–424.

Bach, M., & Meigen, T. (1998). Electrophysiological correlates of human texture segregation, an overview. *Documenta Ophthalmologica, 95*(3–4), 335–347.

Bach, M., & Meigen, T. (1999). Do's and don'ts in Fourier analysis of steady-state potentials. *Documenta Ophthalmologica, 99*(1), 69–82.

Bai, X., Towle, V. L., He, E. J., & He, B. (2007). Evaluation of cortical current density imaging methods using intracranial electrocorticograms and functional MRI. *NeuroImage, 35*(2), 598–608.

Baitch, L. W., & Levi, D. M. (1988). Evidence for nonlinear binocular interactions in human visual cortex. *Vision Research, 28*(10), 1139–1143.

Baldauf, D., & Desimone, R. (2014, April 25). Neural mechanisms of object-based attention. *Science, 344*(6182), 424–427.

Behrens, P. (2009). CircStat: A MATLAB toolbox for circular statistics. *Journal of Statistical Software, 31*(10), 1–21.

Belmonte, M. (1998). Shifts of visual spatial attention modulate a steady-state visual evoked potential. *Brain Research, Cognitive Brain Research, 6*(4), 295–307.

Bentin, S., Allison, T., Puce, A., Perez, E., & McCarthy, G. (1996). Electrophysiological studies of face perception in humans. *Journal of Cognitive Neuroscience, 8*(6), 551–565.

Benucci, A., Frazor, R. A., & Carandini, M. (2007). Standing waves and traveling waves distinguish two circuits in visual cortex. *Neuron, 55*(1), 103–117.

Blake, R., & Logothetis, N. (2002). Visual competition. *Nature Reviews of Neuroscience, 3*(1), 13–21.

Bonds, A. B. (1989). Role of inhibition in the specification of orientation selectivity of cells in the cat striate cortex. *Visual Neuroscience, 2*(1), 41–55.

Boremanse, A., Norcia, A. M., & Rossion, B. (2013). An objective signature for visual binding of face parts in the human brain. *Journal of Vision, 13*(11):6, 1–18, http://www.journalofvision.org/content/13/11/6, doi:10.1167/13.11.6. [PubMed] [Article]

Boremanse, A., Norcia, A. M., & Rossion, B. (2014). Dissociation of part-based and integrated neural responses to faces by means of electroencephalographic frequency tagging. *European Journal of Neuroscience, 40*(6), 2987–2997.

Braddick, O. J., Atkinson, J., & Wattam-Bell, J. R. (1986). Development of the discrimination of spatial phase in infancy. *Vision Research, 26*(8), 1223–1239.

Braddick, O., Birtles, D., Wattam-Bell, J., & Atkinson, J. (2005). Motion- and orientation-specific cortical

responses in infancy. *Vision Research, 45*(25–26), 3169–3179.

Brown, R. J., Candy, T. R., & Norcia, A. M. (1999). Development of rivalry and dichoptic masking in human infants. *Investigative Ophthalmology & Visual Science, 40*(13), 3324–3333, http://www.iovs.org/content/40/13/3324. [PubMed] [Article]

Brown, R. J., & Norcia, A. M. (1997). A method for investigating binocular rivalry in real-time with the steady-state VEP. *Vision Research, 37*(17), 2401–2408.

Buzsaki, G., Anastassiou, C. A., & Koch, C. (2012). The origin of extracellular fields and currents—EEG, ECoG, LFP and spikes. *Nature Reviews Neuroscience, 13*(6), 407–420.

Campbell, F. W., & Kulikowski, J. J. (1972). The visual evoked potential as a function of contrast of a grating pattern. *Journal of Physiology, 222*(2), 345–356.

Campbell, F. W., & Maffei, L. (1970). Electrophysiological evidence for the existence of orientation and size detectors in the human visual system. *Journal of Physiology, 207*(3), 635–652.

Candy, T. R., Skoczenski, A. M., & Norcia, A. M. (2001). Normalization models applied to orientation masking in the human infant. *Journal of Neuroscience, 21*(12), 4530–4541.

Capilla, A., Pazo-Alvarez, P., Darriba, A., Campo, P., & Gross, J. (2011). Steady-state visual evoked potentials can be explained by temporal superposition of transient event-related responses. *PLoS One, 6*(1), e14543.

Chen, Y., Seth, A. K., Gally, J. A., & Edelman, G. M. (2003). The power of human brain magnetoencephalographic signals can be modulated up or down by changes in an attentive visual task. *Proceedings of the National Academy of Sciences, USA, 100*(6), 3501–3506.

Chua, L. O., & Liao, Y. (1991). Measuring Volterra kernels III: How to estimate the highest significant order. *International Journal of Circuit Theory and Applications, 19,* 189–209.

Chun, M. M., Golomb, J. D., & Turk-Browne, N. B. (2011). A taxonomy of external and internal attention. *Annual Review of Psychology, 62,* 73–101.

Cobb, W. A., Morton, H. B., & Ettlinger, G. (1967). Cerebral potentials evoked by pattern reversal and their suppression in visual rivalry. *Nature, 216*(120), 1123–1125.

Cosmelli, D., David, O., Lachaux, J. P., Martinerie, J., Garnero, L., Renault, B., ... Varela, F. (2004). Waves of consciousness: Ongoing cortical patterns during binocular rivalry. *NeuroImage, 23*(1), 128–140.

Cottereau, B. R., Ales, J. M., & Norcia, A. M. (2012). Increasing the accuracy of electromagnetic inverses using functional area source correlation constraints. *Human Brain Mapping, 33*(11), 2694–2713.

Cottereau, B. R., Ales, J. M., & Norcia, A. M. (2014a). How to use fMRI functional localizers to improve EEG/MEG source estimation. *Journal of Neuroscience Methods,* PMC4383720.

Cottereau, B. R., Ales, J. M., & Norcia, A. M. (2014b). The evolution of a disparity decision in human visual cortex. *NeuroImage, 92,* 193–206.

Cottereau, B. R., McKee, S. P., Ales, J. M., & Norcia, A. M. (2011). Disparity-tuned population responses from human visual cortex. *Journal of Neuroscience, 31*(3), 954–965.

Cottereau, B. R., McKee, S. P., Ales, J. M., & Norcia, A. M. (2012). Disparity-specific spatial interactions: Evidence from EEG source imaging. *Journal of Neuroscience, 32*(3), 826–840.

Cottereau, B. R., McKee, S. P., & Norcia, A. M. (2012). Bridging the gap: Global disparity processing in the human visual cortex. *Journal of Neurophysiology, 107*(9), 2421–2429.

Cottereau, B. R., McKee, S. P., & Norcia, A. M. (2014). Dynamics and cortical distribution of neural responses to 2D and 3D motion in human. *Journal of Neurophysiology, 111*(3), 533–543.

Dannhauer, M., Lanfer, B., Wolters, C. H., & Knosche, T. R. (2011). Modeling of the human skull in EEG source analysis. *Human Brain Mapping, 32*(9), 1383–1399.

Davila, C. E., Srebro, R., & Ghaleb, I. A. (1998). Optimal detection of visual evoked potentials. *IEEE Transactions on Biomedical Engineering, 45*(6), 800–803.

Dawson, G. D. (1954). A summation technique for the detection of small evoked potentials. *Electroencephalography and Clinical Neurophysiology, 6*(1), 65–84.

Di Russo, F., Pitzalis, S., Aprile, T., Spitoni, G., Patria, F., ... Hillyard, S.A. (2007). Spatiotemporal analysis of the cortical sources of the steady-state visual evoked potential. *Human Brain Mapping, 28*(4), 232–334.

Di Russo, F., Spinelli, D., & Morrone, M. C. (2001). Automatic gain control contrast mechanisms are modulated by attention in humans: Evidence from visual evoked potentials. *Vision Research, 41*(19), 2435–2447.

Ding, J., Sperling, G., & Srinivasan, R. (2006).

Attentional modulation of SSVEP power depends on the network tagged by the flicker frequency. *Cerebral Cortex, 16*(7), 1016–1029.

Eizenman, M., Westall, C. A., Geer, I., Smith, K., Chatterjee, S., Panton, C. M., … Skarf, B. (1999). Electrophysiological evidence of cortical fusion in children with early- onset esotropia. *Investigative Ophthalmology & Visual Science, 40*(2), 354–362, http://www.iovs.org/content/40/2/354. [PubMed] [Article]

Ellis, K. A., Silberstein, R. B., & Nathan, P. J. (2006). Exploring the temporal dynamics of the spatial working memory *n*-back task using steady state visual evoked potentials (SSVEP). *NeuroImage, 31*(4), 1741–1751.

Farzin, F., Hou, C., & Norcia, A. M. (2012). Piecing it together: Infants' neural responses to face and object structure. *Journal of Vision, 12*(13):6, 1–14, http://www.journalofvision.org/content/12/13/6, doi:10.1167/12.13.6. [PubMed] [Article]

Fawcett, I. P., Barnes, G. R., Hillebrand, A., & Singh, K. D. (2004). The temporal frequency tuning of human visual cortex investigated using synthetic aperture magnetometry. *NeuroImage, 21*(4), 1542–1553.

Fiorentini, A., & Trimarchi, C. (1992). Development of temporal properties of pattern electroretinogram and visual evoked potentials in infants. *Vision Research, 32*(9), 1609–1621.

Freire, A., Lee, K., & Symons, L. A. (2000). The face-inversion effect as a deficit in the encoding of configural information: Direct evidence. *Perception, 29*(2), 159–170.

Friman, O., Volosyak, I., & Graser, A. (2007). Multiple channel detection of steady-state visual evoked potentials for brain–computer interfaces. *IEEE Transactions of Biomedical Engineering, 54*(4), 742–750.

Fuchs, S., Andersen, S. K., Gruber, T., & Muller, M. M. (2008). Attentional bias of competitive interactions in neuronal networks of early visual processing in the human brain. *NeuroImage, 41*(3), 1086–1101.

Galambos, R., Makeig, S., & Talmachoff, P. J. (1981). A 40-Hz auditory potential recorded from the human scalp. *Proceedings of the National Academy of Sciences, USA, 78*(4), 2643–2647.

Garcia, J. O., Srinivasan, R., & Serences, J. T. (2013). Near-real-time feature-selective modulations in human cortex. *Current Biology, 23*(6), 515–522.

Garcia Molina, G., & Zhu, D. (2011). *Optimal spatial filtering for the steady-state visual evoked potential: BCI application*. Paper presented at the Proc. IEEE EMBS Neural Eng.

Geisler, W. S., & Albrecht, D. G. (1992). Cortical neurons: Isolation of contrast gain control. *Vision Research, 32*(8), 1409–1410.

Giani, A. S., Ortiz, E., Belardinelli, P., Kleiner, M., Preissl, H., & Noppeney, U. (2012). Steady-state responses in MEG demonstrate information integration within but not across the auditory and visual senses. *NeuroImage, 60*(2), 1478–1489.

Grech, R., Cassar, T., Muscat, J., Camilleri, K. P., Fabri, S. G., Zervakis, M., … Vanrumste, B. (2008). Review on solving the inverse problem in EEG source analysis. *Journal of Neuro-engineering and Rehabilitation, 5,* 25, 10.1186/1743-0003-5-25.

Gruss, L. F., Wieser, M. J., Schweinberger, S. R., & Keil, A. (2012). Face-evoked steady-state visual potentials: Effects of presentation rate and face inversion. *Frontiers of Human Neuroscience, 6,* 316, 10.3389/fnhum.2012.00316.

Gundlach, C., & Muller, M. M. (2013). Perception of illusory contours forms intermodulation responses of steady state visual evoked potentials as a neural signature of spatial integration. *Biological Psychology, 94*(1), 55–60.

Hamalainen, M., Ilmoniemi, R., Knuutila, J., & Lounasmaa, O. (1993). Magnetoencephalography: theory, instrumentation and applications to the non-invasive study of human brain function. *Reviews of Modern Physics, 65,* 413–497.

Handel, B., Lutzenberger, W., Thier, P., & Haarmeier, T. (2007). Opposite dependencies on visual motion coherence in human area MT+ and early visual cortex. *Cerebral Cortex, 17*(7), 1542–1549.

Handy, T. C. (2005). *Event-related potential: A methods handbook*. Cambridge, MA: MIT Press.

Heeger, D. J. (1992). Normalization of cell responses in cat striate cortex. *Visual Neuroscience, 9*(2), 181–197.

Heinrich, S. P. (2010). Some thoughts on the interpretation of steady-state evoked potentials. *Documenta Ophthalmologica, 120*(3), 205–214.

Heinrich, S. P., Mell, D., & Bach, M. (2009). Frequency-domain analysis of fast oddball responses to visual stimuli: A feasibility study. *International Journal of Psychophysiology, 73*(3), 287–293.

Herrmann, C. S. (2001). Human EEG responses to 1-100 Hz flicker: Resonance phenomena in visual cortex and their potential correlation to cognitive phenomena. *Experimental Brain Research, 137*(3–4), 346–353.

Hillyard, S. A., Hink, R. F., Schwent, V. L., & Picton, T. W. (1973, October 12). Electrical signs of selective attention in the human brain. *Science, 182*(4108), 177–180.

Hillyard, S. A., Hinrichs, H., Tempelmann, C., Morgan, S. T., Hansen, J. C., Scheich, H., & Heinze, H. J. (1997). Combining steady-state visual evoked potentials and fMRI to localize brain activity during selective attention. *Human Brain Mapping, 5*(4), 287–292.

Hindi Attar, C., Andersen, S. K., & Muller, M. M. (2010). Time course of affective bias in visual attention: Convergent evidence from steady-state visual evoked potentials and behavioral data. *NeuroImage, 53*(4), 1326–1333.

Hoffmann, M. B., Unsold, A. S., & Bach, M. (2001). Directional tuning of human motion adaptation as reflected by the motion VEP. *Vision Research, 41*(17), 2187–2194.

Hou, C., Good, W. V., & Norcia, A. M. (2007). Validation study of VEP vernier acuity in normal-vision and amblyopic adults. *Investigative Ophthalmology & Visual Science, 48*(9), 4070–4078, http://www.iovs.org/content/48/9/4070. [PubMed] [Article]

Hou, C., Pettet, M. W., & Norcia, A. M. (2008). Abnormalities of coherent motion processing in strabismic amblyopia: Visual-evoked potential measurements. *Journal of Vision, 8*(4):2, 1–12, http://www.journalofvision.org/content/8/4/2, doi: 10.1167/8.4.2. [PubMed] [Article]

Hou, C., Pettet, M. W., Vildavski, V. Y., & Norcia, A. M. (2006). Neural correlates of shape-from-shading. *Vision Research, 46*(6-7), 1080–1090.

Hubel, D. H., & Wiesel, T. N. (1965). Receptive fields and functional architecture in two nonstriate visual areas (18 and 19) of the cat. *Journal of Neurophysiology, 28,* 229–289.

Hubel, D. H., & Wiesel, T. N. (1968). Receptive fields and functional architecture of monkey striate cortex. *Journal of Physiology, 195*(1), 215–243.

Jonas, J., Rossion, B., Krieg, J., Koessler, L., Colnat-Coulbois, S., Vespignani, H., ... Maillard, L. (2014). Intracerebral electrical stimulation of a face-selective area in the right inferior occipital cortex impairs individual face discrimination. *NeuroImage, 99,* 487–497.

Julesz, B., & Kropfl, W. (1982). Binocular neurons and cyclopean visually evoked potentials in monkey and man. *Annals of the New York Academy of Sciences, 388,* 37–44.

Julesz, B., Kropfl, W., & Petrig, B. (1980). Large evoked potentials to dynamic random-dot correlograms and stereograms permit quick determination of stereopsis. *Proceedings of the National Academy of Sciences, USA, 77*(4), 2348–2351.

Kamp, A., Sem-Jacobsen, C. W. Storm van Leeuwen, W., & van der Tweel, T. L. (1960). Cortical responses to modulated light in the human subject. *Acta Physiologica Scandinavica, 48,* 1–12.

Kashiwase, Y., Matsumiya, K., Kuriki, I., & Shioiri, S. (2012). Time courses of attentional modulation in neural amplification and synchronization measured with steady-state visual-evoked potentials. *Journal of Cognitive Neuroscience, 24*(8), 1779–1793.

Kaspar, K., Hassler, U., Martens, U., Trujillo-Barreto, N., & Gruber, T. (2010). Steady-state visually evoked potential correlates of object recognition. *Brain Research, 1343,* 112–121.

Keil, A., Gruber, T., Muller, M. M., Moratti, S., Stolarova, M., Bradley, M. M., ... Lang, P. J. (2003). Early modulation of visual perception by emotional arousal: Evidence from steady-state visual evoked brain potentials. *Cognitive, Affective & Behavioral Neuroscience, 3*(3), 195–206.

Keitel, C., Quigley, C., & Ruhnau, P. (2014). Stimulus-driven brain oscillations in the alpha range: Entrainment of intrinsic rhythms or frequency-following response? *Journal of Neuroscience, 34*(31), 10137–10140.

Kim, Y. J., Grabowecky, M., Paller, K. A., Muthu, K., & Suzuki, S. (2007). Attention induces synchronization-based response gain in steady-state visual evoked potentials. *Nature Neuroscience, 10*(1), 117–125.

Kimura, M., Kondo, H., Ohira, H., & Schroger, E. (2012). Unintentional temporal context-based prediction of emotional faces: An electrophysiological study. *Cerebral Cortex, 22*(8), 1774–1785.

Klimesch, W. (2012). Alpha-band oscillations, attention, and controlled access to stored information. *Trends in Cognitive Sciences, 16*(12), 606–617.

Lam, K., Kaneoke, Y., Gunji, A., Yamasaki, H., Matsumoto, E., Naito, T., ... Kakigi, K. (2000). Magnetic response of human extrastriate cortex in the detection of coherent and incoherent motion. *Neuroscience, 97*(1), 1–10.

Lamme, V. A., Van Dijk, B. W., & Spekreijse, H. (1992). Texture segregation is processed by primary visual cortex in man and monkey. Evidence from VEP experiments. *Vision Research, 32*(5), 797–807.

Lansing, R. W. (1964, December 4). Electroencephalographic correlates of binocular rivalry in man. *Science, 146,* 1325–1327.

Lauritzen, T. Z., Ales, J. M., & Wade, A. R. (2010).

The effects of visuospatial attention measured across visual cortex using source-imaged, steady-state EEG. *Journal of Vision, 10*(14):39, 1–17, http://www.journalofvision.org/content/10/14/39, doi:10.1167/10.14.39. [PubMed] [Article]

Lee, J., Birtles, D., Wattam-Bell, J., Atkinson, J., & Braddick, O. (2012). Latency measures of pattern-reversal VEP in adults and infants: Different information from transient P1 response and steady-state phase. *Investigative Ophthalmology & Visual Science, 53*(3), 1306–1314, http://www.iovs.org/content/53/3/1306. [PubMed] [Article]

Liu-Shuang, J., Norcia, A. M., & Rossion, B. (2014). An objective index of individual face discrimination in the right occipito-temporal cortex by means of fast periodic oddball stimulation. *Neuropsychologia, 52,* 57–72.

Lochy, A., Van Belle, G., & Rossion, B. (2014). A robust index of lexical representation in the left occipito-temporal cortex as evidenced by EEG responses to fast periodic visual stimulation. *Neuropsychologia, 66C,* 18–31.

Lopes da Silva, F. H., van Rotterdam, A., Storm van Leeuwen, W., & Tielen, A. M. (1970). Dynamic characteristics of visual evoked potentials in the dog. II. Beta frequency selectivity in evoked potentials and background activity. *Electroencephalography and Clinical Neurophysiology, 29*(3), 260–268.

Lorenceau, J., & Shiffrar, M. (1992). The influence of terminators on motion integration across space. *Vision Research, 32*(2), 263–273.

Luck, S. J. (2005). *An introduction to the event-related potential technique*. Cambridge, MA: MIT Press.

Luck, S. J., & Kappenman, E. S. (2012). *The Oxford handbook of event-related potential components*. Oxford, UK: Oxford University Press.

Makeig, S., Westerfield, M., Jung, T. P., Enghoff, S., Townsend, J., Courchesne, E., ... Sejnowski, T. J. (2002, January 25). Dynamic brain sources of visual evoked responses. *Science, 295*(5555), 690–694.

Malach, R., Reppas, J. B., Benson, R. R., Kwong, K. K., Jiang, H., Kennedy, W. A., ... Tootell, R. B. H. (1995). Object-related activity revealed by functional magnetic resonance imaging in human occipital cortex. *Proceedings of the National Academy of Sciences, USA, 92*(18), 8135–8139.

Malinowski, P., Fuchs, S., & Muller, M. M. (2007). Sustained division of spatial attention to multiple locations within one hemifield. *Neuroscience Letters, 414*(1), 65–70.

Maris, E., & Oostenveld, R. (2007). Nonparametric statistical testing of EEG- and MEG-data. *Journal of Neuroscience Methods, 164*(1), 177–190.

Marmarelis, V. (2004). *Non-linear modeling of physiological systems*. Piscataway, NY: IEEE Press.

Mayes, A. K., Pipingas, A., Silberstein, R. B., & Johnston, P. (2009). Steady state visually evoked potential correlates of static and dynamic emotional face processing. *Brain Topography, 22*(3), 145–157.

McTeague, L. M., Shumen, J. R., Wieser, M. J., Lang, P. J., & Keil, A. (2011). Social vision: Sustained perceptual enhancement of affective facial cues in social anxiety. *NeuroImage, 54*(2), 1615–1624.

Meigen, T., & Bach, M. (1999). On the statistical significance of electrophysiological steady-state responses. *Documenta Ophthalmologica, 98*(3), 207–232.

Millodot, M., & Riggs, L. A. (1970). Refraction determined electrophysiologically. Responses to alternation of visual contours. *Archives of Ophthalmology, 84*(3), 272–278.

Mitzdorf, U., & Singer, W. (1979). Excitatory synaptic ensemble properties in the visual cortex of the macaque monkey: A current source density analysis of electrically evoked potentials. *Journal of Comparative Neurology, 187*(1), 71–83.

Moratti, S., Keil, A., & Stolarova, M. (2004). Motivated attention in emotional picture processing is reflected by activity modulation in cortical attention networks. *NeuroImage, 21*(3), 954–964.

Morgan, S. T., Hansen, J. C., & Hillyard, S. A. (1996). Selective attention to stimulus location modulates the steady-state visual evoked potential. *Proceedings of the National Academy of Sciences, USA, 93*(10), 4770–4774.

Muller, M. M., Andersen, S., Trujillo, N. J., Valdes-Sosa, P., Malinowski, P., & Hillyard, S. A. (2006). Feature-selective attention enhances color signals in early visual areas of the human brain. *Proceedings of the National Academy of Sciences, USA, 103*(38), 14250–14254.

Muller, M. M., & Hubner, R. (2002). Can the spotlight of attention be shaped like a doughnut? Evidence from steady-state visual evoked potentials. *Psychological Science, 13*(2), 119–124.

Muller, M. M., Malinowski, P., Gruber, T., & Hillyard, S. A. (2003). Sustained division of the attentional spotlight. *Nature, 424*(6946), 309–312.

Muller, M. M., Picton, T. W., Valdes-Sosa, P., Riera, J., Teder-Salejarvi, W. A., & Hillyard, S. A. (1998). Effects of spatial selective attention on the steady-state visual evoked potential in the 20-28 Hz range.

Brain Research, Cognitive Brain Research, 6(4), 249–261.

Muller, M. M., Teder, W., & Hillyard, S. A. (1997). Magnetoencephalographic recording of steady-state visual evoked cortical activity. *Brain Topography, 9*(3), 163–168.

Muller, M. M., Teder-Salejarvi, W., & Hillyard, S. A. (1998). The time course of cortical facilitation during cued shifts of spatial attention. *Nature Neuroscience, 1*(7), 631–634.

Naatanen, R. (1975). Selective attention and evoked potentials in humans—A critical review. *Biological Psychology, 2*(4), 237–307.

Naatanen, R. (1990). The role of attention in auditory information processing as revealed by event-related potentials and other brain measures of cognitive function. *Behavioral Brain Research, 13,* 201–233.

Nakamura, H., Kashii, S., Nagamine, T., Matsui, Y., Hashimoto, T., Honda, Y., ... Shibasaki, H. (2003). Human V5 demonstrated by magnetoencephalography using random dot kinematograms of different coherence levels. *Neuroscience Research, 46*(4), 423–433.

Nelson, J. I., Kupersmith, M. J., Seiple, W. H., Weiss, P. A., & Carr, R. E. (1984). Spatiotemporal conditions which elicit or abolish the oblique effect in man: Direct measurement with swept evoked potential. *Vision Research, 24*(6), 579–586.

Nelson, J. I., Seiple, W. H., Kupersmith, M. J., & Carr, R. E. (1984). Lock-in techniques for the swept stimulus evoked potential. *Journal of Clinical Neurophysiology, 1*(4), 409–436.

Niedeggen, M., & Wist, E. R. (1999). Characteristics of visual evoked potentials generated by motion coherence onset. *Brain Research, Cognitive Brain Research, 8*(2), 95–105.

Norcia, A. M. (1996). Abnormal motion processing and binocularity: Infantile esotropia as a model system for effects of early interruptions of binocularity. *Eye, 10*(Pt 2), 259–265.

Norcia, A. M., Candy, T. R., Pettet, M. W., Vildavski, V. Y., & Tyler, C. W. (2002). Temporal dynamics of the human response to symmetry. *Journal of Vision, 2*(2):1, 132–139, http://www.journalofvision.org/content/2/2/1, doi:10.1167/2.2.1. [PubMed] [Article]

Norcia, A. M., Clarke, M., & Tyler, C. W. (1985). Digital filtering and robust regression techniques for estimating sensory thresholds from the evoked potential. *IEEE Engineering in Medicine and Biology Magazine, 4,* 26–32.

Norcia, A. M., Pei, F., Bonneh, Y., Hou, C., Sampath, V., & Pettet, M. W. (2005). Development of sensitivity to texture and contour information in the human infant. *Journal of Cognitive Neuroscience, 17*(4), 569–579.

Norcia, A. M., Sampath, V., Hou, C., & Pettet, M. W. (2005). Experience-expectant development of contour integration mechanisms in human visual cortex. *Journal of Vision, 5*(2):3, 116–130, http://www.journalofvision.org/content/5/2/3, doi:10.1167/5.2.3 .[PubMed] [Article]

Norcia, A. M., & Tyler, C. W. (1985). Spatial frequency sweep VEP: Visual acuity during the first year of life. *Vision Research, 25*(10), 1399–1408.

Norcia, A. M., Tyler, C. W., & Hamer, R. D. (1990). Development of contrast sensitivity in the human infant. *Vision Research, 30*(10), 1475–1486.

Norcia, A. M., Tyler, C. W., Hamer, R. D., & Wesemann, W. (1989). Measurement of spatial contrast sensitivity with the swept contrast VEP. *Vision Research, 29*(5), 627–637.

Norcia, A. M., Wesemann, W., & Manny, R. E. (1999). Electrophysiological correlates of vernier and relative motion mechanisms in human visual cortex. *Visual Neuroscience, 16*(6), 1123–1131.

Nozaradan, S., Peretz, I., & Mouraux, A. (2012). Selective neuronal entrainment to the beat and meter embedded in a musical rhythm. *Journal of Neuroscience, 32*(49), 17572–17581.

Painter, D. R., Dux, P. E., Travis, S. L., & Mattingley, J. B. (2014). Neural responses to target features outside a search array are enhanced during conjunction but not unique-feature search. *Journal of Neuroscience, 34*(9), 3390–3401.

Palomares, M., Ales, J. M., Wade, A. R., Cottereau, B. R., & Norcia, A. M. (2012). Distinct effects of attention on the neural responses to form and motion processing: A SSVEP source-imaging study. *Journal of Vision, 12*(10):15, 1–14, http://www.journalofvision.org/content/12/10/15, doi:10.1167/12.10.15. [PubMed] [Article]

Parkkonen, L., Andersson, J., Hamalainen, M., & Hari, R. (2008). Early visual brain areas reflect the percept of an ambiguous scene. *Proceedings of the National Academy of Sciences, USA, 105*(51), 20500–20504.

Pazo-Alvarez, P., Cadaveira, F., & Amenedo, E. (2003). MMN in the visual modality: A review. *Biological Psychology, 63*(3), 199–236.

Pei, F., Pettet, M. W., & Norcia, A. M. (2002). Neural correlates of object-based attention. *Journal of Vision, 2*(9):1, 588–596, http://www.journalofvision.org/content/2/9/1, doi:10.1167/2.9.1. [PubMed] [Article]

Pei, F., Pettet, M. W., Vildavski, V. Y., & Norcia, A. M. (2005). Event-related potentials show configural specificity of global form processing. *NeuroReport, 16*(13), 1427–1430.

Perlstein, W. M., Cole, M. A., Larson, M., Kelly, K., Seignourel, P., & Keil, A. (2003). Steady-state visual evoked potentials reveal frontally-mediated working memory activity in humans. *Neuroscience Letters, 342*(3), 191–195.

Peterson, D. J., Gurariy, G., Dimotsantos, G. G., Arciniega, H., Berryhill, M. E., & Caplovitz, G. P. (2014). The steady-state visual evoked potential reveals neural correlates of the items encoded into visual working memory. *Neuropsychologia, 63,* 145–153.

Picton, T. W., Vajsar, J., Rodriguez, R., & Campbell, K. B. (1987). Reliability estimates for steady-state evoked potentials. *Electroencephalography and Clinical Neurophysiology, 68*(2), 119–131.

Priebe, N. J., Lampl, I., & Ferster, D. (2010). Mechanisms of direction selectivity in cat primary visual cortex as revealed by visual adaptation. *Journal of Neurophysiology, 104*(5), 2615–2623.

Ratliff, F., & Zemon, V. (1982). Some new methods for the analysis of lateral interactions that influence the visual evoked potential. *Annals of the New York Academy of Sciences, 388,* 113–124.

Regan, D. (1964). *A study of the visual system by the correlation of light stimuli and evoked electrical response*. London, UK: Imperial College London.

Regan, D. (1966). Some characteristics of average steady-state and transient responses evoked by modulated light. *Electroencephalography and Clinical Neurophysiology, 20*(3), 238–248.

Regan, D. (1973). Rapid objective refraction using evoked brain potentials. *Investigative Ophthalmology & Visual Science, 12*(9), 669–679, http://www.iovs.org/content/12/9/669. [PubMed] [Article]

Regan, D. (1975). Colour coding of pattern responses in man investigated by evoked potential feedback and direct plot techniques. *Vision Research, 15*(2), 175–183.

Regan, D. (1977). Speedy assessment of visual acuity in amblyopia by the evoked potential method. *Ophthalmologica, 175*(3), 159–164.

Regan, D. (1989). *Human brain electrophysiology: Evoked potentials and evoked magnetic fields in science and medicine*. Amsterdam, the Netherlands: Elsevier.

Regan, D., & Cartwright, R. F. (1970). A method of measuring the potentials evoked by simultaneous stimulation of different retinal regions. *Electroencephalography and Clinical Neurophysiology, 28*(3), 314–319.

Regan, D., & Heron, J. R. (1969). Clinical investigation of lesions of the visual pathway: A new objective technique. *Journal of Neurology, Neurosurgery & Psychiatry, 32*(5), 479–483.

Regan, D., & Regan, M. P. (1988). A frequency domain technique for characterizing nonlinearities in biological systems. *Journal of Theoretical Biology, 133,* 293–317.

Regan, M. P., He, P., & Regan, D. (1995). An audio-visual convergence area in the human brain. *Experimental Brain Research, 106*(3), 485–487.

Regan, M. P., & Regan, D. (1989). Objective investigation of visual function using a nondestructive zoom-FFT technique for evoked potential analysis. *Canadian Journal of Neurological Science, 16*(2), 168–179.

Robson, J. G. (1988). Linear and nonlinear operations of the visual system. *Investigative Ophthalmology & Visual Science, 32,* 429.

Rossion, B. (2013). The composite face illusion: A window on our understanding of holistic face perception. *Visual Cognition, 121,* 139–253.

Rossion, B. (2014). Understanding individual face discrimination by means of fast periodic visual stimulation. *Experimental Brain Research, 232*(6), 1599–1621.

Rossion, B., & Boremanse, A. (2011). Robust sensitivity to facial identity in the right human occipito-temporal cortex as revealed by steady-state visual-evoked potentials. *Journal of Vision, 11*(2):16, 1–21, http://www.journalofvision.org/content/11/2/16, doi:10.1167/11.2.16. [PubMed] [Article]

Rossion, B., & Jacques, C. (2011). The N170: Understanding the time course of face perception in the human brain. In S. J. Luck & E. S. Kappenman (Eds.), *The Oxford handbook of event-related potential components* (pp. 115–141). New York: Oxford University Press.

Rossion, B., Prieto, E. A., Boremanse, A., Kuefner, D., & Van Belle, G. (2012). A steady-state visual evoked potential approach to individual face perception: Effect of inversion, contrast-reversal and temporal dynamics. *NeuroImage, 63*(3), 1585–1600, doi:10.3389/fpsyg.2012.00131.

Rossion, B., Torfs, K., Jacques, C., & Liu-Shuang, J. (2015). Fast periodic presentation of natural images reveals a robust face-selective electrophysiological response in the human brain. *Journal of Vision, 15*(1):18, 1–18, http://www.journalofvision.org/content/15/1/18, doi:10.1167/15.1.18. [PubMed] [Article]

Rousselet, G. A. (2012). Does filtering preclude us from studying ERP time-courses? *Frontiers in Psychology, 3,* 131.

Russell, R., Sinha, P., Biederman, I., & Nederhouser, M. (2006). Is pigmentation important for face recognition? Evidence from contrast negation. *Perception, 35*(6), 749–759.

Saupe, K., Schroger, E., Andersen, S. K., & Muller, M. M. (2009). Neural mechanisms of intermodal sustained selective attention with concurrently presented auditory and visual stimuli. *Frontiers of Human Neuroscience, 3,* 58 doi:10.3389/neuro.09.058.2009.

Sayers, B. M., Beagley, H. A., & Henshall, W. R. (1974). The mechanism of auditory evoked EEG responses. *Nature, 247*(5441), 481–483.

Shah, A. S., Bressler, S. L., Knuth, K. H., Ding, M., Mehta, A. D., Ulbert, I., ... Schroeder, C. E. (2004). Neural dynamics and the fundamental mechanisms of event-related brain potentials. *Cerebral Cortex, 14*(5), 476–483.

Shapley, R. M., & Victor, J. D. (1978). The effect of contrast on the transfer properties of cat retinal ganglion cells. *Journal of Physiology, 285,* 275–298.

Sharon, D., Hamalainen, M. S., Tootell, R. B., Halgren, E., & Belliveau, J. W. (2007). The advantage of combining MEG and EEG: Comparison to fMRI in focally stimulated visual cortex. *NeuroImage, 36*(4), 1225–1235.

Silberstein, R. B., Nunez, P. L., Pipingas, A., Harris, P., & Danieli, F. (2001). Steady state visually evoked potential (SSVEP) topography in a graded working memory task. *International Journal of Psychophysiology, 42*(2), 219–232.

Silberstein, R. B., Schier, M. A., Pipingas, A., Ciorciari, J., Wood, S. R., & Simpson, D. G. (1990). Steady-state visually evoked potential topography associated with a visual vigilance task. *Brain Topography, 3*(2), 337–347.

Skoczenski, A. M., & Norcia, A. M. (2002). Late maturation of visual hyperacuity. *Psychological Science, 13*(6), 537–541.

Spaak, E., de Lange, F. P., & Jensen, O. (2014). Local entrainment of alpha oscillations by visual stimuli causes cyclic modulation of perception. *Journal of Neuroscience, 34*(10), 3536–3544.

Spekreijse, H. (1967). *Analysis of EEG responses in man*. The Hague, the Netherlands: University of Amsterdam.

Spekreijse, H. (1978). Maturation of contrast EPs and development of visual resolution. *Archives Italiennes de Biologie, 116*(3-4), 358–369.

Spekreijse, H., & Oosting, H. (1970). Linearizing: A method for analysing and synthesizing nonlinear systems. *Kybernetik, 7*(1), 22–31.

Spekreijse, H., & Reits, D. (1982). Sequential analysis of the visual evoked potential system in man: Nonlinear analysis of a sandwich system. *Annals of the New York Academy of Sciences, 388,* 72–97.

Spekreijse, H., van der Twell, L. H., & Zuidema, T. (1973). Contrast evoked responses in man. *Vision Research, 13*(8), 1577–1601.

Srinivasan, R., Bibi, F. A., & Nunez, P. L. (2006). Steady-state visual evoked potentials: Distributed local sources and wave-like dynamics are sensitive to flicker frequency. *Brain Topography, 18*(3), 167–187.

Srinivasan, R., Russell, D. P., Edelman, G. M., & Tononi, G. (1999). Increased synchronization of neuromagnetic responses during conscious perception. *Journal of Neuroscience, 19*(13), 5435–5448.

Stormer, V. S., & Alvarez, G. A. (2014). Feature-based attention elicits surround suppression in feature space. *Current Biology, 24*(17), 1985–1988.

Stormer, V. S., Alvarez, G. A., & Cavanagh, P. (2014). Within-hemifield competition in early visual areas limits the ability to track multiple objects with attention. *Journal of Neuroscience, 34*(35), 11526–11533.

Stormer, V. S., Winther, G. N., Li, S. C., & Andersen, S. K. (2013). Sustained multifocal attentional enhancement of stimulus processing in early visual areas predicts tracking performance. *Journal of Neuroscience, 33*(12), 5346–5351.

Strasburger, H. (1987). The analysis of steady state evoked potentials revisited. *Clinical Vision Science, 1*(3), 245–256.

Sutoyo, D., & Srinivasan, R. (2009). Nonlinear SSVEP responses are sensitive to the perceptual binding of visual hemifields during conventional "eye" rivalry and interocular "percept" rivalry. *Brain Research, 1251,* 245–255.

Sutter, E. E. (2001). Imaging visual function with the multifocal m-sequence technique. *Vision Research, 41*(10–11), 1241–1255.

Sutton, S., Braren, M., Zubin, J., & John, E. R. (1965, November 26). Evoked-potential correlates of stimulus uncertainty. *Science, 150*(3700), 1187–1188.

Tanaka, J. W., & Farah, M. J. (1993). Parts and wholes in face recognition. *Quarterly Journal of Experimental Psychology A, 46*(2), 225–245.

Tang, Y., & Norcia, A. M. (1995). An adaptive filter

for steady-state evoked responses. *Electroencephalography and Clinical Neurophysiology, 96*(3), 268–277.

Toffanin, P., de Jong, R., Johnson, A., & Martens, S. (2009). Using frequency tagging to quantify attentional deployment in a visual divided attention task. *International Journal of Psychophysiology, 72*(3), 289–298.

Tononi, G., Srinivasan, R., Russell, D. P., & Edelman, G. M. (1998). Investigating neural correlates of conscious perception by frequency-tagged neuromagnetic responses. *Proceedings of the National Academy of Sciences, USA, 95*(6), 3198–3203.

Tsai, J. J., Wade, A. R., & Norcia, A. M. (2012). Dynamics of normalization underlying masking in human visual cortex. *Journal of Neuroscience, 32*(8), 2783–2789.

Tyler, C. W., Apkarian, P., Levi, D. M., & Nakayama, K. (1979). Rapid assessment of visual function: An electronic sweep technique for the pattern visual evoked potential. *Investigative Ophthalmology & Visual Science, 18*(7), 703–713, http://www.iovs.org/content/18/7/703. [PubMed] [Article]

Tyler, C. W., & Kaitz, M. (1977). Movement adaptation in the visual evoked response. *Experimental Brain Research, 27*(2), 203–209.

Van Der Tweel, L. H., & Lunel, H. F. (1965). Human visual responses to sinusoidally modulated light. *Electroencephalography and Clinical Neurophysiology, 18,* 587–598.

van der Tweel, L. H., & Spekreijse, H. (1969). Signal transport and rectification in the human evoked-response system. *Annals of the New York Academy of Sciences, 156*(2), 678–695.

Vaughan, H. G., Jr. (Ed.). (1969). *The relationship of brain activity to scalp recordings of event-related potentials*. Washington, DC: National Aeronautics and Space Administration.

Verghese, P., Kim, Y. J., & Wade, A. R. (2012). Attention selects informative neural populations in human V1. *Journal of Neuroscience, 32*(46), 16379–16390.

Vialatte, F. B., Maurice, M., Dauwels, J., & Cichocki, A. (2010). Steady-state visually evoked potentials: Focus on essential paradigms and future perspectives. *Progress in Neurobiology, 90*(4), 418–438.

Victor, J. D., & Conte, M. M. (2000). Two-frequency analysis of interactions elicited by Vernier stimuli. *Visual Neuroscience, 17*(6), 959–973.

Victor, J. D., & Mast, J. (1991). A new statistic for steady-state evoked potentials. *Electroencephalography and Clinical Neurophysiology, 78*(5), 378–388.

Wagemans, J., Elder, J. H., Kubovy, M., Palmer, S. E., Peterson, M. A., Singh, M., ... von der Heydt, R. (2012). A century of Gestalt psychology in visual perception: I. Perceptual grouping and figure-ground organization. *Psychological Bulletin, 138*(6), 1172–1217.

Walter, W. G., Dovey, V. J., & Shipton, H. (1946). Analysis of the electrical response of the human cortex to photic stimulation. *Nature, 158,* 540–541.

Wattam-Bell, J. (1991). Development of motion-specific cortical responses in infancy. *Vision Research, 31*(2), 287–297.

Wattam-Bell, J., Birtles, D., Nystrom, P., von Hofsten, C., Rosander, K., Anker, S., ... Braddick, O. (2010). Reorganization of global form and motion processing during human visual development. *Current Biology, 20*(5), 411–415.

Wieser, M. J., & Keil, A. (2011). Temporal trade-off effects in sustained attention: dynamics in visual cortex predict the target detection performance during distraction. *Journal of Neuroscience, 31*(21), 7784–7790.

Winawer, J., Kay, K. N., Foster, B. L., Rauschecker, A. M., Parvizi, J., & Wandell, B. A. (2013). Asynchronous broadband signals are the principal source of the BOLD response in human visual cortex. *Current Biology, 23*(13), 1145–1153.

Zemon, V., & Ratliff, F. (1982). Visual evoked potentials: Evidence for lateral interactions. *Proceedings of the National Academy of Sciences, USA, 79*(18), 5723–5726.

Zemon, V., & Ratliff, F. (1984). Intermodulation components of the visual evoked potential: Responses to lateral and superimposed stimuli. *Biological Cybernetics, 50*(6), 401–408.

Zemon, V., Victor, J. D., & Ratliff, F. (1986). Functional subsystems in the visual pathways of humans characterized using evoked potentials. In R. Q. Cracco & I. Bodis-Wollner (Eds.), *Evoked potentials: Frontiers of clincal neuroscience*, Vol. 3 (pp. 203-210). New York: Alan R. Liss, Inc.

Zhang, P., Jamison, K., Engel, S., He, B., & He, S. (2011). Binocular rivalry requires visual attention. *Neuron, 71*(2), 362–369.

Zhu, D., Bieger, J., Garcia Molina, G., & Aarts, R. M. (2010). A survey of stimulation methods used in SSVEP-based BCIs. *Computational Intelligence & Neuroscience,* 702357, doi:10.1155/2010/702357.

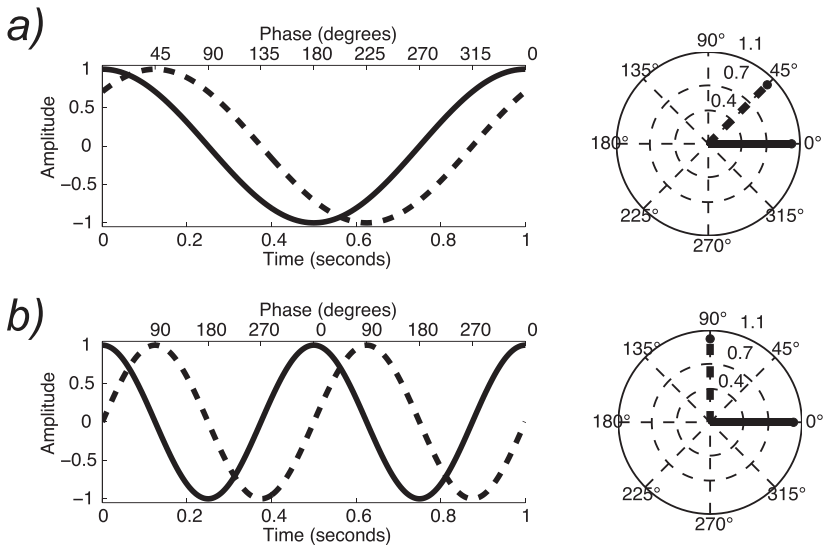

Figure A1. Schematic showing a response of two systems, one with no delay (solid lines) and one with a 0.125-s delay. (a) Waveforms and phasor diagram for 1-Hz input, showing that a 0.125-s delay translates to a 45° phase angle. (b) Waveforms and phasor diagram for a 2-Hz input, showing that the same 0.125-s delay causes a 90° phase angle.

Appendices

Appendix 1. Estimating delay from SSVEP responses

One of the advantages of EEG recording is that it can measure activity on the scale of milliseconds. This level of temporal resolution enables the measurement of the dynamics of brain processes at their native time scale. An important parameter of response dynamics is response latency, i.e., the time it takes for a response to be generated after the stimulus is present. This concept is straightforward in the time domain, where a commonly used latency measure is the first deviation of a signal from baseline. However, this latency is difficult to quantify because it requires measuring signals that are at the edge of detectability. An arbitrary choice must be made as to what constitutes a significant deviation. This choice is further complicated because one must repeatedly test successive time points for deviation, and there can thus be many false alarms due to the multiple-testing problem (Maris & Oostenveld, 2007). A common strategy to reduce this problem is to require multiple significant samples in a row, akin to a cluster-wise correction in fMRI. In addition, the choice of the number of significant samples must be carefully made with regard to the filtering of the signal. Another problem is that the latency of the first deviation will correlate with the SNR of the measurements. As noise levels decrease, earlier latencies become significantly different from baseline. If one is not careful, this can cause difficulties in comparison between different conditions and experiments.

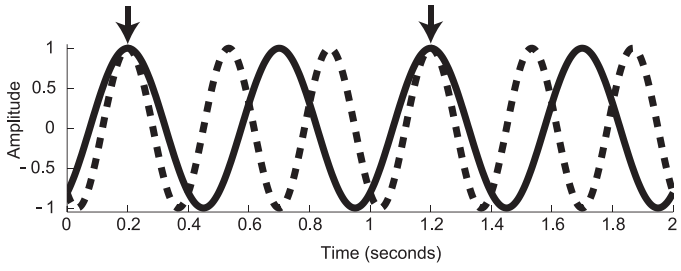

Figure A2. Waveforms from a system with a 200-ms delay and two stimulation frequencies: 2 Hz (solid line) and 3 Hz (dashed line). The arrows indicate the time that the responses coincide. Because there is a 1-Hz difference between stimulation frequencies, the repetition period is 1 s.

In order get away from the small-signal problems, an alternative is to use a peak in the measured time-averaged response. This requires first defining the corresponding peaks, e.g., the first positive maximum or the maximum response between 140 and 210 ms. Peaks provide strong signals but have the problem that using them to measure latency does not distinguish between a signal that starts early and rises slowly from a signal that starts late and rises fast. Aside from these methods, there are various other ways to determine latency in the time domain. No matter what method is used in the time domain, extreme caution should be used when latency measures are derived after temporal filtering has been performed, because temporal filtering will distort the shape of the response (Acunzo, Mackenzie, & van Rossum, 2012; Rousselet, 2012).

The frequency-domain analog to delay is phase, which measures latency using the entire waveform,

obviating the need to choose any specific feature. Phase is directly related to delay, and the relationship directly scales with the frequency of the response. For example, at 1 Hz a 90° phase delay translates into 0.25 s, while at 2 Hz a 90° phase delay is 0.125 s (see axis labels in Figure A1). A constant delay of 0.125 s correspond to a 45° phase delay at 1 Hz and a 90° phase delay at 2 Hz (Figure A1). In other words, if the delay is constant, doubling the frequency doubles the phase angle. It should be noted that two different sign conventions for phase exist in the literature. The one used here is that *positive* phase change means increasing delay. In other works, including most engineering literature, *negative* phase change means increasing delay.

Phase as a measure of delay differs from time-domain measures in ways that are important to understand. Phase is a *circular* variable, with a 0° phase angle identical to a 360° phase angle. Because of this circularity, care must be taken to respect the fundamental circularity of the distribution of phase values when doing phase analysis. In particular, circular statistics should be used (for a thorough treatment of this issue and a MATLAB toolbox for circular statistics, see Behrens, 2009).

A major issue with the circularity of the phase variable is that at high stimulation rates, response phase can wrap around one or more times, making the phase measurement ambiguous in terms of absolute latency. For example, at 10 Hz the same phase angle repeats every 100 ms. Another ambiguity exists because negative and positive responses are equally informative in EEG. If one is interested in the absolute delay of the response, this effectively halves the absolute repetition period (e.g., from 100 to 50 ms). This is not a problem if one is interested in small *relative* latency differences between conditions. This is illustrated nicely in the phase values plotted for the contrast and spatial-frequency sweeps in the lower panels of Figure 2, which show smooth changes in response phase associated with changes in contrast or spatial frequency. These smooth changes can be understood as follows: A general principle of sensory systems is that responses speed up as the stimuli become increasingly visible (Shapley & Victor, 1978). Speeding up of the response corresponds to a smaller lag of phase with respect to the stimulus. In the plots, 0 phase indicates 0 phase (time) lag with respect to the stimulus. Decreasing phase lag (faster response) is indicated in the contrast-sweep plot as a downward shift of the phase going from low to high contrasts, i.e., from low to high visibility. In the spatial-frequency sweep, visibility increases with decreasing spatial frequency. As in the case of the contrast sweep, we see the same direction of phase shift as we go from high spatial frequency (low visibility) to low spatial frequency (high visibility). In the case of the contrast sweep, phase changed by ~30°. At the 5-Hz stimulus frequency, 30° of phase shift is 1/12 of a period of the fundamental, or ~17 ms of decreased lag going from low to high contrast. With a single response-frequency measurement, it is often not possible to determine the absolute amount of delay with respect to the stimulus.

For the more general case when an absolute measure of delay is desired, it is possible to derive such a measure by recording response phase at multiple stimulation frequencies (Lee et al., 2012; Lopes da Silva et al., 1970; Regan, 1966; Spekreijse, 1978). This approach follows directly from the earlier argument regarding the correspondence between delay and phase shift. The choice of the frequencies used to estimate delay is important. In the limit, only two are needed, but when only two different frequencies are used, there is still an ambiguity in absolute terms that is equal to the *difference* between the two frequencies. Figure A2 illustrates this with 2-Hz and 3-Hz responses, both with latencies of 200 ms. The only places the two signals are commensurate occurs precisely at the delay and then again 1 s later (the difference between 2 and 3 Hz). It is much more plausible, physiologically, that the delay is 200 ms rather than 1200 ms for most stimuli.

This method works for any two frequencies, but care must be exercised in choosing these frequencies. Frequencies should be close enough together to reduce the ambiguity of absolute latency, as in the example just given. However, the closer together the frequencies, the stronger the influence of noise on the latency estimate. Put simply, the measured phase difference should be larger than the uncertainty in the phase measurement itself. Formally, the relationship is that latency is proportional to the derivative of phase with respect to frequency. This relationship, along with fitting a line to the change in phase versus frequency, has been used for many years (Fiorentini & Trimarchi, 1992; Lopes da Silva et al., 1970; Regan, 1966). One difficulty is that because phase is only measured between 0° and 360°, the method to fit the data must respect this nonlinearity, either by unwrapping phase prior to fitting the line (Lee et al., 2012; Strasburger, 1987) or using a nonlinear fitting procedure.

Appendix 2. Detecting significant SSVEP activity

There are several approaches available to determine whether a statistically reliable SSVEP response is present. One common method is based on a threshold SNR. The SNR is obtained by dividing the EEG amplitude at response frequency f by a noise value. Noise can be computed at the same frequency f during a baseline period (Meigen & Bach, 1999; see also Cottereau et al., 2011). It can also be extracted from the average of the amplitude at frequency bins adjacent to the tagged frequency f (i.e., $f - \delta f$ and $f + \delta f$, where δf is

the frequency resolution of the Fourier analysis). By averaging noise values from frequencies immediately above and below the response frequency, one can interpolate the additive background noise likely to be present at the response frequency during the actual SSVEP recording. This has two advantages: The first is that the noise is estimated under the same state conditions (e.g., movements and arousal are the same), and the second is that the interpolation takes into account the slope of the background EEG spectrum, which can be quite steep at low frequencies. Threshold values for SNR corresponding to different levels of statistical significance can be obtained from empirical sampling distributions (Norcia et al., 1989).

When long-duration recordings are used, the noise can be also computed over a larger number of narrow frequency bins (e.g., by using 20 neighboring bins; see Rossion et al., 2012; Srinivasan et al., 1999). This approach is valid as long as the chosen frequency bands do not include any of the harmonics of the input frequency (or IM frequencies for multiple input designs; see Multiple periodic visual inputs). The advantage of this approach is that the variance of the noise around the frequency of interest can be estimated, so that statistical tests (i.e., a t value or a z-score) can be performed to determine if the response at the frequency bin of interest is significant (e.g., Liu-Shuang et al., 2014). If the noise is not distributed normally around the frequency bin of interest, nonparametric tests can be used. The SNR at higher order harmonics of the stimulus tagging frequency F (i.e., at $2f$, $3f$, ...) can be computed following the same approach.

If the multiple harmonics are thought to reflect a common response (see Heinrich, 2010), it is possible to compute a global SNR for multiple harmonics (e.g., the two first odd harmonics of the tagged frequency) by pooling together all the moduli of their Fourier coefficients using their root-mean-square value. This operation is equivalent to summing the powers of the individual harmonics and then taking the square root (Appelbaum et al., 2006). This pooled value is then divided by the root-mean-square of the associated noise magnitudes (see Cottereau, McKee, & Norcia, 2014).

Several approaches have been proposed to characterize the variability of the Fourier components at a given frequency during a steady-state stimulation. These approaches use the distribution of the Fourier coefficients produced by the individual trials of an SSVEP recording to compute variance estimates for response amplitude. They were adapted from standard statistics from other contexts (see e.g., Picton, Vajsar, Rodriguez, & Campbell, 1987; Strasburger, 1987). More developed versions, such as the well-known T^2_{circ} statistic (Victor & Mast, 1991), use the real and imaginary parts of Fourier components to determine confidence limits for the SSVEP response at a given frequency. These approaches can be used to determine if a signal is significantly different from zero and to compare the SSVEPs obtained from different conditions. As a statistical test, T^2_{circ} achieves the highest efficiency for detecting a true activation out of noise. It achieves this efficiency by making the strong parametric assumption of independent identically distributed Gaussian noise on the Fourier coefficients. A limitation of this approach is that it requires more than approximately five independent samples. If these samples have a short duration, the experiment can be reasonably limited in time. Single long-duration recordings, while providing high SNR, do not provide error estimates for amplitude or phase unless they are segmented into separate epochs or variability is measured across another dimension, such as across participants. In theory, averaging many short-duration trials or a few long-duration trials should give rise to roughly identical SNRs. But practically, different trial lengths may have a variety of uncontrolled differences between them (e.g., different artifacts and participant compliance), and empirical tests of the difference are currently lacking.